NASA/TM—2005-213414

A Comparative Propulsion System Analysis for the High-Speed Civil Transport

Jeffrey J. Berton, William J. Haller, Paul F. Senick, Scott M. Jones, and Jonathan A. Seidel
Glenn Research Center, Cleveland, Ohio

February 2005

The NASA STI Program Office . . . in Profile

Since its founding, NASA has been dedicated to the advancement of aeronautics and space science. The NASA Scientific and Technical Information (STI) Program Office plays a key part in helping NASA maintain this important role.

The NASA STI Program Office is operated by Langley Research Center, the Lead Center for NASA's scientific and technical information. The NASA STI Program Office provides access to the NASA STI Database, the largest collection of aeronautical and space science STI in the world. The Program Office is also NASA's institutional mechanism for disseminating the results of its research and development activities. These results are published by NASA in the NASA STI Report Series, which includes the following report types:

- TECHNICAL PUBLICATION. Reports of completed research or a major significant phase of research that present the results of NASA programs and include extensive data or theoretical analysis. Includes compilations of significant scientific and technical data and information deemed to be of continuing reference value. NASA's counterpart of peer-reviewed formal professional papers but has less stringent limitations on manuscript length and extent of graphic presentations.

- TECHNICAL MEMORANDUM. Scientific and technical findings that are preliminary or of specialized interest, e.g., quick release reports, working papers, and bibliographies that contain minimal annotation. Does not contain extensive analysis.

- CONTRACTOR REPORT. Scientific and technical findings by NASA-sponsored contractors and grantees.

- CONFERENCE PUBLICATION. Collected papers from scientific and technical conferences, symposia, seminars, or other meetings sponsored or cosponsored by NASA.

- SPECIAL PUBLICATION. Scientific, technical, or historical information from NASA programs, projects, and missions, often concerned with subjects having substantial public interest.

- TECHNICAL TRANSLATION. English-language translations of foreign scientific and technical material pertinent to NASA's mission.

Specialized services that complement the STI Program Office's diverse offerings include creating custom thesauri, building customized databases, organizing and publishing research results . . . even providing videos.

For more information about the NASA STI Program Office, see the following:

- Access the NASA STI Program Home Page at ***http://www.sti.nasa.gov***

- E-mail your question via the Internet to help@sti.nasa.gov

- Fax your question to the NASA Access Help Desk at 301–621–0134

- Telephone the NASA Access Help Desk at 301–621–0390

- Write to:
  NASA Access Help Desk
  NASA Center for AeroSpace Information
  7121 Standard Drive
  Hanover, MD 21076

NASA/TM—2005-213414

A Comparative Propulsion System Analysis for the High-Speed Civil Transport

Jeffrey J. Berton, William J. Haller, Paul F. Senick, Scott M. Jones, and Jonathan A. Seidel
Glenn Research Center, Cleveland, Ohio

National Aeronautics and
Space Administration

Glenn Research Center

February 2005

Document History

This research was originally published internally as HSR007 in October 1995.

This report is a formal draft or working paper, intended to solicit comments and ideas from a technical peer group.

This report contains preliminary findings, subject to revision as analysis proceeds.

Note that at the time of writing, the NASA Lewis Research Center was undergoing a name change to the NASA John H. Glenn Research Center at Lewis Field. Both names may appear in this report.

Available from

NASA Center for Aerospace Information
7121 Standard Drive
Hanover, MD 21076

National Technical Information Service
5285 Port Royal Road
Springfield, VA 22100

Available electronically at http://gltrs.grc.nasa.gov

A Comparative Propulsion System Analysis for the High-Speed Civil Transport

Jeffrey J. Berton, William J. Haller, Paul F. Senick, Scott M. Jones, and Jonathan A. Seidel
National Aeronautics and Space Administration
Glenn Research Center
Cleveland, Ohio 44135

Abstract

Six of the candidate propulsion systems for the High-Speed Civil Transport are the turbojet, turbine bypass engine, mixed flow turbofan, variable cycle engine, Flade engine, and the inverting flow valve engine. A comparison of these propulsion systems by NASA's Lewis Research Center, paralleling studies within the aircraft industry, is presented. This report describes the Lewis Aeropropulsion Analysis Office's contribution to the High-Speed Research Program's 1993 and 1994 propulsion system selections. A parametric investigation of each propulsion cycle's primary design variables is analytically performed. Performance, weight, and geometric data are calculated for each engine. The resulting engines are then evaluated on two airframer-derived supersonic commercial aircraft for a 5000 nautical mile, Mach 2.4 cruise design mission. The effects of takeoff noise, cruise emissions, and cycle design rules are examined. (This report was written in 1995 for NASA's High Speed Research Program.)

Introduction

There is a renewed, worldwide interest in developing an economically viable and environmentally acceptable commercial supersonic transport to begin operations early in the twenty-first century. Several attempts have been made over the last quarter century to develop a U.S. supersonic commercial transport. The Supersonic Transport Program, which ran from the mid-1960s to 1971, focused on establishing an airframe and propulsion system that could compete in the international supersonic transport marketplace. The program was canceled when political support waned in the face of increasing technical, environmental, and economic concerns. From 1972 to 1981, NASA conducted the Supersonic Cruise Research Program. This cooperative government/industry effort investigated areas where advanced technology would produce significant enhancements in supersonic cruise performance. New engine concepts and better jet noise reduction techniques were developed (ref. 1). In 1989, the NASA-sponsored High-Speed Research (HSR) Program was initiated with the objective of providing solutions to the environmental issues associated with a proposed future High-Speed Civil Transport (HSCT). NASA-sponsored studies involving both airframe and engine manufacturers have determined that an economically viable, environmentally acceptable Mach 2.4 HSCT could enter the market as early as 2005. The HSCT's potential economic impact is enormous. The findings of Boeing's 1993 Focus Group indicate that due to increased productivity, time savings, and passenger preference, the HSCT could capture up to seventy percent of the long-haul markets in cases where it can offer significant time savings over long-range subsonic aircraft. Boeing's market research also suggests that sufficient profitability is possible with little or no fare premiums.

The problems that plagued the U.S. Supersonic Transport Program are still present today. In addition to difficult economic challenges, there are problems posed by environmental concerns. Namely, the stratospheric propulsion emissions must be minimized such that the HSCT fleet will have no significant effect on the ozone layer, and the propulsion noise must be reduced to meet current Federal Aviation Regulation (FAR) Part 36 Stage 3 noise rules (ref. 2). Indeed, noise regulations of the near future may become even more stringent in the airport vicinity, and additional rules may regulate noise levels many miles from the airport as the aircraft climbs. These economic and environmental requirements pose a significant propulsion engineering challenge.

This study builds upon earlier research performed by the NASA Lewis mission analysis team (refs. 3 and 4). The candidate propulsion systems evaluated here for the HSCT are the turbojet, turbine bypass engine, mixed flow turbofan, variable cycle engine, Flade engine, and the inverting flow valve family of engines (see figs. 1 to 7). The design variables of each of these cycles are parametrically varied and the performance and weight data are analytically computed. The resulting engines are then evaluated on two airframer-derived HSCTs for 5000 nautical mile, Mach 2.4 cruise missions. The effects of takeoff noise, cruise emissions, and the addition of alternate missions are also examined.

The intent of this study was to provide guidance for the NASA/industry propulsion system downselect team. This team, consisting of representatives from NASA, General Electric, Pratt & Whitney, Boeing, and McDonnell Douglas, selected two propulsion system concepts, a prime and a backup, in October, 1993. Additional updated propulsion system evaluations are also presented for the downselect confirmation of April, 1994. Contained in this paper are the NASA Lewis mission analysis team's recommendations for the selection of these two propulsion system concepts based on our independent engine cycle and mission analysis.

The reader who is familiar with the ongoing HSR Program will note that many changes have been made to the HSCT propulsion system concepts since the 1994 downselect confirmation. Even the propulsion system choices themselves would have been made very differently had the results of many studies and component tests been known in 1993. This paper is written to describe the state of affairs as they were known to exist in April, 1994. The reader is asked to consider the data and conclusions in this paper from that point of view.

Method of Analysis

Propulsion System Analysis

Cycle, Aeromechanical, Flowpath, and Weight Analyses

The uninstalled performance of each engine is predicted by the NASA Engine Performance Program (refs. 5 and 6). This computer code calculates the uninstalled performance of each engine based on a steady, one-dimensional, thermodynamic cycle analysis. Off-design engine performance is calculated with the aid of individual component performance maps supplied by the HSR engine manufacturers, General Electric and Pratt & Whitney. The physical and thermodynamic limitations used in this analysis have been identified by NASA and industry as being commensurate with a 2005 entry into service date. An abridged list of these design "ground rules" are shown in tables 1 through 3. The first set of ground rules is used for the initial, 1993, downselect. Due to independent detailed materials study recommendations, the compressor discharge, turbine rotor inlet, and nozzle throat temperature limits became more conservative during the course of the program (see table 1). The effects of these changes have been calculated for the 1994 downselect confirmation and are also presented in this paper.

Bare engine weights and dimensions are calculated using an extensively updated version of the Boeing weight and flowpath analysis code described in reference 7. The weight and flowpath design parameters shown in table 2 are used in this analysis. Miscellaneous pod weights (i.e., nacelle, pylon, mounts, firewall, and controls and accessories) are computed using empirical relations for commercial transports (refs. 8, 9, 10, and table 2).

Installation Effects

A mixed-compression translating centerbody inlet is used for each of the engine cycles in this study. The performance and aerodynamic characteristics of this inlet are derived from reference 7 and some of its more dominant performance characteristics are plotted in figures 8 to 12. The throttle-dependent, isolated nacelle inlet installation drags consist of pre-entry spillage drag, bypass drag, bleed drag, and cowl lip drag. These installation drags are calculated and are subtracted from the uninstalled net thrust determined from the thermodynamic cycle analysis described above. The inlet's weight and dimensions are computed by the mission analysis team from a method incorporating empirically-derived actuation system weights and analytically-derived structural weights modeled using the Internally Pressurized Structural Synthesis and Optimization code (refs. 8 to 11).

The throttle-dependent, isolated nacelle nozzle boattail drags are also subtracted from the uninstalled net thrust. These drags are computed, in part, from inviscid linearized aerodynamic perturbation theory. Inviscid boattail drag coefficients are computed for this study using the program described in reference 12 for both axisymmetric and 2D nozzle exit geometries. To account for the additional viscous drag component, boattail drag coefficients derived from a set of agreed-upon experimental axisymmetric data by NASA Lewis, General Electric, and Pratt & Whitney are used. This viscous drag component is determined by subtracting the analytically derived inviscid drag from the empirical total drag for each axisymmetric geometry. The viscous drags are then added to the inviscid drags of the 2D geometries, resulting in a total drag database for 2D exit nozzles. For reasons that are explained below, each of the propulsion systems analyzed in this study is assumed to have a 2D nozzle exit. For the valved engines, however, an axisymmetric nozzle may be a superior choice when propulsion-airframe integration effects are considered. These 2D boattail drag coefficients are plotted for various external area ratios in figures 13 to 15.

Since these boattail drags are calculated simultaneously with the nozzle's thrust, the opportunity is taken to optimize thrust. Specifically, the nozzle is operated in a slightly overexpanded flow configuration. Without considering boattail drag, this would seem to be detrimental due to the pressure drag and possible flow separation near the nozzle exit plane. However, the artificially larger exit area of an overexpanded nozzle reduces the boattail drag by lowering the nozzle's boattail angle. The exact amount of overexpansion is calculated by optimizing the installed thrust. In the transonic regime, where boattail drags are greatest, this technique can improve the installed gross thrust for some configurations by as much as six percent. This significant thrust improvement can help the

HSCT pass through the transonic regime more quickly and, if it is sized at the transonic drag rise, with potentially smaller engines.

Mixer-Ejector Nozzles

High velocity jet noise, which dominates the acoustic signature of the HSCT, can be reduced by ejecting large amounts of ambient air into the primary jet within an acoustically lined duct. The resultant mixed jet has a lower velocity than an unmixed primary jet. The mixed jet generates less shear layer interaction with the ambient air and is quieter than a conventional convergent-divergent nozzle operating under the same conditions. Shock cell noise can be reduced by careful, shock-free, expansion of the jet. Nozzles with these characteristics are called mixer-ejector nozzles, and their use currently appears to be the best approach to suppressing the jet noise of the turbojet, turbine bypass engine, mixed flow turbofan, and the variable cycle engine. In this study, engines that are already inherently quiet (i.e., the Flade and valved engines described below) are not equipped with these nozzles. Other propulsion noise sources, such as fan, turbine, and core noise, do not dominate the acoustic signature and are not specifically calculated in this study. An acoustic margin is used to account for these sources (as described later) to ensure compliance with noise regulations.

The weights and dimensions of the mixer-ejector nozzles described here are calculated using a nozzle model created by the Lewis team specifically for this study. This model is database-oriented and draws upon the characteristics of a family of hybrid axisymmetric and 2D mixer-ejector nozzles analytically designed by General Electric. The model assumes that the amount of secondary entrained air that is required to suppress the jet noise to certification levels can be determined from the primary stream conditions. Specifically, this entrained mass flow augmentation is assumed to be a function of the velocity of the primary jet hypothetically expanded through a convergent-divergent nozzle with a velocity coefficient of 0.95. This relationship is shown in figure 16. Since the weight and dimensions of the nozzle are assumed to increase with increasing mass flow augmentation, the curve shown in this figure can therefore be viewed as a nozzle weight and size severity model. The shape of this curve has been calibrated to reflect current estimates of mixer-ejector nozzle weights and dimensions with respect to their suppression requirements. The mixer-ejector nozzle length (fig. 17), maximum nozzle cross-sectional area (fig. 19), and weight (fig. 20) are derived from the database for various nozzle pressure ratios for the 1993 model. These relationships were used for the initial October, 1993 downselect. In January of 1994, the model's database was updated to reflect General Electric's decision to remove excessive acoustic liner material at the nozzle entrance. These changes resulted in shorter, lighter nozzles. The revised nozzle length and weight relationships of the 1994 model are shown in figures 18 and 21, respectively. These relations were used for the April, 1994 downselect confirmation. The nozzle thrust coefficient with the ejectors in their stowed position is also assumed to be a function of the nozzle pressure ratio and is shown in figure 22. The nozzle thrust coefficient with ejectors deployed is assumed to be 0.95 throughout the takeoff segment of the mission. These mixer-ejector nozzle aeroacoustic performance models are considered to be representative and achievable if HSR nozzle development continues along its present course.

Exhaust Emissions

Nitric oxide (NO) and nitrogen dioxide (NO_2), collectively known as NO_X, are products of combustion that are known to affect stratospheric ozone. An emission index, defined as the ratio of an emittant's mass to one thousand times the mass of fuel burned, is computed for NO_X for every engine data point of every engine cycle studied. These emission indices, which are a function of Mach number, altitude, and power setting, are integrated over the HSCT's flight path to give a total mass of NO_X produced for the mission. The NO_X emission index (EI) is calculated from the following set of relations:

$$EI = 0.01555\,T_3 - 8.3$$

for compressor discharge total temperatures (T_3, in degrees Rankine) less than 1100 °R, or

$$EI = 2.899\left(\frac{T_{3max}}{1000} - 0.46\right)\left(\frac{P_4}{P4_{toc}}\frac{T_{4toc}}{T_4}\frac{w_{toc}}{w}\right) \times \exp\left(-72.28 + 2.087\sqrt{T_f} - 0.014611\,T_f\right)$$

for T_3 greater than 1100 °R. The subscript "toc" denotes the top-of-climb cycle conditions, T_{3max} is the highest compressor discharge total temperature in degrees Rankine encountered by the engine over the entire mission, P_4 is the combustor exit total pressure, T_4 is the combustor exit total temperature, w is the combustor airflow, and T_f is the combustor flame total temperature in degrees Rankine, defined as the greater of either 3600 °R or

$$T_f = T_3 + 1.1765\left(T_4 - T_3\right)$$

These relations are based on a simplified generic low-emissions HSR combustor model developed jointly by the combustor analysis and design groups at General Electric, Pratt & Whitney, and NASA Lewis.

Turbojet and Turbine Bypass Engines

The conventional single-spool turbojet (fig. 1) is evaluated in this study to measure the advantages and disadvantages of the other cycles relative to this classical standard. The single-spool Turbine Bypass Engine (TBE, fig. 2) is similar to the turbojet operating with a fixed-area, choked turbine. The advantage a TBE holds over a turbojet is a bypass valve that routes compressor exit air through a duct around the combustor and turbine. This bypass stream allows the engine to maintain constant corrected turbine airflow throughout the flight envelope without reducing the turbomachinery's rotational speed. Bypassing this compressor discharge air around the turbine allows cycle pressures, temperatures, and total engine airflow to remain higher than those in a turbojet operating under similar conditions. In addition, this bypass flow helps to maintain high total engine airflow during part-power operation, which reduces both spillage and boattail drags in throttled conditions.

The TBE and turbojet are desirable because of their high specific thrust. Due to the turbine bypass flow, however, the subsonic cruise air-handling capabilities make the TBE a better candidate for the HSCT than a turbojet. Unfortunately, both the turbojet's and the TBE's high sea level primary jet velocities necessitate the addition of a relatively large noise-suppressing mixer-ejector nozzle to meet takeoff noise regulations. A small, lightweight mixer-ejector nozzle with good aeroacoustic performance is crucial to the success of the TBE.

The cycle design parameters investigated for the TBE are the combustor exit temperature, the overall pressure ratio (OPR), and the turbine bypass flow (TBP), expressed as a percentage of the total engine airflow. Values quoted for each of these parameters are always at sea level static (SLS) conditions. During previous studies of the NASA Lewis downselect team (refs. 3 and 4), the OPRs and TBPs investigated for the TBE ranged from 11.0 to 18.5 and from 2.5 to 18.4 percent, respectively. It was discovered that the TBEs resulting in the lowest takeoff gross weight aircraft were those that had the highest allowable OPRs and the lowest TBPs. This is due to the improvement in thrust-specific fuel consumption (TSFC) provided by high OPRs and the improvement in top-of-climb specific thrust provided by low TBPs. Therefore, the TBEs and the turbojet presented here have the highest OPRs allowed by the 1993 maximum compressor discharge temperature limit: 18.5 at T_3 = 1710 °R. The TBEs presented here have SLS TBPs of 8.7 percent, which results in no bypass flow at top-of-climb conditions. The ranges of SLS combustor exit temperatures and turbine rotor inlet temperatures (T_4 and T_{41}, respectively) for the turbojet and TBEs investigated are shown below.

Engine Designation	T_4 (°R)	T_{41} (°R)
TJ3010	3489	3360
TBE3010	3489	3360
TBE3021	3309	3207
TBE3031	3202	3120
TBE3041	2990	2930

The turbine rotor inlet temperatures are calculated by mass-averaging the core stream and cooling stream enthalpies. Note that the highest temperature cycles, TJ3010 and TBE3010, are T_{41}-limited at 3360 °R for the initial 1993 downselect study. Since the TBE was eliminated in the 1993 downselect (as discussed below), no turbojets or TBEs are presented for the 1994 downselect study's ground rules (see table 1).

Understanding the tradeoffs between the high- and low-temperature cycles is difficult without performing an aircraft mission and sizing analysis (to be discussed below). The high-temperature engines provide higher specific thrust and could likely be sized smaller than the lower temperature engines, but their high primary jet velocities require larger, heavier mixer-ejector nozzles. The low-temperature engines benefit from lower TSFCs, smaller mixer-ejector nozzles, and potentially greater turbine blade life, but they would need to be sized larger to meet mission thrust requirements because of their lower specific thrust.

The influence of transonic afterburning is also investigated. These additional afterburning engine data are calculated for flight Mach numbers between 0.90 and 1.40 to provide supplementary thrust throughout the drag rise of the transonic regime. The amount of afterburning is limited by either a 600 °R stream temperature rise or by the maximum allowable mixer-ejector nozzle temperature of 2710 °R, whichever occurs first. The relatively small temperature increase of 600 °R is chosen to reflect the use of a compact, lightweight, limited-performance afterburner. The level of supplementary thrust is a maximum at Mach 1.10, and decreases linearly to zero at Mach numbers 0.90 and 1.40. The additional weight and dimensions of an afterburning duct are considered.

Mixed Flow Turbofan

The two-spool Mixed Flow Turbofan (MFTF, fig. 3) has a core bypass stream that rejoins the core flow through a forced mixer downstream of the turbine. Bypassing the engine core results in a loss of specific thrust, but leads to lower TSFCs and jet velocities than a comparable TBE. Depending on the amount of bypass airflow designed in the cycle, these potentially low primary jet velocities make the MFTF an inherently quieter engine than the TBE. Its mixer-ejector nozzle is therefore typically required to provide less noise suppression than the TBE's nozzle. Because of these reduced noise suppression requirements, the MFTF benefits from potentially lower nozzle size, weight, and boattail drag levels. And since the maximum propulsion pod cross sectional area occurs in the nozzle's ejector region, better nacelle forebody shapes can be designed on a MFTF pod than the TBE's pod, leading to more favorable airframe integration aerodynamics.

The key cycle parameters investigated for the MFTF are the fan pressure ratio (FPR), overall pressure ratio (OPR), mixer secondary-to-primary total pressure ratio, and the temperature throttle ratio (TTR). The TTR is defined as the ratio of the maximum T_{41} encountered to the SLS design point T_{41} and is directly related to the airflow lapse of the inlet. Greater inlet airflow lapses lead to lower TTRs. By choosing to vary these four design parameters, the engine bypass ratio (BPR) becomes a dependent variable.

A series of MFTFs are examined using the 1993 ground rules. The values of TTR (1.13) and SLS OPR (21.0) are determined by the inlet airflow schedule and the desire to achieve the maximum compressor discharge temperature at the top of the aircraft climb path, respectively. Like the TBE, earlier NASA Lewis studies (refs. 3 and 4) determined that the highest OPR allowed by the compressor discharge temperature limit leads to the best cycle performance. These studies also determined that a SLS design point mixer pressure ratio slightly greater than unity is optimal. All of the turbofans evaluated here have a mixer pressure ratio design value of 1.02. Higher values produce supersonic mixing problems. Consequently, the only parameters varied for this particular evaluation are the maximum allowable T_{41}, FPR, and BPR. The following five cycles are modeled using the maximum T_{41} allowed by the 1993 ground rules (3360 °R) with SLS FPRs ranging from 3.0 to 4.6. The ranges of SLS FPRs and BPRs of these high-temperature MFTFs using the 1993 ground rules are shown below.

Maximum T_{41} = 3360 °R		
Engine Designation	FPR	BPR
MFTF1093	3.00	1.20
MFTF2093	3.40	0.83
MFTF3093	3.80	0.55
MFTF4093	4.20	0.35
MFTF5093	4.60	0.18

Another effect investigated is the reduction of the maximum allowable T_{41}. Each of the five MFTFs described above are redesigned for reductions in maximum T_{41} of 150 and 250 °R. This analysis expands the analytical design envelope of the turbofan. The specific thrust penalty of a low-temperature turbofan can be partially offset by the benefits of reduced specific fuel consumption and jet noise. Engines with lower combustor temperatures also produce fewer NO_X emissions and may potentially have greater hot section life. The same FPR range above is used for this evaluation. The OPR and T_{3max} for these turbofans remains constant at 21.0 and 1710 °R, respectively. By dropping T_{41} but holding the OPR constant, the engine BPR must decrease to compensate. Because of this, an engine with an FPR of 4.6 is not achievable for a T_{41} of 3110 °R and there are therefore only four turbofans analyzed at that temperature. The ranges of SLS FPRs and BPRs of these low-temperature MFTFs using the 1993 cycle ground rules are shown below.

Maximum T_{41} = 3210 °R		
Engine Designation	FPR	BPR
MFTF1193	3.00	0.98
MFTF2193	3.40	0.64
MFTF3193	3.80	0.40
MFTF4193	4.20	0.21
MFTF5193	4.60	0.06

Maximum T_{41} = 3110 °R		
Engine Designation	FPR	BPR
MFTF1293	3.00	0.81
MFTF2293	3.40	0.50
MFTF3293	3.80	0.27
MFTF4293	4.20	0.10

The effect of transonic afterburning is investigated for the 1993 MFTFs. Like the TBE, an afterburner temperature increase of up to 600 °R is permitted between flight Mach numbers 0.90 and 1.40. For the low bypass turbofans, the maximum temperature augmentation must be limited to observe the mixer-ejector nozzle temperature limit. The engines that include thrust augmentation have an additional weight and length increase to account for the augmentor.

For the 1994 cycle ground rules, the decrease in maximum allowable T_3 and T_{41} requires the MFTF cycle design process to be repeated. A similar procedure to the one explained above is employed to obtain five new MFTFs. The drop in maximum allowable T_3 to 1660 °R forces the cycle OPR from 21.0 to 19.5. As before, five MFTFs are derived with the same FPR range. Since it will be shown that the aircraft noise, mission, and sizing analyses of the reduced combustor temperature 1993 turbofans resulted in poor aircraft performance, no reduced temperature turbofans are investigated using the 1994 ground rules. The ranges of SLS FPRs and BPRs of the MFTFs investigated using the 1994 cycle ground rules are shown below.

Maximum T_{41} = 3260 °R		
Engine Designation	FPR	BPR
MFTF1094	3.00	1.06
MFTF2094	3.40	0.71
MFTF3094	3.80	0.44
MFTF4094	4.20	0.25
MFTF5094	4.60	0.09

In selecting the optimum MFTF for this application, several factors must be considered. A low bypass, high temperature MFTF has a higher specific thrust than a high bypass, low temperature MFTF and has a smaller installed engine size requirement. The corresponding high takeoff jet velocities produced, however, have greater noise suppression requirements, which lead to a larger mixer-ejector nozzle. The overall thrust benefit of a small capture area may be offset by a large nozzle diameter that could produce unreasonably high boattail drag levels. These nozzles are also heavier than those requiring less suppression. For a given airflow, the low bypass MFTF's bare engine weight is also higher. This occurs because a greater portion of the engine airflow must pass through the core, requiring larger, heavier turbomachinery components. Therefore, like the TBE, the trade between the MFTF's cycle performance, engine and nozzle weight, and installation effects must be derived through the aircraft noise, mission, and sizing analyses.

Variable Cycle Engine

The Variable Cycle Engine (VCE, fig. 4) has been used in various applications since being proposed for the Supersonic Cruise Research Program, the most notable application being a variant used in the U.S. Air Force's Advanced Tactical Fighter. The VCE is similar to the conventional two-spool MFTF described above with two exceptions. The first is the additional secondary outer bypass duct, which can be used to increase the overall BPR and flow handling capability of the engine. This second bypass stream, at the expense of additional complexity and weight, improves TSFC and improves fan surge control by allowing the fan to pass its maximum amount of air throughout a broader flight regime. This allows greater flexibility in cycle operation at both high flight speeds and part-power operation. The second difference is the presence of a core-driven fan stage (CDFS) placed directly in front of the high-pressure compressor. This stage gives a boost in pressure to both the core and inner bypass flow streams. Unlike the MFTF, the VCE enjoys a nearly constant overall BPR regardless of flight condition because the front fan is allowed to pass only as much airflow as the core-driven fan can handle. Depending on the amount of bypass flow, the VCE is also a relatively quiet engine whose mixer-ejector nozzle is required to deliver less noise suppression.

In previous studies made for the Supersonic Cruise Research Program, the front fan was oversized and the secondary bypass duct was opened during takeoff in an effort to reduce jet noise. Operating the cycle in this manner increased the amount of low-energy bypass flow which reduced the overall exhaust velocity and resulted in a quieter engine. It was determined, however, that this reduction in jet velocity was not great enough to justify the increased size and weight of the front fan. Recent studies performed by the NASA Lewis team and General Electric confirm this conclusion. In the current HSR Program, the VCE's secondary bypass is only opened at flight speeds in excess of Mach 1.6 to provide fan surge control and to improve TSFC. Designed this way, the VCE produces takeoff and climb exhaust jet velocities comparable to a similar BPR MFTF cycle. Because there is no significant inner bypass growth, the VCE designer is allowed greater latitude in selecting design parameters which would otherwise result in unacceptably high inner bypass and thrust lapse values at top-of-climb conditions.

The ranges of the parameters investigated for the VCE are shown below. All values are given at SLS conditions except the outer BPR, which is given at top-of-climb conditions.

Parameter	Range
FPR	2.75 - 4.00
OPR	16.8 - 26.7
T_4 (°R)	3260 - 3560
Inner BPR	0.15 - 0.80
Top-of-Climb Outer BPR	0 - 0.30
TTR	1.00 - 1.21
CDFS PR	1.10 - 1.38

Like the TBE and MFTF, the VCE's optimum OPR is determined by the highest T_3 allowed by the 1993 ground rules. The high pressure compressor's pressure ratio is chosen to maximize T_3 at top-of-climb conditions. The fan pressure ratio is chosen to achieve a mixing balance of inner bypass and core streams. Due to experience gained from the TBE and MFTF, the VCE uses the highest T_4 allowed by the 1993 T_{41} limit. Inner BPRs greater than 0.8 produce VCEs with too little thrust during climb and are not considered in this study. Outer BPRs are optimized for performance and flow control and are a function of the inner BPR. For inner BPRs less than 0.4, an outer BPR of 0.1 is found to provide the best trade between TSFC reduction and front fan surge margin. For inner BPRs between 0.3 and 0.9, the front fan surge margin requires more flow from the secondary bypass and the outer BPR is increased to 0.2. TTRs between 1.00 and 1.05 lead to VCEs with attractive TSFCs and acceptable thrust throughout the mission. The CDFS pressure ratio is varied within the bounds and strategies already mentioned.

The four primary 1993 study VCEs are listed below. Each of these cycles have SLS OPR, SLS T_4, and TTR values of 22.3, 3560 °R, and 1.00, respectively.

Engine Designation	FPR	Inner BPR	Outer BPR
VCE701510	4.00	0.15	0.10
VCE703010	3.52	0.30	0.10
VCE706520	2.96	0.65	0.20
VCE708020	2.75	0.80	0.20

The effect of transonic afterburning is investigated for the VCE. Since the VCE was eliminated in the 1993 downselect (as discussed below), no VCEs are presented for the 1994 downselect ground rules.

Flade Engine

The Fan-on-Blade (Flade) cycle (fig. 5) is a hybrid propulsion system that consists of a core engine surrounded by a bypass duct. This bypass duct, or flade stream duct, contains variable inlet guide vanes and a single compression stage created by extending one row of the core engine's fan blades into the stream. The flade stream is ducted downward to the lower half of the engine where it is exhausted through a variable area nozzle. The flade stream, in addition to lowering the overall primary jet noise, acts as a fluid acoustic shield that partially masks the jet noise perceived by ground observers. One benefit of this nozzle is its reduction of weight and length relative to the mixer-ejector nozzles used with the TBE, MFTF, and VCE cycles. Due to the relatively small nozzle diameter, the maximum cross sectional area of the pod is located near the fan, which results in steep angles in the nacelle forebody region and may create adverse aerodynamic installation effects. The amount of noise suppression achieved from this nozzle is discussed below.

Initial versions of the Flade concept contained a VCE as its core engine. After the VCE was eliminated in the initial 1993 propulsion selection (as discussed below), the MFTF became the Flade's core engine. Only fladed VCEs using the 1993 cycle ground rules are evaluated in this study.

The key cycle design parameters investigated for the Flade engine are similar to those of the MFTF and VCE: the FPR, CDFS pressure ratio, TTR, and the mixer secondary-to-primary total pressure ratio. The design value of the flade stage pressure ratio could be varied as well; however, it is held constant for this analysis at 1.8. This is very near the maximum achievable pressure ratio in a single stage at the tip speeds encountered in this application. There has been debate on the merits of flading multiple stages of the fan, which would increase the low speed thrust of the overall engine. The Flade appears, however, to produce ample thrust in this regime, and such a design is contrary to the flade stream's purpose of providing low velocity air for the fluid acoustic shield. Like the MFTF, all Flades in this study have the same design mixer pressure ratio. The total design engine airflow for the cycle screening is 900 lb/s, with 650 lb/s entering the VCE and 250 lb/s entering the flade duct. This airflow split is another design parameter that may warrant future investigation. The inner BPR is the dependent variable in this analysis.

A series of Flade engines are investigated. Two TTRs, two FPRs, and two CDFS pressure ratios produce a matrix of eight candidate cycles. The major SLS design point parameters of these eight Flades are shown in the following table.

Engine	FPR	TTR	OPR	CDFS PR	BPR (VCE)
F193	3.30	1.06	20.5	1.50	0.14
F293	3.00	1.06	20.5	1.50	0.28
F393	3.30	1.06	20.5	1.60	0.05
F493	3.00	1.06	20.5	1.60	0.18
F593	3.30	1.03	21.0	1.50	0.21
F693	3.00	1.03	21.0	1.50	0.37
F793	3.30	1.03	21.0	1.60	0.12
F893	3.00	1.03	21.0	1.60	0.26

The primary jets of the above Flade engines have velocities ranging from 2300 to 2600 ft/s. These jets would produce noise levels well in excess of allowable limits when unattenuated. With the addition of the flade stream's fluid acoustic shield, however, significant noise reduction is possible.

Inverting Flow Valve Engines

The inverting flow valve family of engines consists of turbojets (TJ/IFVs, fig. 6) and turbofans (TF/IFVs, fig. 7) with a valve downstream of the fan or low-pressure compressor that allows for dual-mode cycle operation. During normal, high-speed flight operations, with the outer stream of air ducted around the core, these engines provide the relatively high specific thrust typical of a turbojet or moderate-bypass turbofan. At takeoff, however, the valve is turned to a position that inverts, or switches, the paths of the inner and outer streams through the engine. At the same time, auxiliary inlet doors are opened to provide additional airflow, or flow shift, to the engine core. The bypass stream is either mixed downstream of the turbine or is allowed to remain separate, and exits through either a single or dual flow conventional convergent-divergent exhaust nozzle, respectively. During takeoff high-flow operations, the resultant nozzle jet velocities become comparable to those of a low-noise, high-bypass turbofan. All IFV engines in this analysis are designed with maximum dry jet velocities low enough such that no jet noise suppression is required for FAR 36 Stage 3 noise certification. This jet velocity, approximately 1450 ft/s, is determined using the noise analysis tools described below. These valved engines have the advantage of not requiring a heavy, complex, mixer-ejector noise suppression nozzle. This advantage is offset, of course, by the large flow inversion valve that contributes to weight, complexity, and nacelle aerodynamic integration challenges of its own.

The original concept for the IFV engine was a single-spool turbine bypass engine with the flow inversion valve located behind the first stage of the high pressure compressor. Previous studies have shown, however, that a twin-spool TBE can have a larger amount of additional airflow than the single-spool TBE can when the flow inversion valve is located behind the low pressure compressor. Since the IFV engines are designed for low nozzle jet velocities at takeoff, a large flow shift is critical to achieving takeoff thrust levels comparable to other cycles. The turbine bypass feature is therefore eliminated in this study because it degrades the full-power performance of a twin-spool turbojet with a flow inversion valve, and its added complexity offsets any potential part-power benefit.

The cycle design parameters investigated for the IFV engines are the combustor exit temperature, the overall pressure ratio, the fan or low-pressure compressor pressure ratio, and the amount of additional airflow used at takeoff. In addition, the bypass ratio for the TF/IFV cycles is also investigated. Like the other cycles in this investigation, it was discovered that the IFV cycles resulting in the lowest takeoff gross weight aircraft are those having the highest allowable combustor exit temperatures and the highest allowable OPRs. Thus, all IFV cycles presented here have the highest OPR and T_4 allowed by the T_3 and T_{41} limits of the 1993 cycle ground rules: 1710 °R and 3360 °R, respectively. Since the IFV engines were eliminated in the 1993 downselect (as discussed below), no IFV engines are presented for the 1994 downselect study's ground rules.

The relatively poor takeoff thrust of the IFV cycles results in aircraft that are severely field length constrained. Large thrust loadings and small wing loadings, resulting in heavy aircraft, are required to meet the minimum field length requirement (to be discussed below). Consequently, these IFV cycles are designed for the maximum possible flow augmentation at takeoff subject to other cycle constraints. Due to this flow augmentation, the HPC never operates at corrected speeds greater than 86 percent while in low-flow mode. When in high-flow mode, the flow to the core increases and the HPC corrected speed operates at 100 percent. Even when the flow augmentation and thrust are maximized, severe field length penalties cannot be avoided. Therefore, the additional thrust gained through ground run afterburning is assumed. Each of the IFV engines has afterburning data calculated for takeoff ground run operations. The aircraft begins its ground run with its afterburners turned on. The added noise of the afterburners during this phase is alleviated by both ground attenuation and engine-by-engine shielding effects. As the aircraft climbs through the second segment of the takeoff, the afterburners are gradually and automatically turned off so that the jet noise over the measurement points is reduced to acceptable levels. It is assumed that future regulations will allow computer-controlled throttling to occur under the minimum 689-foot altitude restriction described in FAR 25 (ref. 13). The afterburners are later activated once again through the transonic drag rise. As with the other engines, the amount of afterburning is limited by either a 600 °R stream temperature rise or by the maximum allowable nozzle temperature of 2710 °R.

For the twin-spool turbojet IFV cycles, the range of low pressure compressor pressure ratios is limited. For a TJ/IFV with a mixed exhaust, the LPC pressure ratio can vary between 2.0 and 2.4. Pressure ratios outside this range make a static pressure balance in the mixer unachievable. This range is small enough that varying the pressure ratio has a negligible influence on airplane performance. For a TJ/IFV with separate exhaust streams, the LPC pressure ratio must equal 3.0 for the highest specific thrust while still meeting the noise requirements.

The range of fan pressure ratios for the turbofan IFV cycles is similarly limited. For a TF/IFV with a mixed exhaust, both the fan pressure ratio and the bypass ratio become linked. The higher bypass ratios at takeoff needed to meet the noise goals require a low fan pressure ratio to achieve a static pressure balance in the mixer. This mixing requirement also means that there is a minimum low-flow mode bypass ratio that is attainable by this cycle type. This minimum BPR is approximately 0.8. The turbofan IFV with separate exhaust streams, on the other hand, can have any low-flow mode bypass ratio desirable; but, like the separate flow TJ/IFV, the fan pressure ratio for the separate flow TF/IFV must be equal to 3.0. The range of bypass ratios for the IFV engines investigated are shown below.

Engine Designation	Low-Flow BPR	High-Flow BPR
AIV222	0.41	2.22
AIV216	0.35	2.16
AIV209	0.29	2.09
AIV202	0.24	2.02
AIV196	0.19	1.96
AIV189	0.14	1.89
AIV181	0.08	1.81
AIV139	0.00	1.39

All of the bypass ratios above are quoted at SLS conditions. AIV139 is the only TJ/IFV engine evaluated.

The most challenging part of the aeromechanical design of the IFV cycle is the inverting flow valve. Given two concentric flow streams, the IFV flips the inner stream flow to the outer passage and flips the outer stream flow to the inner passage without ever mixing the two streams. In the high-flow mode, when the valve is inverting the flow streams, the high pressure compressor maximum corrected speed is 100 percent. The corrected speed quickly decreases to 85 percent during the transition to the low-flow mode. The transient behavior when converting from high-flow to low-flow mode may cause surging or stalling in either compressor and is one of the critical design issues for IFV engines. Except for the flow inversion valve, the mechanical design of the IFV cycles is similar to the mixed-flow turbofan cycle described above.

Aircraft Analysis

Airframe Design and Sizing

The U.S. HSR airframers, Boeing and McDonnell Douglas, provided the NASA Lewis mission analysis team with sufficient information to model each of their proposed HSCTs under a strict, limited distribution agreement. The general arrangements of each of the planforms are shown in figures 23 and 24. The Boeing model 1080-924 HSCT has a double-cranked delta wing which provides relatively good aerodynamic performance at subsonic cruise and low speed takeoff conditions. The McDonnell Douglas model D-3235-2.4-7A HSCT, with its arrow wing, has a configuration designed with emphasis on the optimization of supersonic cruise aerodynamics. A comparison of some of the major design parameters of each company's HSCT using the 1994 MFTF5000 Lewis turbofan is shown below.

	Boeing	Douglas
Still-Air Range (nm)	5000	5186
MTOGW (lb)	747800	762800
OEW (lb)	288900	328400
Payload (lb)	64890	61500
Passengers	309	300
Overall Length (ft)	313	334
Wingspan (ft)	136	160
Effective Wing Area (ft^2)	7860	10210
SLS Net Thrust (lb)	45400	47900
Aspect Ratio	2.36	2.50
Wing Loading (lb/ft^2)	95.2	74.7
Thrust Loading	0.243	0.251
Subsonic L/D	16.1	14.8
Supersonic L/D	8.4	9.0

The aircraft loadings are given at maximum takeoff weight conditions, and the subsonic and supersonic lift/drag ratios are given at the subsonic and supersonic cruise midpoint aircraft weights, respectively.

The mission and sizing analyses are performed for each aircraft/engine combination using the Flight Optimization System code (ref. 14). The wing and engine sizes are parametrically varied to obtain minimum gross weight, design point aircraft that satisfy the design mission requirements. As the wing and engine vary in size, the aircraft weights and aerodynamics are systematically altered according to accepted methods applicable to high-speed transport aircraft. The aspect ratio remains constant as the wing area changes. This analysis is graphically typified in so-called aircraft sizing "thumbprints," where the effects of various constraining parameters show the required sizes of the engine and wing that result in a minimum gross weight, constrained aircraft. For example, the thumbprint for the 1993 TBE3010 on the Boeing HSCT is shown in figure 25. In this particular case, the vehicle is constrained by the FAR 25 takeoff field length and fuel volume requirements and the engine thrust and wing are sized at 43000 lb and 7935 ft^2, respectively. The constrained airplane's maximum takeoff gross weight is minimized at 744046 lb. In cases where engine and wing sizes can be traded with little or no gross weight penalty, airframers will frequently choose larger wing and smaller engine sizes. This should allow for the less expensive purchase of engines, which are typically priced on a thrust basis, and larger wings often allow for future growth of the airplane. Because of the preliminary nature of this study, no such trades are performed. Aircraft gross weight is the measure of merit assigned to each of the propulsion cycles.

Inputs required for the Flight Optimization System program include the engine data (calculated as described previously), airplane dry weight data and scaling relationships, airplane aerodynamics and scaling relationships, the mission profile, and airplane constraining details. Each is discussed below.

The dry airplane weight scaling relationships are provided by the airframers and are illustrated in figures 26 and 27. The operating empty weight (less the propulsion system weight, which is calculated by the Lewis team as described above) is a function of both the maximum takeoff gross and wing weights. The wing weight, in turn, varies with the wing area and with the propulsion pod weight, both of which change during the sizing process. The changes with respect to pod weight reflect the design requirements of the supporting wing spar. The weight scaling relationships in figures 26 and 27 are presented for the reference pod weights and for a range of wing loadings.

Aerodynamics

The aircraft aerodynamics are also provided by the airframers and are shown in figures 28 and 29. These aerodynamics are also a function of Reynolds number, but are accurate as shown in the figure at altitudes along the trajectory. Low-speed aerodynamics are also provided by each airframer for takeoff trajectory calculations. The pods used in Boeing's and McDonnell Douglas' aerodynamic calculations are Pratt & Whitney's STJ989 TBE and General Electric's D6 Flade engine, respectively. Ideally, these aerodynamics should be scaled with respect to the propulsion pod size and shape. Studies have shown, however (e.g., ref. 15), that if careful consideration is given to the proper nacelle placement, nacelle contours, wing cambering, and wing twist, the overall effect of reasonable pod size and shape variations on the overall airplane aerodynamics can be relatively small. Therefore, in the interest of screening a large number of engine sizes and types in a short time, changes in aerodynamics due to propulsion-airframe integration effects are not considered directly in this study. The throttle-dependent, isolated nacelle installation drags discussed previously, of course, are included in the installed engine data, but the Boeing and McDonnell Douglas nacelle aerodynamics remain unchanged with respect to the original STJ989 and D6 engine pods, respectively. Nevertheless, these propulsion-airframe integration issues are important and are studied in other NASA Lewis in-house efforts (see ref. 16). The study described in this reference shows that incorporating propulsion-airframe integration effects does not affect the propulsion system selections.

Mission Definitions and Constraints

The missions suggested by Boeing and McDonnell Douglas are shown in figures 30 through 32. The Boeing design mission (fig. 30) consists of typical taxi-out, takeoff, and climb segments, followed by an over-water, Mach 2.4 climbing cruise segment. A traditional step-cruise profile typical of subsonic aircraft is not used, since air traffic between 55000 and 65000 feet will be light compared to the subsonic fleet's cruise altitudes. In addition, air traffic control technology will likely be able to handle climbing cruise flight profiles when the HSCT enters service. Typical descent, approach, landing, and taxi-in segments follow, for a still-air range of 5000 nm. A reserve mission, consisting of a six percent of trip fuel contingency allowance, a 260 nm subsonic alternate airport diversion, and a 30-minute hold, is also included. The design mission occurs with the full payload complement of 309 passengers. To prevent sonic boom noise, the regulations of reference 17 prohibit supersonic flight of civil aircraft over U.S. land. For this reason, and for the need to provide a more "typical" HSCT mission for economic direct operating cost calculations, an off-design, "economic" mission which includes a subsonic cruise leg is also analyzed. This economic mission, shown in figure 31, includes a 600 nm outbound cruise leg at Mach 0.90, has a reduced, 201-passenger complement, and has a reduced range of 3436 nm. Performing the subsonic cruise leg on the outbound side of the supersonic cruise leg requires less fuel and is more optimistic than the reverse, since the airplane is therefore lighter during the remaining climb to supersonic cruise.

The McDonnell Douglas design mission (fig. 32) uses a 300-passenger complement and incorporates an overland, Mach 0.95 outbound subsonic leg. Its range is 5000 nm with headwinds, which is equivalent to a still-air distance of 5186 nm. A reserve mission, consisting of a three percent block fuel contingency allowance and a 200 nm subsonic alternate airport diversion, is also included. Climb and descent altitude-Mach number profiles suggested by the airframers are shown in figures 33 and 34.

Every airplane sized in this study is constrained to an 11000 foot, 86 °F FAR 25 field length to allow operations out of most of the world's major airports. The approach velocity is limited to 155 keas. A minimum potential rate of climb constraint is also applied to the entire climb profile. This minimum value is 500 and 1000 ft/min for the Boeing and McDonnell Douglas HSCTs, respectively. Each HSCT's wing area is also constrained by the amount of available fuel volume for its design mission. The wing area and fuel volume relationships are provided by the manufacturers. In addition to these constraints, each HSCT must also comply with the FAR 36 Stage 3 noise regulations. Although no domestic noise regulations exist for future supersonic commercial aircraft, the FAA has stated its intentions (ref. 18) to restrict these aircraft to FAR 36 Stage 3 noise levels. The takeoff noise constraining process is described below.

Takeoff and Noise Analysis

Operational Procedures

Applying the methods of reference 14, a detailed takeoff analysis is performed for each HSCT using the aircraft physical characteristics and low-speed aerodynamics supplied by the airframers. Since the FAR 36 noise certification field length need not necessarily coincide with the FAR 25 performance field length, this constraint is relaxed from 11000 feet to 12000 feet for noise certification evaluations. The arrangement of the Effective Perceived Noise Level (EPNL) measurement points used in FAR 36 certification is shown in figure 35. Approach power settings are not available and approach noise levels are not calculated. The noise constraining process for each aircraft is determined only by the sideline and community noise levels.

The regulations of reference 2 specify the operational procedures that may be used for takeoff. For a four-engine aircraft, the throttle setting during takeoff must remain constant from the point of brake release until the aircraft reaches an altitude of at least 689 feet. Above this altitude, with all engines operating, the thrust may be reduced to a level that maintains a four percent minimum climb gradient. This standard throttle cutback is designed to reduce the noise perceived by the community observer (see fig. 35). During the ground roll, the throttle may be set at either a part-power setting or at maximum power. Both of these tactics can be used to reduce noise.

A simple part-power takeoff reduces noise directly through quieter engine operation. The part-power setting used in this type of takeoff is determined by the thrust necessary to achieve the 12000 foot field requirement using the minimum allowable rotation velocity. A maximum dry power takeoff, although producing more direct engine noise, may indirectly generate lower effective perceived noise levels by delaying rotation until the 12000 foot field limit is reached. This allows the aircraft to build up greater speeds on the runway, achieve a higher climbout velocity, and increase its rate of climb. The EPNLs can be reduced because passage by the sideline and community measurement points occurs at higher altitudes. Further noise reduction for the community observer occurs when this higher climbout velocity allows the pilot to cutback to a lower power setting. Other, smaller, benefits of a high-speed, delayed rotation takeoff include noise reduction due to reduced aircraft-observer dwell time, reduced frequency of the received noise due to increased Doppler shift, and greater forward-velocity jet noise attenuation (refs. 19 and 20).

Note that even an HSCT that is field length constrained at 11000 feet for performance reasons may take some advantage of part-power or delayed rotation takeoffs due to the extra one thousand feet of available field length used in noise certification. The TBE HSCT shown previously in figure 25 is one example of this. Conversely, aircraft with relatively low specific thrust engines are typically sized to meet climb constraints and therefore may have very short performance field lengths. These aircraft, such as the Boeing HSCT with the MFTF2000, can take much greater advantage of part-power or delayed rotation 12000 foot takeoffs. Further, this engine is already inherently much quieter than its high specific thrust relative, the MFTF5000. When performing advanced takeoff procedures (discussed below), this engine requires very little mixer-ejector nozzle noise suppression at all.

Some advanced takeoff procedures are proposed that do not yet strictly conform to current FAA safety and noise certification regulations. One such procedure, called the auto-throttle, or programmed lapse rate (PLR) maneuver, is considered in this study. FAR 36's requirement of maintaining a constant throttle setting under the 689 foot altitude limit is thought to be avoidable if computer-controlled throttle scheduling is used. After the 35 foot commercial obstacle is cleared, but before the conventional throttle cutback takes place, the throttle setting is automatically reduced to lessen the sideline noise. The final level and rate of this PLR thrust reduction are considered to be free variables in this study. Their optimization for minimum total EPNL production is discussed below. The level to which the throttle may be reduced is limited by the second- and final-segment climb gradient criteria. It will be shown that the PLR maneuver can greatly reduce the problematic sideline noise levels and considerably lower the amount of overall nozzle noise suppression required. This noise reduction, however, is not without consequences. The PLR throttle reduction adversely affects the aircraft's rate of climb and forces the aircraft to pass over the community noise measurement point at a lower altitude than it would if a standard takeoff had been performed. For this reason, PLR maneuvers, despite their sideline noise reduction advantages, are in direct conflict with keeping community noise levels low.

Since the 2005 subsonic fleet is expected to be, on average, more than 5 EPNdB under current FAR 36 Stage 3 regulations, unfavorable comparisons will undoubtedly be made with the HSCT. Many think that the HSCT should not be designed with a low-suppression nozzle to be used in conjunction with a PLR takeoff. For many propulsion cycles, however, meeting the sideline noise requirement is a serious challenge, and the advantages of a PLR are not easily dismissed. For these reasons, both standard and advanced takeoffs are calculated in this study. Each is described below.

Standard Takeoff

A standard takeoff is defined in this study as one which uses only a fixed, part-power initial throttle setting and a throttle cutback. The fixed, part-power throttle setting is determined by the ground run thrust derate level required to achieve a 12000 foot field length using the minimum rotation velocity. This throttle setting remains constant throughout the ground run, rotation, liftoff, obstacle clearance, and first constant climb segments of the takeoff. A throttle cutback is then performed. Although regulations governing four-engine aircraft allow cutbacks at altitudes as low as 689 feet, the cutbacks performed in this study occur at a point 19000 feet downrange from the point of brake release. At this point, depending on the amount of ground run derate, typical Boeing HSCTs are generally at altitudes of about one thousand feet. Even though a late cutback increases sideline noise somewhat (ref. 21), it is used because it improves the rate of climb throughout the second constant climb segment to the benefit of the community noise observer. The trajectory and throttle history of the Boeing TBE3010 HSCT using a standard takeoff is shown in figure 36. The ground run derate for this configuration is four percent less than SLS maximum dry thrust. The throttle in this case is cut back to 61 percent of maximum dry net thrust at ten percent per second.

Advanced Takeoff

An advanced takeoff is defined in this study as one which uses both part-power derate and delayed rotation ground run tactics and combines them with PLR and throttle cutback maneuvers. The effects of the derated throttle setting and the amount of delayed rotation overspeed must combine to yield no more than a 12000 foot field length. The ground run derate and delayed rotation speed of the TBE3010 Boeing HSCT in figure 36, for example, are three percent less than SLS maximum dry net thrust and 30 percent more than the aircraft stall speed, respectively. The PLR is considered to consist of two free variables: the thrust lapse and the thrust lapse rate. The PLR shown in figure 36, for example, has a lapse rate of two percent per second and lapses to a level of 78 percent of SLS maximum dry net thrust. A throttle cutback to 59 percent thrust at a downrange distance of 19000 feet is performed as before. Note that due to the greater climbout velocity achieved through runway overspeeding, the advanced takeoff method allows a lower, quieter throttle cutback power setting to be used than the standard takeoff method's setting. Both trajectories are constrained to the four percent second-segment climb gradient requirement. These values of derate, delayed rotation overspeed, and thrust lapse and lapse rate above are the optimum values for minimum noise production of the TBE3010 Boeing HSCT. The actual amounts of ground run derate and overspeed, though linked through the field length requirement, are systematically varied and numerically optimized along with the PLR's two lapse variables to yield minimum overall noise production as described below.

Noise Evaluation

The takeoff trajectory, aircraft orientation, primary jet properties, and throttle history data for each HSCT are passed to the noise analysis portion of the mission analysis code derived from reference 22. Jet noise is calculated for each propulsion system using the Motsinger-Sieckman single-stream convergent jet noise model (ref. 23). This jet noise model, which is incorporated into the mission analysis code specifically for this study, is chosen for its accuracy in predicting high pressure ratio jet noise. The jet noise is corrected for spherical spreading, atmospheric attenuation (ref. 24), extra ground attenuation (ref. 25), and shielding effects (ref. 22). The resulting tone-weighted perceived noise level (PNLT) time traces for the TBE Boeing HSCT trajectories of figure 36 are shown in figure 37. Note that the theoretically continuous sideline is approximated by an array of observers at discrete intervals of one thousand feet along the sideline. These noise levels are numerically integrated on a logarithmic basis with respect to time to yield the EPNLs at the noise measurement points. The greatest of these sideline EPNLs is the sideline noise defined by FAR 36. Note that the sideline noise for the TBE HSCT occurs at the ninth sideline observer location for both the standard and advanced takeoff profiles. The PNLT trace at this position is integrated with respect to time to yield sideline EPNLs of 119.3 and 116.1 EPNdB for the standard and advanced profiles, respectively. The community EPNLs are coincidentally identical at 118.9 EPNdB. The overall results for the TBE profiles shown in figure 37 are summarized in tables 4 and 5. Note that the gross weight-dependent FAR 36 Stage 3 rule is slightly different due to the difference in weight between the two aircraft.

Optimization of the advanced takeoff profile for minimum sideline and community EPNLs is conducted using the individual procedures discussed above. The ground roll derate, thrust lapse, and thrust lapse rate are parametrically varied by a Hooke and Jeeves optimization algorithm modified with a gradient search correction. The level of delayed rotation used in each optimization iteration is determined by the amount of throttle derate used and the 12000 foot field requirement. The sideline and community EPNL exceedance levels relative to the rule for the TBE Boeing HSCT are graphically shown in figures 38 and 39, respectively. A ground run derate of three percent is pictured. It can be seen from figure 38 that the more severe PLR maneuvers greatly reduce the sideline noise. The community noise levels of figure 39, however, are adversely affected by these same PLR maneuvers. An overall required suppression level, defined as the maximum of either sideline or community EPNLs, is therefore the object function necessary for optimization with respect to FAR 36. This parameter, shown in figure 40, graphically illustrates the tradeoff of the PLR maneuver with respect to the two noise measurements. Overlaid on the object function is the optimization path computed by the modified Hooke and Jeeves algorithm. The trajectory defined by the final, optimized values of derate, delayed rotation, and PLR is checked to ensure that the minimum climb gradients required by the regulations of reference 2 are not violated.

Since jet noise is the only noise source calculated in this study, an additional two decibels are added to each aircraft's nozzle noise suppression requirement to account for propulsion noise sources other than the jet and to provide a noise sizing assurance margin for each airplane. The jet noise suppression requirements for the TBE of tables 4 and 5, for example, are 18.9 and 15.8 dB for the standard and advanced takeoff profiles, respectively. For aircraft with engines equipped with mixer-ejector nozzles, subsequent sizing iterations are necessary and are calculated using the results of each previous noise calculation. This iteration process is illustrated in figure 41. For each iteration, aircraft sizing thumbprints are prepared using engine and aircraft data, a performance-constrained aircraft is designed, and detailed takeoff and noise analyses are performed. Since the nozzle mass flow augmentation used for the first iteration is based on the primary stream's maximum dry jet velocity (via fig. 16), the amount of noise suppression the mixer-ejector nozzle provides is always too great for takeoffs using noise abatement procedures with lower jet velocities. Ideally, a specific mass flow augmentation value for each engine is required that is commensurate with suppressing the amount of noise generated. The iteration on flow augmentation is considered necessary. Using an augmentation that is too low would violate noise requirements, while using an augmentation that is too high would unnecessarily penalize the aircraft with excessive nozzle weight, boattail drag, and more complex airframe integration problems. This ideal mass flow augmentation is derived iteratively using the mixer-ejector severity model relationship to the primary jet velocity shown in figure 16. This primary jet velocity, in turn, is derived analytically from the sideline EPNL-jet velocity relationship determined by the jet noise analysis of reference 23. Convergence, thankfully, is quick: no more than three sizing iterations are typically required before the appropriate amount of mass flow augmentation and noise suppression is achieved. Note that after the first iteration, the primary jet velocity used for the nozzle model calculations is no longer the actual, physical primary jet velocity, but is rather an "effective," or "average" primary jet velocity whose magnitude is that which generates the EPNLs calculated at the noise measurement points. The tacit assumption in this method is that the mixer-ejector nozzle's assumed noise suppression capability is independent of the primary jet velocity's variations with throttle setting. This assumption is borne out in many recent nozzle acoustic tests, but as the design of mixer-ejector nozzles becomes more finely calibrated to primary stream conditions, this assumption may ultimately prove to be flawed. Ideally, in addition to mass flow augmentation, the nozzle noise suppression's dependency on throttle setting should be included. Such information, however, is not available at the time of this writing.

Flade Engine Considerations

The Flade-engined HSCTs' unique noise sizing process is illustrated in figure 42. Unlike the mixer-ejector nozzles, whose noise suppression ability is an adjustable variable depending on the amount of flow augmentation assumed, the Flade nozzle is assumed to be capable of delivering a fixed, limited amount of suppression. This level of suppression, shown in figure 43, is based on General Electric's studies and is assumed to be a function of the mixed jet velocity of the flade and primary streams. Flade-engined HSCTs have a distinct disadvantage relative to HSCTs with mixer-ejector nozzles. If the amount of flade suppression is not adequate to suppress the noise to acceptable levels, the entire Flade engine must be sized larger than that required by simple performance requirements. These oversized engines are then throttled to a greater degree during takeoff to reduce the EPNLs. The iteration on engine size proceeds by following the locus of minimum gross weight increases with respect to increasing engine size until FAR 36 is satisfied. This will be shown to be an inefficient method to reduce noise. In general, with mixer-ejector nozzle weights and dimensions determined by the model illustrated in figures 17 through 21, the ability to design the level of noise suppression into the airplane through the nozzle is always preferable to reducing the noise through oversizing the engines. Indeed, as shown below, the increased propulsion weights and corresponding increased gross weights of Flade HSCTs due to oversized engines make all but one of the Flade HSCTs unreasonably heavy.

Results and Discussion

Results for each of the propulsion systems evaluated are presented in tables 6 through 46.

The maximum takeoff gross weight results for the 1993 turbojet and TBE Boeing HSCTs are shown in figures 44 and 45. Note that for the TBE, there is virtually no gross weight penalty in reducing the design combustor exit temperature from the maximum 3489 °R (TBE3010) to 3309 °R (TBE3021). The cooler TBE's specific thrust penalty is offset by its lower specific fuel consumption rates and its smaller, lighter, mixer-ejector nozzle. At design combustor temperatures less than 3309 °R, however, the airplane requires increasingly larger engines to satisfy its thrust requirements and the gross weight begins to increase. The dramatic effect of the advanced takeoff procedure on the noise suppression requirement can be seen in figure 45. The nozzle noise suppression requirement for the TBE3010 Boeing HSCT, for example, can be reduced from 18.9 to 15.8 dB by employing the advanced takeoff procedures described above. The mixer-ejector flow augmentation requirement, which falls from 126 to 74 percent, results in an aircraft gross weight reduction of 15000 pounds. The benefits of a PLR advanced takeoff for the TBE are clear. The influence of the design combustor exit temperature on noise production is dramatic as well. The noise suppression requirement drops 1.5 and 3.4 dB over the temperature range investigated for the standard and advanced takeoff procedures, respectively.

The increased fuel flow and added weight of the afterburners adversely affects the transonic afterburning TBEs. Gross weight penalties of about 4000 pounds due to transonic afterburning can be seen in figures 44 and 45. Even the lower temperature, lower specific thrust TBEs have sufficient thrust to climb through the transonic drag rise without the aid of an afterburner.

The benefit of the turbine bypass feature is clear. The reference turbojets shown in figure 44 have gross weights over 30000 pounds more than the corresponding TBEs. Interestingly, however, due to their considerably poorer SLS thrust, the high-temperature turbojets shown in figure 45 require much less noise suppression than the high-temperature TBEs.

The maximum takeoff gross weight results for the 1993 and 1994 MFTFs are shown in figures 46 through 53. The influence of bypass ratio and maximum allowed T_{41} for the 1993 MFTFs using the Boeing HSCT is shown for both standard and advanced takeoff procedures in figures 46 and 47. Minimum gross weight aircraft are achieved in this study by designing the highest temperature and lowest bypass turbofans possible. A mixer-ejector weight model that more conservatively penalizes large mass flow nozzles, however, can easily force the gross weight minimum towards somewhat larger bypass ratios. Optimum bypass ratio selection is also heavily affected by boattail drag models, mission requirements, and airplane characteristics. The noise impact of these 1993 MFTFs is shown in figure 48. Note that for the Boeing HSCT, the best 1993 turbofan (MFTF5093) enjoys 23000 pound gross weight and 1.9 dB noise suppression advantages over the best 1993 TBE.

Unlike the TBEs, the lower specific thrust MFTFs generally have more difficulty climbing through the higher drag of the transonic regime. It is therefore possible for the MFTFs to benefit from transonic afterburning while the TBEs do not. The increasing gross weight benefit of transonic afterburning with increasing bypass ratio for the 1993 turbofans using the Boeing HSCT is shown in figure 49.

The influence of the more conservative 1994 cycle ground rules on the MFTF is shown in figure 50. The 4.6 fan pressure ratio MFTF carries more than a 25000 pound gross weight penalty due to the lower maximum allowable T_3 and T_{41} requirements (see table 1).

The results of airplane selection on the 1994 turbofans are shown in figures 51 through 53. Although the aerodynamics, empty weights, scaling models, constraining requirements, and design mission profiles of the Boeing and McDonnell Douglas HSCTs differ, their calculated gross weights are remarkably similar. The McDonnell Douglas HSCT has lower gross weights than the Boeing HSCT when designed with the higher bypass MFTFs (figs. 51 and 52). This is primarily due to the presence of the subsonic cruise leg in the McDonnell Douglas design mission. The airplane is able to take better advantage of the higher bypass turbofans' good subsonic performance. The advantages of good low-speed aerodynamics can be seen in figure 53. The Boeing HSCT, with its superior lift-drag ratio over a greater range of angle of attack, is able to take better advantage of advanced takeoff procedures than the McDonnell Douglas HSCT. The noise suppression requirement for the MFTF5094 HSCTs using a standard takeoff profile is identical at 18.8 dB. In an advanced takeoff, however, a much more effective PLR can be implemented with Boeing's better low-speed aerodynamics. This results in a 1.6 dB reduction in the nozzle suppression requirement for the MFTF5094 Boeing HSCT.

The maximum takeoff gross weight results for the 1993 VCE Boeing HSCTs are shown in figures 54 and 55. Like the turbofans, the lowest inner bypass VCE produces the lowest gross weight aircraft. Unlike the MFTF, however, the better transonic air-handling qualities of the VCE negate any benefit of transonic afterburning. Even at the relatively high inner bypass ratio of 0.80, a level at which the turbofan profits from transonic afterburning, the additional weight and fuel expenditure of the afterburner reverses any advantage of afterburning for the VCE. Note that the gross weight of the VCE701510 HSCT is nearly identical to the weight of the low bypass MFTF5093 HSCT. Although capable of slightly better performance than the turbofan, the VCE has a larger propulsion pod weight that results in 1.5 and 1.2 percent gross weight penalties for the standard and advanced takeoff procedures, respectively.

Each of the eight 1993 Flade engines are initially analyzed from a simple performance standpoint using the Boeing HSCT without a noise analysis. The special noise constraining analysis for the Flade cycles described above is then performed. This noise analysis is applied to the Flade HSCTs in order of increasing gross weight until a minimum gross weight noise-constrained airplane is found. Due to the limited noise suppression capabilities of the unique fluid acoustic shield Flade nozzle, however (see fig. 43), not all of the Flade cycles can meet the FAR 36 Stage 3 noise requirements. The F393 and F793 Flade HSCTs, for example, have the lowest gross weights without a noise constraint, but are unable to meet the noise requirements without incurring excessive engine oversizing gross weight penalties. The F193 HSCT, although ranked third in gross weight for Flades without noise constraints, has the lowest noise-constrained gross weight of all eight Flade cycles considered. This performance is achieved by implementing an advanced takeoff procedure with PLR, delayed rotation, and ten percent engine oversizing. This analysis results in a 748373 lb aircraft that is 6.1 percent heavier than the 1993 MFTF5093 Boeing HSCT using advanced takeoff procedures. Due to the tedium involved in the noise analysis process, the remaining five heavier Flade HSCTs remain unconstrained with respect to the noise requirement. None of the Flade engines are analyzed using the

1994 cycle ground rules, transonic afterburning, or the McDonnell Douglas airplane.

The maximum takeoff gross weight results for the 1993 IFV Boeing HSCTs are shown in figure 56. Like the other cycles evaluated in this study, the highest specific thrust TF/IFV results in the lowest gross weight aircraft. The AIV181 Boeing HSCT has a gross weight of 728173 lb, which is 3.2 percent greater than the 1993 MFTF5093 Boeing HSCT using advanced takeoff procedures, and only one percent greater than the MFTF5093 Boeing HSCT using a standard takeoff. The TJ/IFV HSCT, due to its reduced versatility relative to the TF/IFV HSCTs, has a 19 percent higher gross weight than the AIV181 HSCT. None of the IFV engines are analyzed using the 1994 cycle ground rules or the McDonnell Douglas airplane.

A maximum takeoff gross weight, design mission block fuel weight, and economic mission block fuel weight comparison is shown in figure 57 for the best of each of the 1993 cycles evaluated on the Boeing HSCT using advanced takeoff procedures. Note that the cycle ranking is similar regardless of which weight measure of merit is chosen. The low bypass MFTF5093 HSCT is the lowest weight aircraft and has the best fuel economy of the group. A similar weight comparison for aircraft using standard takeoff procedures is shown in figure 58. The Flade and IFV HSCTs, which exclusively use only advanced takeoff procedures as explained above, are not represented in the figure.

Emissions comparisons of the same engines are shown in figures 59 and 60. The emission indices shown are taken at the mid-weight supersonic cruise point of the Boeing HSCT design mission. A new emissions parameter called specific NO_X is introduced. Defined as the amount of cruise NO_X generated per passenger mile, it delineates the effect of both aircraft fuel consumption performance and payload-carrying capabilities. Using the generic HSR combustor emissions model described previously, cruise emission indices ranging from 6.7 to 8.5 lb/klb are indicated for the HSCTs using advanced takeoff procedures. These indices are greater than the HSR combustor emission index goal of 5 lb/klb. A fleet of 600 HSCTs with combustors operating at the emissions goal performance levels will likely have little or no effect on the steady-state amount of atmospheric ozone (ref. 26). One method of reducing these emission indices to the goal value is to reduce the design T_4 of the cycles. A gross weight and emissions sensitivity of the 1993 TBEs and MFTFs across the temperature range investigated is shown in figure 61. Note that for a given temperature reduction, the MFTF is able to reduce cruise emissions much more effectively than the TBE. Another method of reducing these emission indices comes as a natural consequence of adopting the newer, more conservative, 1994 cycle ground rules. These ground rules, which reduce both T_4 and T_3, lower the supercruise emission index of the 4.6 FPR MFTF from 8.2 lb/klb to the near-goal performance value of 5.7 lb/klb.

Concluding Remarks

Although maximum gross weight, fuel burned, noise, and emissions data are very important in selecting the primary and secondary propulsion systems, other effects that are not directly evaluated in this study must also be considered. Engine cost, operating life, reliability, maintainability, manufacturing complexity, versatility, risk, operating cost, and airframe integration considerations all contribute to the downselect process. Many of these issues are addressed in various NASA-sponsored studies throughout industry.

For example, the use of afterburning is rejected by the NASA/industry propulsion downselect team due to its high temperature material requirements and impact on component life. This decision is made despite studies that indicate modest performance benefits in some low specific thrust applications. The valved engine HSCTs, which require afterburning thrust performance during the takeoff ground run to shorten their exceptionally long field lengths, are severely penalized by the lack of afterburners. Afterburning jet noise produced during the ground run and transient performance during valve clocking movements are also concerns. Although capable of respectable performance (see e.g., fig. 57), the afterburning issue, combined with their somewhat unconventional design and element of risk, effectively eliminates the IFV engines from contention.

Added complexity is also an undesirable characteristic. Although the VCE is capable of good performance, its additional aeromechanical requirements are difficult to justify for an HSCT application. Although the VCE's thrust and fuel consumption performance is slightly better than the MFTF's, it is the VCE's additional engine weight that contributes to its overall heavier aircraft weight. For these reasons, the VCE is dropped from the competition.

Interestingly, unlike the IFV and VCE, the TBE is the only cycle analyzed here that is eliminated from consideration by using aircraft sizing and noise data alone. This conclusion was established using these criteria as early as 1991 (ref. 3). Although the TBE is the simplest of the concepts considered, the MFTF is only slightly more complex and holds a three percent gross weight advantage over the TBE. Due to the difficulty involved in suppressing the noise of its high pressure primary flow stream, the TBE also has a poor ability to cope with the possible introduction of more restrictive future noise regulations.

The primary propulsion concept selected by the NASA/industry propulsion team for further study is the MFTF. Its good performance, resulting in low aircraft weights, and low risk and complexity lead to the best direct operating costs of any propulsion system considered to date. And since its design bypass ratio can be varied, its performance can be adjusted somewhat to more effectively match both mixer-ejector nozzle and aircraft design requirements.

The secondary propulsion concept selected is the Flade engine with a fluid acoustic shield nozzle. The Flade cycle represents a reasonable balance of design compromises and pursues distinctly different technologies than the mixer-ejector propulsion systems. Should the mixer-ejector design of the MFTF provide insufficient noise suppression, the Flade cycle provides an alternative technology path to follow.

Continued studies of both of these engines, as well as other concepts, are needed to secure our stake in the revolutionary supersonic aircraft of the future.

References

1. Fishbach, L.; Stitt, L.; Stone, J.; and Whitlow, Jr., J.: *NASA Research in Supersonic Propulsion - A Decade of Progress.* NASA TM 82862, 1982.
2. *Noise Standards: Aircraft Type and Airworthiness Certification.* FAR, Part 36, Federal Aviation Administration, 1974. (Consolidated Reprint Aug. 12, 1985.)
3. Seidel, J.; Haller, W.; and Berton, J.: *Comparison of Turbine Bypass and Mixed Flow Turbofan Engines for a High-Speed Civil Transport.* AIAA Aircraft Design Systems and Operations Meeting, AIAA 91-3132, 1991.
4. Berton, J.; Haller, W.; Seidel, J.; and Senick, P.: *A NASA Lewis Comparative Propulsion System Assessment for the High-Speed Civil Transport.* First Annual High-Speed Research Workshop, NASA Conference Publication 10087, Part II, 1991.
5. Plencner, R.; and Snyder, C.: *The Navy/NASA Engine Program (NNEP89) - A User's Manual.* NASA TM 105186, 1991.
6. Klann, J.; and Snyder, C.: *NEPP Programmer's Manual (NASA Engine Performance Program), Volumes I and II.* NASA TM 106575, 1994.
7. Onat, E.; and Klees, G.: *A Method to Estimate Weight and Dimensions of Large and Small Gas Turbine Engines.* NASA CR 159481, 1979.
8. Kowalski, E.; and Atkins, Jr., R.: *A Computer Code for Estimating Installed Performance of Aircraft Gas Turbine Engines, Volumes I, II, and III.* NASA CRs 159691, 159692, and 159693, 1979.
9. Los Angeles Aircraft Division of Rockwell International Corporation: *Methods for Comparative Evaluations of Propulsion System Designs for Supersonic Aircraft.* NASA CR 135110, 1976.
10. Schmidt, A.: *Preliminary Weight Estimation of Engine Section Structure.* SAWE Paper No. 1311, Index Category No. 23, 1979.
11. Moses, P.; and Jones, S.: *Internally Pressurized Structural Synthesis and Optimization Code.* Documentation, first updated release: April 24, 1987, NASA LaRC.
12. Craidon, C.: *User's Guide for a Computer Program for Calculating the Zero-Lift Wave Drag of Complex Aircraft Configurations.* NASA TM 85670, 1983.
13. *Airworthiness Standards, Transport Category Airplanes.* FAR, Part 25, Federal Aviation Administration, March, 1984.
14. McCullers, L.: *Aircraft Configuration Optimization Including Optimized Flight Profiles.* Proceedings of the Symposium on Recent Experiences in Multidisciplinary Analysis and Optimization, NASA CP 2327, April 1984.
15. Barnhart, P.: *A Supersonic Through Flow Fan Engine Airframe Integration Study.* NASA CR 185140, 1989.
16. Baumgarten, W.: *Propulsion / Airframe Aerodynamic Integration Effects for a Mach 2.4 High-Speed Civil Transport.* Limited Distribution NASA TM 106673, 1995. Date for general release: July, 1999.
17. *General Operating and Flight Rules.* FAR, Part 91, Federal Aviation Administration, 1974. (Consolidated Reprint with changes 1 through 67 as of May 1, 1986.)
18. *Civil Supersonic Aircraft Noise Type Certification Standards and Operating Rules; Notice of Proposed Rulemaking.* Federal Register vol. 55, no. 104, May 30, 1990.
19. Stone, J.: *Interim Prediction Method for Jet Noise.* NASA TMX-71618, 1975.
20. Stone, J.; Groesbeck, D.; and Zola, C.: *An Improved Prediction Method for Noise Generated by Conventional Profile Coaxial Jets.* NASA TM 82712, AIAA-81-1991, 1981.
21. Olson, E.: *Advanced Takeoff Procedures for High-Speed Civil Transport Community Noise Reduction.* SAE Paper No. 921939, 1992.
22. Clark, B.: *A Computer Program to Predict Aircraft Noise Levels.* NASA TP 1913, 1981.
23. Gliebe, P.; Motsinger, R.; and Sieckman, A.: *High Velocity Jet Noise Source Location and Reduction, Task 3 - Experimental Investigation of Suppression Principles.* Report No. FAA RD 76-79, III-I (R78AEG27), 1978.
24. *Standard Values of Atmospheric Absorption as a Function of Temperature and Humidity.* Aerospace Recommended Practice 866, 1964, SAE.
25. *Method for Calculating the Attenuation of Aircraft Ground to Ground Noise Propagation during Takeoff and Landing.* Aerospace Information Report 923, Aug. 15, 1966, SAE.
26. Shaw, R.; Gilkey, S.; and Hines, R.: *Engine Technology Challenges for a 21st Century High-Speed Civil Transport.* NASA TM 106216, 1993.

Appendix: Nomenclature

Symbol	Description
A_9	Nozzle exit area
A_{10}	Maximum propulsion pod cross-sectional area
A_C	Inlet capture area
A_O	Inlet streamtube area
A_{Oi}	Inlet streamtube area plus bleed area
AB	Afterburning
AN^2	Blade root centrifugal stress parameter
AR	Blade aspect ratio
BPR	Bypass Ratio
CD	Convergent-Divergent (Laval) nozzle
CDFS	Core-Driven Fan Stage
C_{DSP}	Inlet spillage drag coefficient
$C_{D\beta}$	Nozzle boattail drag coefficient
CET	Combustor Exit Temperature
C_M	Mixer momentum coefficient
C_V	Nozzle velocity coefficient
C&A	Controls and Accessories
D_{max}	Maximum propulsion pod diameter
E	Mixer effectiveness
EI	Emissions Index
ESAD	Equivalent Still Air Distance
F_G	Gross Thrust
F_N	Net Thrust
HPC	High Pressure Compressor
HPT	High Pressure Turbine
ISA	International Standard Atmosphere
IFV	Inverting Flow Valve
keas	equivalent airspeed in knots
L_{bare}	Bare engine length
L/D	Lift/Drag ratio
L/H	Length/height ratio

Symbol	Description
LHV	Fuel Lower Heating Value
LPC	Low Pressure Compressor
LPT	Low Pressure Turbine
M_∞	Freestream Mach number
ME	Mixer-Ejector nozzle
MFA	Mixer-Ejector nozzle Mass Flow Augmentation
MFTF	Mixed Flow Turbofan
MTOGW	Maximum Takeoff Gross Weight
N_{bl}	Number of blades
NPR	Nozzle Pressure Ratio
PAX	Passengers
PR	Pressure Ratio
PROC	Potential Rate of Climb
RF	Range Factor
R_h/R_t	Hub-to-tip ratio
S	Effective wing reference area
SLS	Sea Level Static
t_r	Combustor residence time
T_3	Compressor exit total temperature
T_4	Combustor exit total temperature
T_{41}	Turbine rotor inlet total temperature
T_8	Nozzle throat total temperature
TBE	Turbine Bypass Engine
TJ	Turbojet
TO	Takeoff
TOGW	Takeoff Gross Weight
TSFC	Thrust Specific Fuel Consumption
U_{tip}	Blade tip velocity
$U_{tip\ corr}$	Corrected blade tip velocity
V_{comb}	Combustor throughflow velocity
V_{JP}	Hypothetically expanded primary jet velocity
VABI	Variable Area Bypass Injector

Symbol	Description
VCE	Variable Cycle Engine
w_{corr}	Corrected Airflow
w_l/w_t	Combustor liner to total flow ratio (Fraction of air not heated)
W	Weight
β	Nozzle boattail angle
$\Delta P/P$	Pressure drop
η	Inlet total pressure recovery
η_{ad}	Adiabatic efficiency
η_b	Burner efficiency
η_p	Polytropic efficiency
λ	Turbine loading parameter
ρ	Material density
σ	Turbomachinery blade solidity
σ_d	Disk stress

Table 1.—Abridged HSR Cycle Design Ground rules (Thermodynamic)

Component	Specification	Specification Revision, 1/94
Inlet	w_{corr}= 650 lb/s @ SLS, Recoveries given in Figs 8-10.	
Fan/LPC	η_p = 0.895 @ SLS	
CDFS	η_p = 0.845 @ SLS	
HPC	η_p = 0.920 @ SLS $T_{3\ max}$ = 1250 °F (1710 °R)	 $T_{3\ max}$ = 1200 °F (1660 °R)
Combustor	η_b = 0.999 LHV = 18,500 BTU/lb $\Delta P/P$ = 0.060 w_l/w_t = 0.14	
HPT	η_{ad} = 0.920 (Peak) $T_{41\ max}$ = 2900 °F (3360 °R)	 $T_{41\ max}$ = 2800 °F (3260 °R)
LPT	η_{ad} = 0.925 (Peak)	
Mixer	E = 0.40 (Unforced mixers) E = 0.80 (Forced mixers) C_M = 0.95	
Ducts	$\Delta P/P$ = 0.010 (duct, splitter, or VABI) $\Delta P/P$ = 0.005 (turbine exit frame) $\Delta P/P$ = 0.040 (IFV) $\Delta P/P$ = 0.020 (VCE/Flade bypass) $\Delta P/P$ = 0.020 (IFV bypass)	
Augmentor	η_b = 0.920 $\Delta P/P$ = 0.020	
Nozzles	$T_{8\ max}$ = 2250 °F (2710 °R) C_V = 0.982 (conventional CD Nozzle) $C_V = C_V(NPR)$ (ME nozzles, see fig. 22)	$T_{8\ max}$ = 1700 °F (2160 °R)
Parasitics	200 HP high spool power extraction 1.0 lb/s customer bleed (ref.: 650 lb/s airflow)	

Table 2.—Abridged HSR Cycle Design Ground rules (Flowpath/Mechanical/Weight)

Component	Specification
Inlet	See figs. 11 and 12
Fan/LPC	PR_{max} = 2.65 (for single stage) PR_{max} = 4.00 (for two stages) $U_{tip\ corr\ max}$ = 1720 ft/s $U_{tip\ max}$ = 1800 ft/s $M_{in\ max}$ = 0.625 $M_{out\ max}$ = 0.500 $R_h/R_{t\ min,\ entrance}$ = 0.37 σ = 0.95 N_{bl} = 30 to 35 AR_{in} = 3.5 AR_{out} = 2.5 ρ = 0.12 lb/in^3
CDF	PR_{max} = 2.10 (for single stage) $U_{tip\ corr\ max}$ = 1650 ft/s $U_{tip\ max}$ = 1865 ft/s $M_{in\ max}$ = 0.550 $R_h/R_{t\ min,\ entrance}$ = 0.40 σ = 0.90 N_{bl} = 40 to 55 AR_{in} = 2.0 to 2.5
HPC	PR_{max} = 1.80 (for single stage) $U_{tip\ corr\ max}$ = 1600 ft/s $M_{in\ max}$ = 0.400 (0.550 for IFV engines) $M_{out\ max}$ = 0.350 $R_h/R_{t\ min,\ entrance}$ = 0.400 $R_h/R_{t\ max,\ exit}$ = 0.935 σ = 0.85 N_{bl} = 50 to 60 AR_{in} = 2.0

Table 2 (Continued)

Component	Specification
HPC	$AR_{out} = 1.4$ $\rho = 0.16$ lb/in^3
Combustor	$V_{comb} = 200$ ft/s $t_r = 0.0075$ s $\rho_{liner} = 0.20$ lb/in^3 $\rho_{inner\ case} = 0.20$ lb/in^3 $\rho_{outer\ case} = 0.20$ lb/in^3 $L/H_{diffuser} = 5.75$
HPT	$U_{tip\ max} = 1900$ ft/s $AN^2_{max} = 45\text{x}10^9$ in^2-RPM^2 $M_{out\ max} = 0.670$ $\lambda_{min} = 0.210$ $\sigma = 0.90$ $AR_{in} = 1.6$ $AR_{out} = 2.5$ $\sigma_{d\ max} = 200{,}000$ psi
LPT	$R_h/R_{t\ exit\ min} = 0.60$ $AN^2_{max} = 50\text{x}10^9$ in^2-RPM^2 $M_{out\ max} = 0.600$ $\lambda_{min} = 0.30$ $\sigma = 0.80$ $AR_{in} = 2.0$ to 3.0 $AR_{out} = 3.0$ to 4.0 $\sigma_{d\ max} = 200{,}000$ psi
Nozzles	See figs. 16 to 21.

Table 2 (Concluded)

Component	Specification
Miscellaneous	$W_{nacelle}$ (lb) = 1.956 L_{bare} (ft) D^2_{max} (ft^2) W_{mounts} (lb) = 0.003 $F_{N\ SLS}$ (lb) $W_{firewall}$ (lb) = 3.1 L_{bare} (ft) D_{max} (ft) $W_{pylon}\text{ (lb)} = 8.407\text{x}10^{-5}\,\frac{F_{N\ SLS}\text{ (lb)}}{D_{max}\text{ (ft)}}\left(L_{bare}\text{ (ft)} + 2.184\sqrt{A_{capt}\text{ (ft}^2)}\right)\sqrt{A_{capt}\text{ (ft}^2)}$ $W_{C\&A}$ (lb) = 0.10 W_{bare} (lb)

Table 3.—Flight Data Performance Envelope

Altitude (ft)	Mach
0	***0.00, 0.20,*** *0.30, 0.40*
689	*0.00, 0.20,* ***0.30,*** *0.40*
2000	*0.00, 0.20, 0.30,* ***0.40,*** 0.60
10000	0.40, **0.60,** 0.90
15000	0.40, 0.60, 0.90
20000	0.40, 0.60, 0.90, 1.10
30000	**0.90,** 1.10, 1.40, 1.60, 1.63
36089	0.90, **1.10,** 1.40, 1.60, 1.63, 1.80
40000	0.90, 1.10, 1.40, 1.60, 1.63, 1.80, 2.10
50000	1.40, **1.60,** 1.63, 1.80, 2.10, 2.40
55000	**1.80, 2.10,** 2.40
60000	1.60, 1.63, 1.80, 2.10, **2.40**
65000	1.80, 2.10, 2.40
70000	1.80, 2.10, 2.40
80000	2.10, 2.40

Key:
Bold indicates throttle hook is computed
Italic indicates hot day (ISA + 18 °F) data

Table 4.—TBE3010 Boeing HSCT Noise Summary, Standard Takeoff

Downrange Distance (ft)	Lateral Distance (ft)	Maximum PNLT (PNdB)	FAR36 Stage 3 Rule (EPNdB)	EPNL (EPNdB)	Exceedance of Rule (EPNdB)
21325	0	122.0	105.2	118.9	13.7
9500	1476	115.2	102.4	112.8	10.4
10500	1476	116.5	102.4	113.6	11.2
11500	1476	118.0	102.4	114.8	12.4
12500	1476	119.7	102.4	116.2	13.8
13500	1476	120.3	102.4	116.9	14.5
14500	1476	120.7	102.4	117.6	15.2
15500	1476	121.2	102.4	118.3	15.9
16500	1476	121.5	102.4	118.8	16.4
17500	**1476**	**121.7**	**102.4**	**119.3**	**16.9**
18500	1476	120.8	102.4	118.6	16.2
19500	1476	116.8	102.4	116.4	14.0
20500	1476	115.3	102.4	115.4	13.0

Key:
Bold indicates maximum sideline noise location

Table 5.—TBE3010 Boeing HSCT Noise Summary, Advanced Takeoff

Downrange Distance (ft)	Lateral Distance (ft)	Maximum PNLT (PNdB)	FAR36 Stage 3 Rule (EPNdB)	EPNL (EPNdB)	Exceedance of Rule (EPNdB)
21325	0	124.5	105.1	118.9	13.8
9500	1476	115.1	102.3	113.1	10.8
10500	1476	115.6	102.3	113.5	11.2
11500	1476	116.3	102.3	114.0	11.7
12500	1476	117.0	102.3	114.4	12.1
13500	1476	117.2	102.3	114.9	12.6
14500	1476	117.6	102.3	115.3	13.0
15500	1476	118.0	102.3	115.7	13.4
16500	1476	118.4	102.3	116.0	13.7
17500	**1476**	**118.8**	**102.3**	**116.1**	**13.8**
18500	1476	115.5	102.3	115.3	13.0
19500	1476	114.7	102.3	114.6	12.3
20500	1476	114.9	102.3	114.0	11.7

Key:
Bold indicates maximum sideline noise location

Table 6.—TJ3010 Results, 1993 Propulsion Ground rules, Boeing HSCT

	Adv TO, Dry Throughout	Std TO, Dry Throughout	Adv TO, Transonic AB	Std TO, Transonic AB
Sized Airplane				
MTOGW (lb)	762279	778566		
Landing Weight (lb)	402790	412424		
OEW (lb)	287519	296025		
SLS F_G (ISA + 18 °F, lb)	44500	45817		
Effective Wing Area (ft^2)	8078	8185		
Span (ft)	138	139		
Bare Engine Weight (lb)	7022	7240		
Nozzle Weight (lb)	3580	4619		
Total Pod Weight (lb)	14711	16096		
Nozzle MFA (%)	59	110		
Nozzle Suppression (dB)	14.0	17.9		
FAR 25 Field Length (ft)	11000	11000		
Wing Loading (lb/ft^2)	94.36	95.12		
Thrust Loading	.2335	.2354		
Design Mission				
Block Fuel (lb)	361243	367948		
Block Time (hr)	4.65	4.63		
Reserve Fuel (lb)	50381	51509		
Total Fuel (lb)	409870	417651		
Begin Supercruise Altitude (ft)	57534	57602		
End Supercruise Altitude (ft)	67144	67292		
L/D (Mid supercruise wt)	8.56	8.57		
TSFC (Mid supercruise wt, lb/hr/lb)	1.358	1.358		
RF (Mid supercruise wt, nm)	8679	8690		
EI (Mid supercruise wt, lb/1000 lb)	6.52	6.52		
Supercruise NO_X (lb)	1557	1610		
Min PROC/Mach (ft/min)	527/1.18	582/1.18		
Climb Time (min)	56.5	53.7		
Approach Velocity (keas)	136.4	136.9		
Economic Mission				
TOGW (lb)	596040	610452		
Block Fuel (lb)	226667	231612		
Block Time (hr)	4.02	4.01		
L/D (Mid subcruise wt)	16.13	16.13		
TSFC (Mid subcruise wt, lb/hr/lb)	1.205	1.207		
RF (Mid subcruise wt, nm)	7011	6998		
L/D (Mid supercruise wt)	8.55	8.57		
TSFC (Mid supercruise wt, lb/hr/lb)	1.361	1.361		
RF (Mid supercruise wt, nm)	8649	8668		

Table 7.— TBE3010 Results, 1993 Propulsion Ground rules, Boeing HSCT

	Adv TO, Dry Throughout	Std TO, Dry Throughout	Adv TO, Transonic AB	Std TO, Transonic AB
Sized Airplane				
MTOGW (lb)	729055	744046	732634	748225
Landing Weight (lb)	384575	393496	386744	395952
OEW (lb)	272033	279937	273960	282106
SLS F_G (ISA + 18 °F, lb)	41800	43000	42100	43350
Effective Wing Area (ft^2)	7835	7935	7858	7963
Span (ft)	136	137	136	137
Bare Engine Weight (lb)	6065	6248	6337	6534
Nozzle Weight (lb)	3210	4223	3234	4259
Total Pod Weight (lb)	12670	13969	12992	14321
Nozzle MFA (%)	74	126	74	126
Nozzle Suppression (dB)	15.8	18.9	15.7	18.9
FAR 25 Field Length (ft)	11000	11000	11000	11000
Wing Loading (lb/ft^2)	93.05	93.77	93.23	93.96
Thrust Loading	.2293	.2312	.2299	.2317
Design Mission				
Block Fuel (lb)	346285	352408	347709	354145
Block Time (hr)	4.56	4.55	4.53	4.52
Reserve Fuel (lb)	47652	48669	47895	48956
Total Fuel (lb)	392132	399219	393785	401229
Begin Supercruise Altitude (ft)	56579	56301	56422	56150
End Supercruise Altitude (ft)	66255	66034	66198	65978
L/D (Mid supercruise wt)	8.52	8.53	8.52	8.53
TSFC (Mid supercruise wt, lb/hr/lb)	1.366	1.364	1.366	1.363
RF (Mid supercruise wt, nm)	8585	8609	8589	8613
EI (Mid supercruise wt, lb/1000 lb)	7.42	6.90	7.28	6.77
Supercruise NO_X (lb)	1701	1623	1698	1624
Min PROC/Mach (ft/min)	1147/1.18	1228/1.18	1342/2.40	1465/1.44
Climb Time (min)	50.8	48.6	46.9	44.8
Approach Velocity (keas)	135.4	136.0	135.6	136.1
Economic Mission				
TOGW (lb)	566450	579671	569798	583471
Block Fuel (lb)	215153	219625	216360	221012
Block Time (hr)	3.96	3.96	3.94	3.94
L/D (Mid subcruise wt)	16.11	16.13	16.12	16.13
TSFC (Mid subcruise wt, lb/hr/lb)	1.162	1.164	1.162	1.165
RF (Mid subcruise wt, nm)	7260	7254	7260	7252
L/D (Mid supercruise wt)	8.52	8.53	8.52	8.53
TSFC (Mid supercruise wt, lb/hr/lb)	1.369	1.367	1.368	1.366
RF (Mid supercruise wt, nm)	8567	8593	8571	8597

Table 8.— TBE3021 Results, 1993 Propulsion Ground rules, Boeing HSCT

	Adv TO, Dry Throughout	Std TO, Dry Throughout	Adv TO, Transonic AB	Std TO, Transonic AB
Sized Airplane				
MTOGW (lb)	729610	744445	733261	748379
Landing Weight (lb)	386630	395454	388951	397846
OEW (lb)	274114	281926	276192	284051
SLS F_G (ISA + 18 °F, lb)	42100	43300	42400	43617
Effective Wing Area (ft^2)	7815	7913	7838	7938
Span (ft)	136	137	136	137
Bare Engine Weight (lb)	6308	6497	6593	6792
Nozzle Weight (lb)	3264	4251	3310	4284
Total Pod Weight (lb)	13136	14418	13493	14774
Nozzle MFA (%)	68	121	70	121
Nozzle Suppression (dB)	15.4	18.6	15.4	18.6
FAR 25 Field Length (ft)	11000	11000	11000	11000
Wing Loading (lb/ft^2)	93.36	94.08	93.55	94.28
Thrust Loading	.2308	.2327	.2313	.2331
Design Mission				
Block Fuel (lb)	344744	350806	346087	352362
Block Time (hr)	4.57	4.56	4.53	4.52
Reserve Fuel (lb)	47625	48638	47869	48904
Total Fuel (lb)	390605	397629	392179	399438
Begin Supercruise Altitude (ft)	56683	56383	56495	56208
End Supercruise Altitude (ft)	66079	65863	66014	65803
L/D (Mid supercruise wt)	8.52	8.53	8.52	8.53
TSFC (Mid supercruise wt, lb/hr/lb)	1.354	1.352	1.354	1.352
RF (Mid supercruise wt, nm)	8663	8683	8665	8685
EI (Mid supercruise wt, lb/1000 lb)	6.39	6.41	6.40	6.41
Supercruise NO_X (lb)	1426	1478	1458	1510
Min PROC/Mach (ft/min)	789/2.40	1067/2.40	860/2.40	1137/2.40
Climb Time (min)	55.2	52.5	50.3	47.9
Approach Velocity (keas)	135.7	136.2	135.8	136.3
Economic Mission				
TOGW (lb)	567977	581046	571482	584740
Block Fuel (lb)	214521	218941	215728	220273
Block Time (hr)	3.97	3.96	3.94	3.94
L/D (Mid subcruise wt)	16.12	16.13	16.12	16.13
TSFC (Mid subcruise wt, lb/hr/lb)	1.159	1.161	1.160	1.162
RF (Mid subcruise wt, nm)	7280	7272	7280	7271
L/D (Mid supercruise wt)	8.52	8.53	8.52	8.53
TSFC (Mid supercruise wt, lb/hr/lb)	1.357	1.355	1.356	1.354
RF (Mid supercruise wt, nm)	8645	8666	8648	8670

Table 9.— TBE3031 Results, 1993 Propulsion Ground rules, Boeing HSCT

	Adv TO, Dry Throughout	Std TO, Dry Throughout	Adv TO, Transonic AB	Std TO, Transonic AB
Sized Airplane				
MTOGW (lb)	734219	748214	737156	750965
Landing Weight (lb)	391506	399592	392937	401430
OEW (lb)	278716	285934	280031	287588
SLS F_G (ISA + 18 °F, lb)	43150	43917	43033	44150
Effective Wing Area (ft^2)	7813	7910	7835	7925
Span (ft)	136	137	136	137
Bare Engine Weight (lb)	6815	6943	7052	7244
Nozzle Weight (lb)	3365	4341	3345	4314
Total Pod Weight (lb)	14023	15198	14228	15493
Nozzle MFA (%)	61	115	60	112
Nozzle Suppression (dB)	14.2	18.3	14.1	18.1
FAR 25 Field Length (ft)	10916	11000	11000	11000
Wing Loading (lb/ft^2)	93.97	94.59	94.09	94.76
Thrust Loading	.2351	.2348	.2335	.2352
Design Mission				
Block Fuel (lb)	344457	350399	345960	351321
Block Time (hr)	4.58	4.58	4.54	4.53
Reserve Fuel (lb)	47901	48768	48016	48952
Total Fuel (lb)	390613	397390	392235	398487
Begin Supercruise Altitude (ft)	56549	56523	56338	56342
End Supercruise Altitude (ft)	65436	65430	65289	65461
L/D (Mid supercruise wt)	8.50	8.52	8.49	8.53
TSFC (Mid supercruise wt, lb/hr/lb)	1.337	1.337	1.337	1.337
RF (Mid supercruise wt, nm)	8748	8771	8741	8782
EI (Mid supercruise wt, lb/1000 lb)	6.34	6.34	6.34	6.34
Supercruise NO_X (lb)	1381	1408	1396	1438
Min PROC/Mach (ft/min)	500/2.40	528/2.40	500/2.40	583/2.40
Climb Time (min)	58.6	58.4	55.7	53.3
Approach Velocity (keas)	136.1	136.6	136.2	136.7
Economic Mission				
TOGW (lb)	573353	585284	575609	588029
Block Fuel (lb)	214962	218962	215817	219880
Block Time (hr)	3.97	3.97	3.95	3.94
L/D (Mid subcruise wt)	16.12	16.14	16.13	16.14
TSFC (Mid subcruise wt, lb/hr/lb)	1.152	1.152	1.150	1.152
RF (Mid subcruise wt, nm)	7326	7338	7344	7337
L/D (Mid supercruise wt)	8.49	8.52	8.49	8.53
TSFC (Mid supercruise wt, lb/hr/lb)	1.339	1.339	1.339	1.339
RF (Mid supercruise wt, nm)	8728	8754	8727	8766

Table 10.—TBE3041 Results, 1993 Propulsion Ground rules, Boeing HSCT

	Adv TO, Dry Throughout	Std TO, Dry Throughout	Adv TO, Transonic AB	Std TO, Transonic AB
Sized Airplane				
MTOGW (lb)	747038	759460	750614	763440
Landing Weight (lb)	400744	407925	402350	409600
OEW (lb)	286978	293389	288450	294926
SLS F_G (ISA + 18 °F, lb)	45067	45733	44867	45450
Effective Wing Area (ft^2)	7878	7960	7908	7993
Span (ft)	137	137	137	138
Bare Engine Weight (lb)	7640	7759	7890	7997
Nozzle Weight (lb)	3504	4372	3488	4377
Total Pod Weight (lb)	15380	16432	15593	16648
Nozzle MFA (%)	50	99	50	100
Nozzle Suppression (dB)	12.4	17.4	12.4	17.4
FAR 25 Field Length (ft)	10782	10867	10891	11000
Wing Loading (lb/ft^2)	94.83	95.41	94.92	95.51
Thrust Loading	.2413	.2409	.2391	.2381
Design Mission				
Block Fuel (lb)	348048	353316	350011	355609
Block Time (hr)	4.58	4.58	4.55	4.55
Reserve Fuel (lb)	48877	49645	49010	49784
Total Fuel (lb)	395170	401181	397274	403624
Begin Supercruise Altitude (ft)	55899	55896	55663	55632
End Supercruise Altitude (ft)	64640	64621	64460	64400
L/D (Mid supercruise wt)	8.46	8.48	8.45	8.47
TSFC (Mid supercruise wt, lb/hr/lb)	1.319	1.319	1.319	1.319
RF (Mid supercruise wt, nm)	8830	8847	8821	8837
EI (Mid supercruise wt, lb/1000 lb)	6.27	6.27	6.27	6.27
Supercruise NO_X (lb)	1356	1376	1363	1380
Min PROC/Mach (ft/min)	500/2.40	500/2.40	500/2.40	500/2.40
Climb Time (min)	61.3	61.3	59.3	59.9
Approach Velocity (keas)	136.7	137.2	136.8	137.2
Economic Mission				
TOGW (lb)	585692	596280	588278	598998
Block Fuel (lb)	218087	221632	219113	222738
Block Time (hr)	3.97	3.97	3.95	3.95
L/D (Mid subcruise wt)	16.14	16.13	16.14	16.13
TSFC (Mid subcruise wt, lb/hr/lb)	1.151	1.149	1.147	1.145
RF (Mid subcruise wt, nm)	7344	7352	7368	7378
L/D (Mid supercruise wt)	8.47	8.49	8.46	8.47
TSFC (Mid supercruise wt, lb/hr/lb)	1.322	1.322	1.322	1.322
RF (Mid supercruise wt, nm)	8822	8842	8811	8823

Table 11.—MFTF5093 Results, 1993 Propulsion Ground rules, Boeing HSCT

	Adv TO, Dry Throughout	Std TO, Dry Throughout	Adv TO, Transonic AB	Std TO, Transonic AB
Sized Airplane				
MTOGW (lb)	705592	721046	706981	721825
Landing Weight (lb)	382295	390610	382025	389990
OEW (lb)	273684	281155	273524	280684
SLS F_G (ISA + 18 °F, lb)	44067	44483	43033	43400
Effective Wing Area (ft^2)	7483	7595	7503	7613
Span (ft)	133	134	133	134
Nozzle Weight (lb)	3615	4691	3540	4571
Total Pod Weight (lb)	14215	15395	14139	15265
Nozzle MFA (%)	58	119	60	119
Nozzle Suppression (dB)	13.9	18.6	14.0	18.6
FAR 25 Field Length (ft)	10285	10481	10543	10737
Wing Loading (lb/ft^2)	94.29	94.94	94.23	94.81
Thrust Loading	.2498	.2468	.2435	.2405
Design Mission				
Block Fuel (lb)	324944	332098	326564	333457
Block Time (hr)	4.57	4.59	4.53	4.55
Reserve Fuel (lb)	43721	44565	43611	44416
Total Fuel (lb)	367019	375000	368567	376251
Begin Supercruise Altitude (ft)	55780	55613	55139	55018
End Supercruise Altitude (ft)	64795	64572	64262	64042
L/D (Mid supercruise wt)	8.44	8.45	8.40	8.40
TSFC (Mid supercruise wt, lb/hr/lb)	1.310	1.310	1.310	1.310
RF (Mid supercruise wt, nm)	8871	8878	8827	8828
EI (Mid supercruise wt, lb/1000 lb)	8.19	8.19	8.20	8.20
Supercruise NO_X (lb)	1758	1774	1752	1761
Min PROC/Mach (ft/min)	500/2.40	500/2.40	500/2.40	500/2.40
Climb Time (min)	54.5	56.9	53.6	56.3
Approach Velocity (keas)	136.3	136.8	136.3	136.7
Economic Mission				
TOGW (lb)	551992	564421	551692	563556
Block Fuel (lb)	202267	206568	202295	206373
Block Time (hr)	3.99	3.99	3.95	3.96
L/D (Mid subcruise wt)	16.13	16.14	16.13	16.14
TSFC (Mid subcruise wt, lb/hr/lb)	1.113	1.108	1.104	1.100
RF (Mid subcruise wt, nm)	7592	7626	7650	7683
L/D (Mid supercruise wt)	8.44	8.45	8.40	8.40
TSFC (Mid supercruise wt, lb/hr/lb)	1.313	1.313	1.313	1.312
RF (Mid supercruise wt, nm)	8849	8860	8810	8811

Table 12.—MFTF5093 Results, 1993 Propulsion Ground rules, McDonnell Douglas HSCT

	Adv TO, Dry Throughout	Std TO, Dry Throughout	Adv TO, Transonic AB	Std TO, Transonic AB
Sized Airplane				
MTOGW (lb)		728271		
Landing Weight (lb)		385202		
OEW (lb)		313470		
SLS F_G (ISA + 18 °F, lb)		45117		
Effective Wing Area (ft^2)		9840		
Span (ft)		157		
Nozzle Weight (lb)		4808		
Total Pod Weight (lb)		15672		
Nozzle MFA (%)		121		
Nozzle Suppression (dB)		18.5		
FAR 25 Field Length (ft)		11000		
Wing Loading (lb/ft^2)		74.01		
Thrust Loading		.2478		
Design Mission				
Block Fuel (lb)		344072		
Block Time (hr)		5.27		
Reserve Fuel (lb)		10232		
Total Fuel (lb)		353301		
L/D (Mid subcruise wt)		14.74		
TSFC (Mid subcruise wt, lb/hr/lb)		1.114		
RF (Mid subcruise wt, nm)		7377		
EI (Mid subcruise wt, lb/1000 lb)		5.97		
Subcruise NO_X (lb)		379		
Begin Supercruise Altitude (ft)		57833		
End Supercruise Altitude (ft)		65204		
L/D (Mid supercruise wt)		8.97		
TSFC (Mid supercruise wt, lb/hr/lb)		1.314		
RF (Mid supercruise wt, nm)		9399		
EI (Mid supercruise wt, lb/1000 lb)		7.62		
Supercruise NO_X (lb)		1483		
Min PROC/Mach (ft/min)		1000/2.40		

Table 13.—MFTF5094 Results, 1994 Propulsion Ground rules, Boeing HSCT

	Adv TO, Dry Throughout	Std TO, Dry Throughout	Adv TO, Transonic AB	Std TO, Transonic AB
Sized Airplane				
MTOGW (lb)	730775	747843		
Landing Weight (lb)	390760	400067		
OEW (lb)	280509	288861		
SLS F_G (ISA + 18 °F, lb)	44850	45417		
Effective Wing Area (ft^2)	7740	7860		
Span (ft)	135	136		
Nozzle Weight (lb)	3283	4465		
Total Pod Weight (lb)	14706	16039		
Nozzle MFA (%)	64	129		
Nozzle Suppression (dB)	14.4	18.8		
FAR 25 Field Length (ft)	10444	10633		
Wing Loading (lb/ft^2)	94.42	95.15		
Thrust Loading	.2455	.2429		
Design Mission				
Block Fuel (lb)	341729	349512		
Block Time (hr)	4.57	4.59		
Reserve Fuel (lb)	45361	46316		
Total Fuel (lb)	385376	394092		
Begin Supercruise Altitude (ft)	54588	54476		
End Supercruise Altitude (ft)	64047	63836		
L/D (Mid supercruise wt)	8.36	8.37		
TSFC (Mid supercruise wt, lb/hr/lb)	1.341	1.341		
RF (Mid supercruise wt, nm)	8586	8598		
EI (Mid supercruise wt, lb/1000 lb)	5.67	5.67		
Supercruise NO_X (lb)	1254	1269		
Min PROC/Mach (ft/min)	500/2.40	500/2.40		
Climb Time (min)	58.8	60.8		
Approach Velocity (keas)	136.4	137.0		
Economic Mission				
TOGW (lb)	568099	581981		
Block Fuel (lb)	210491	215293		
Block Time (hr)	3.98	3.99		
L/D (Mid subcruise wt)	16.13	16.14		
TSFC (Mid subcruise wt, lb/hr/lb)	1.107	1.104		
RF (Mid subcruise wt, nm)	7627	7655		
L/D (Mid supercruise wt)	8.38	8.39		
TSFC (Mid supercruise wt, lb/hr/lb)	1.344	1.344		
RF (Mid supercruise wt, nm)	8580	8593		

Table 14.—MFTF5094 Results, 1994 Propulsion Ground rules, McDonnell Douglas HSCT

	Adv TO, Dry Throughout	Std TO, Dry Throughout	Adv TO, Transonic AB	Std TO, Transonic AB
Sized Airplane				
MTOGW (lb)	733553	762750		
Landing Weight (lb)	383916	400732		
OEW (lb)	311991	328437		
SLS F_G (ISA + 18 °F, lb)	46927	47885		
Effective Wing Area (ft^2)	9710	10208		
Span (ft)	156	160		
Nozzle Weight (lb)	3586	4764		
Total Pod Weight (lb)	15564	17000		
Nozzle MFA (%)	77	126		
Nozzle Suppression (dB)	16.0	18.8		
FAR 25 Field Length (ft)	11000	11000		
Wing Loading (lb/ft^2)	75.55	74.72		
Thrust Loading	.2559	.2511		
Design Mission				
Block Fuel (lb)	350705	363107		
Block Time (hr)	5.25	5.25		
Reserve Fuel (lb)	10425	10795		
Total Fuel (lb)	360062	372813		
L/D (Mid subcruise wt)	14.71	14.82		
TSFC (Mid subcruise wt, lb/hr/lb)	1.125	1.122		
RF (Mid subcruise wt, nm)	7289	7366		
EI (Mid subcruise wt, lb/1000 lb)	7.67	7.53		
Subcruise NO_X (lb)	497	501		
Begin Supercruise Altitude (ft)	57494	57251		
End Supercruise Altitude (ft)	65647	65305		
L/D (Mid supercruise wt)	8.96	9.01		
TSFC (Mid supercruise wt, lb/hr/lb)	1.357	1.357		
RF (Mid supercruise wt, nm)	9092	9143		
EI (Mid supercruise wt, lb/1000 lb)	5.15	5.14		
Supercruise NO_X (lb)	1051	1082		
Min PROC/Mach (ft/min)	1000/2.40	1000/2.40		

Table 15.—MFTF5193 Results, 1993 Propulsion Ground rules, Boeing HSCT

	Adv TO, Dry Throughout	Std TO, Dry Throughout	Adv TO, Transonic AB	Std TO, Transonic AB
Sized Airplane				
MTOGW (lb)	715649	732074		
Landing Weight (lb)	387738	396525		
OEW (lb)	278476	286367		
SLS F_G (ISA + 18 °F, lb)	44917	45367		
Effective Wing Area (ft^2)	7558	7678		
Span (ft)	134	135		
Nozzle Weight (lb)	3664	4785		
Total Pod Weight (lb)	14958	16198		
Nozzle MFA (%)	60	121		
Nozzle Suppression (dB)	14.0	18.7		
FAR 25 Field Length (ft)	10266	10468		
Wing Loading (lb/ft^2)	94.69	95.35		
Thrust Loading	.2511	.2479		
Design Mission				
Block Fuel (lb)	329609	337264		
Block Time (hr)	4.59	4.60		
Reserve Fuel (lb)	44372	45268		
Total Fuel (lb)	372284	380817		
Begin Supercruise Altitude (ft)	55912	55744		
End Supercruise Altitude (ft)	64907	64698		
L/D (Mid supercruise wt)	8.46	8.47		
TSFC (Mid supercruise wt, lb/hr/lb)	1.310	1.310		
RF (Mid supercruise wt, nm)	8893	8903		
EI (Mid supercruise wt, lb/1000 lb)	5.14	5.14		
Supercruise NO_X (lb)	1115	1126		
Min PROC/Mach (ft/min)	500/2.40	500/2.40		
Climb Time (min)	55.3	57.9		
Approach Velocity (keas)	136.6	137.1		
Economic Mission				
TOGW (lb)	560458	573592		
Block Fuel (lb)	205428	209993		
Block Time (hr)	3.99	4.00		
L/D (Mid subcruise wt)	16.13	16.14		
TSFC (Mid subcruise wt, lb/hr/lb)	1.113	1.108		
RF (Mid subcruise wt, nm)	7589	7626		
L/D (Mid supercruise wt)	8.47	8.47		
TSFC (Mid supercruise wt, lb/hr/lb)	1.313	1.313		
RF (Mid supercruise wt, nm)	8878	8886		

Table 16.—MFTF4093 Results, 1993 Propulsion Ground rules, Boeing HSCT

	Adv TO, Dry Throughout	Std TO, Dry Throughout	Adv TO, Transonic AB	Std TO, Transonic AB
Sized Airplane				
MTOGW (lb)	715768	729760	715830	729622
Landing Weight (lb)	389965	397380	389313	396395
OEW (lb)	280746	287421	280300	286686
SLS F_G (ISA + 18 °F, lb)	46450	46767	45350	45467
Effective Wing Area (ft^2)	7528	7630	7533	7638
Span (ft)	134	134	134	135
Nozzle Weight (lb)	3876	4841	3795	4746
Total Pod Weight (lb)	15340	16387	15270	16253
Nozzle MFA (%)	45	104	48	106
Nozzle Suppression (dB)	11.9	17.9	12.6	18.0
FAR 25 Field Length (ft)	10298	10488	10539	10769
Wing Loading (lb/ft^2)	95.08	95.64	95.03	95.53
Thrust Loading	.2596	.2563	.2534	.2493
Design Mission				
Block Fuel (lb)	327434	334021	328109	334824
Block Time (hr)	4.59	4.60	4.54	4.56
Reserve Fuel (lb)	44329	45069	44123	44819
Total Fuel (lb)	370132	377449	370640	378046
Begin Supercruise Altitude (ft)	55609	55444	55023	54832
End Supercruise Altitude (ft)	64428	64209	63916	63605
L/D (Mid supercruise wt)	8.44	8.45	8.40	8.39
TSFC (Mid supercruise wt, lb/hr/lb)	1.295	1.295	1.295	1.294
RF (Mid supercruise wt, nm)	8972	8979	8932	8927
EI (Mid supercruise wt, lb/1000 lb)	7.88	7.88	7.88	7.88
Supercruise NO_X (lb)	1679	1687	1672	1668
Min PROC/Mach (ft/min)	500/2.40	500/2.40	500/2.40	500/2.40
Climb Time (min)	57.1	59.9	55.5	59.5
Approach Velocity (keas)	136.9	137.3	136.9	137.2
Economic Mission				
TOGW (lb)	561828	572904	560589	571170
Block Fuel (lb)	204407	208254	203855	207550
Block Time (hr)	3.99	4.00	3.95	3.96
L/D (Mid subcruise wt)	16.13	16.13	16.13	16.13
TSFC (Mid subcruise wt, lb/hr/lb)	1.102	1.097	1.094	1.088
RF (Mid subcruise wt, nm)	7660	7697	7721	7766
L/D (Mid supercruise wt)	8.45	8.44	8.40	8.39
TSFC (Mid supercruise wt, lb/hr/lb)	1.298	1.298	1.297	1.297
RF (Mid supercruise wt, nm)	8963	8960	8913	8905

Table 17.—MFTF4093 Results, 1993 Propulsion Ground rules, McDonnell Douglas HSCT

	Adv TO, Dry Throughout	Std TO, Dry Throughout	Adv TO, Transonic AB	Std TO, Transonic AB
Sized Airplane				
MTOGW (lb)		729915		
Landing Weight (lb)		388178		
OEW (lb)		316485		
SLS F_G (ISA + 18 °F, lb)		46620		
Effective Wing Area (ft^2)		9674		
Span (ft)		156		
Nozzle Weight (lb)		4832		
Total Pod Weight (lb)		16340		
Nozzle MFA (%)		105		
Nozzle Suppression (dB)		17.6		
FAR 25 Field Length (ft)		11000		
Wing Loading (lb/ft^2)		75.45		
Thrust Loading		.2555		
Design Mission				
Block Fuel (lb)		342719		
Block Time (hr)		5.28		
Reserve Fuel (lb)		10193		
Total Fuel (lb)		351931		
L/D (Mid subcruise wt)		14.70		
TSFC (Mid subcruise wt, lb/hr/lb)		1.101		
RF (Mid subcruise wt, nm)		7446		
EI (Mid subcruise wt, lb/1000 lb)		5.97		
Subcruise NO_X (lb)		377		
Begin Supercruise Altitude (ft)		57386		
End Supercruise Altitude (ft)		64656		
L/D (Mid supercruise wt)		8.93		
TSFC (Mid supercruise wt, lb/hr/lb)		1.298		
RF (Mid supercruise wt, nm)		9471		
EI (Mid supercruise wt, lb/1000 lb)		7.11		
Supercruise NO_X (lb)		1367		
Min PROC/Mach (ft/min)		1000/2.40		

Table 18.—MFTF4094 Results, 1994 Propulsion Ground rules, Boeing HSCT

	Adv TO, Dry Throughout	Std TO, Dry Throughout	Adv TO, Transonic AB	Std TO, Transonic AB
Sized Airplane				
MTOGW (lb)	736347	749718		
Landing Weight (lb)	396362	403599		
OEW (lb)	285794	292304		
SLS F_G (ISA + 18 °F, lb)	46267	46683		
Effective Wing Area (ft^2)	7743	7840		
Span (ft)	135	136		
Nozzle Weight (lb)	3458	4372		
Total Pod Weight (lb)	15619	16648		
Nozzle MFA (%)	50	104		
Nozzle Suppression (dB)	12.8	17.8		
FAR 25 Field Length (ft)	10343	10493		
Wing Loading (lb/ft^2)	95.10	95.63		
Thrust Loading	.2513	.2491		
Design Mission				
Block Fuel (lb)	341642	347791		
Block Time (hr)	4.59	4.60		
Reserve Fuel (lb)	45678	46405		
Total Fuel (lb)	385663	392525		
Begin Supercruise Altitude (ft)	54467	54373		
End Supercruise Altitude (ft)	63563	63396		
L/D (Mid supercruise wt)	8.37	8.38		
TSFC (Mid supercruise wt, lb/hr/lb)	1.323	1.323		
RF (Mid supercruise wt, nm)	8709	8719		
EI (Mid supercruise wt, lb/1000 lb)	5.57	5.57		
Supercruise NO_X (lb)	1217	1225		
Min PROC/Mach (ft/min)	500/2.40	500/2.40		
Climb Time (min)	61.2	63.2		
Approach Velocity (keas)	136.9	137.3		
Economic Mission				
TOGW (lb)	574548	585373		
Block Fuel (lb)	211228	214978		
Block Time (hr)	3.99	4.00		
L/D (Mid subcruise wt)	16.13	16.14		
TSFC (Mid subcruise wt, lb/hr/lb)	1.100	1.096		
RF (Mid subcruise wt, nm)	7680	7709		
L/D (Mid supercruise wt)	8.37	8.38		
TSFC (Mid supercruise wt, lb/hr/lb)	1.326	1.326		
RF (Mid supercruise wt, nm)	8692	8703		

Table 19.—MFTF4094 Results, 1994 Propulsion Ground rules, McDonnell Douglas HSCT

	Adv TO, Dry Throughout	Std TO, Dry Throughout	Adv TO, Transonic AB	Std TO, Transonic AB
Sized Airplane				
MTOGW (lb)	735468	757910		
Landing Weight (lb)	387313	400822		
OEW (lb)	315429	328671		
SLS F_G (ISA + 18 °F, lb)	47057	48270		
Effective Wing Area (ft^2)	9738	10068		
Span (ft)	156	159		
Nozzle Weight (lb)	3644	4578		
Total Pod Weight (lb)	16023	17293		
Nozzle MFA (%)	64	106		
Nozzle Suppression (dB)	14.6	17.9		
FAR 25 Field Length (ft)	11000	11000		
Wing Loading (lb/ft^2)	75.53	75.28		
Thrust Loading	.2559	.2548		
Design Mission				
Block Fuel (lb)	349158	358118		
Block Time (hr)	5.26	5.26		
Reserve Fuel (lb)	10384	10651		
Total Fuel (lb)	358539	367739		
L/D (Mid subcruise wt)	14.72	14.79		
TSFC (Mid subcruise wt, lb/hr/lb)	1.112	1.112		
RF (Mid subcruise wt, nm)	7379	7415		
EI (Mid subcruise wt, lb/1000 lb)	5.74	5.73		
Subcruise NO_X (lb)	369	378		
Begin Supercruise Altitude (ft)	56849	56879		
End Supercruise Altitude (ft)	64500	64471		
L/D (Mid supercruise wt)	8.91	8.98		
TSFC (Mid supercruise wt, lb/hr/lb)	1.333	1.333		
RF (Mid supercruise wt, nm)	9198	9273		
EI (Mid supercruise wt, lb/1000 lb)	4.97	4.96		
Supercruise NO_X (lb)	996	1019		
Min PROC/Mach (ft/min)	1000/2.40	1000/2.40		

Table 20.—MFTF4193 Results, 1993 Propulsion Ground rules, Boeing HSCT

	Adv TO, Dry Throughout	Std TO, Dry Throughout	Adv TO, Transonic AB	Std TO, Transonic AB
Sized Airplane				
MTOGW (lb)	725106	739747		
Landing Weight (lb)	394837	402984		
OEW (lb)	285024	292351		
SLS F_G (ISA + 18 °F, lb)	46450	47017		
Effective Wing Area (ft^2)	7598	7698		
Span (ft)	134	135		
Nozzle Weight (lb)	3859	4889		
Total Pod Weight (lb)	16017	17202		
Nozzle MFA (%)	45	106		
Nozzle Suppression (dB)	11.9	17.9		
FAR 25 Field Length (ft)	10195	10345		
Wing Loading (lb/ft^2)	95.43	96.10		
Thrust Loading	.2562	.2542		
Design Mission				
Block Fuel (lb)	331930	338445		
Block Time (hr)	4.60	4.61		
Reserve Fuel (lb)	44923	45743		
Total Fuel (lb)	375193	382506		
Begin Supercruise Altitude (ft)	55522	55432		
End Supercruise Altitude (ft)	64400	64270		
L/D (Mid supercruise wt)	8.45	8.46		
TSFC (Mid supercruise wt, lb/hr/lb)	1.295	1.295		
RF (Mid supercruise wt, nm)	8985	8997		
EI (Mid supercruise wt, lb/1000 lb)	5.15	5.15		
Supercruise NO_X (lb)	1108	1120		
Min PROC/Mach (ft/min)	500/2.40	500/2.40		
Climb Time (min)	58.2	59.7		
Approach Velocity (keas)	137.2	137.6		
Economic Mission				
TOGW (lb)	569427	581438		
Block Fuel (lb)	207275	211321		
Block Time (hr)	4.00	4.00		
L/D (Mid subcruise wt)	16.14	16.13		
TSFC (Mid subcruise wt, lb/hr/lb)	1.101	1.098		
RF (Mid subcruise wt, nm)	7671	7693		
L/D (Mid supercruise wt)	8.45	8.47		
TSFC (Mid supercruise wt, lb/hr/lb)	1.299	1.298		
RF (Mid supercruise wt, nm)	8961	8979		

Table 21.—MFTF4293 Results, 1993 Propulsion Ground rules, Boeing HSCT

	Adv TO, Dry Throughout	Std TO, Dry Throughout	Adv TO, Transonic AB	Std TO, Transonic AB
Sized Airplane				
MTOGW (lb)	738225	753277		
Landing Weight (lb)	401549	409824		
OEW (lb)	290815	298252		
SLS F_G (ISA + 18 °F, lb)	46383	46917		
Effective Wing Area (ft^2)	7700	7805		
Span (ft)	135	136		
Nozzle Weight (lb)	3851	4885		
Total Pod Weight (lb)	16903	18094		
Nozzle MFA (%)	50	108		
Nozzle Suppression (dB)	12.7	18.0		
FAR 25 Field Length (ft)	10431	10592		
Wing Loading (lb/ft^2)	95.87	96.51		
Thrust Loading	.2513	.2491		
Design Mission				
Block Fuel (lb)	338354	345151		
Block Time (hr)	4.60	4.62		
Reserve Fuel (lb)	45845	46682		
Total Fuel (lb)	382520	390135		
Begin Supercruise Altitude (ft)	55510	55409		
End Supercruise Altitude (ft)	64350	64204		
L/D (Mid supercruise wt)	8.46	8.47		
TSFC (Mid supercruise wt, lb/hr/lb)	1.298	1.298		
RF (Mid supercruise wt, nm)	8973	8981		
EI (Mid supercruise wt, lb/1000 lb)	5.12	5.12		
Supercruise NO_X (lb)	1115	1127		
Min PROC/Mach (ft/min)	500/2.40	500/2.40		
Climb Time (min)	59.3	61.1		
Approach Velocity (keas)	137.5	137.9		
Economic Mission				
TOGW (lb)	580058	592341		
Block Fuel (lb)	211372	215572		
Block Time (hr)	4.00	4.01		
L/D (Mid subcruise wt)	16.13	16.13		
TSFC (Mid subcruise wt, lb/hr/lb)	1.106	1.102		
RF (Mid subcruise wt, nm)	7638	7663		
L/D (Mid supercruise wt)	8.47	8.48		
TSFC (Mid supercruise wt, lb/hr/lb)	1.301	1.301		
RF (Mid supercruise wt, nm)	8958	8972		

Table 22.—MFTF3093 Results, 1993 Propulsion Ground rules, Boeing HSCT

	Adv TO, Dry Throughout	Std TO, Dry Throughout	Adv TO, Transonic AB	Std TO, Transonic AB
Sized Airplane				
MTOGW (lb)	732078	744231	729881	741339
Landing Weight (lb)	400076	406932	397237	403150
OEW (lb)	289640	295810	287346	292674
SLS F_G (ISA + 18 °F, lb)	48150	48683	46017	46183
Effective Wing Area (ft^2)	7633	7715	7633	7718
Span (ft)	134	135	134	135
Nozzle Weight (lb)	4131	4989	3973	4749
Total Pod Weight (lb)	16533	17535	16135	16958
Nozzle MFA (%)	30	85	37	86
Nozzle Suppression (dB)	8.9	16.5	10.1	16.7
FAR 25 Field Length (ft)	9822	9932	10211	10380
Wing Loading (lb/ft^2)	95.91	96.47	95.62	96.05
Thrust Loading	.2631	.2617	.2522	.2492
Design Mission				
Block Fuel (lb)	333647	338961	334216	339765
Block Time (hr)	4.61	4.62	4.57	4.59
Reserve Fuel (lb)	45546	46232	45001	45586
Total Fuel (lb)	377549	383531	377646	383774
Begin Supercruise Altitude (ft)	55523	55469	54686	54588
End Supercruise Altitude (ft)	64164	64076	63243	63014
L/D (Mid supercruise wt)	8.46	8.47	8.37	8.37
TSFC (Mid supercruise wt, lb/hr/lb)	1.284	1.284	1.283	1.283
RF (Mid supercruise wt, nm)	9070	9083	8983	8981
EI (Mid supercruise wt, lb/1000 lb)	7.99	7.99	8.00	8.00
Supercruise NO_X (lb)	1704	1721	1653	1647
Min PROC/Mach (ft/min)	500/2.40	500/2.40	500/2.40	500/2.40
Climb Time (min)	60.7	61.8	63.1	66.5
Approach Velocity (keas)	137.5	137.9	137.3	137.6
Economic Mission				
TOGW (lb)	576809	586904	572210	581024
Block Fuel (lb)	209344	212728	207634	210697
Block Time (hr)	4.01	4.01	3.96	3.97
L/D (Mid subcruise wt)	16.13	16.13	16.13	16.13
TSFC (Mid subcruise wt, lb/hr/lb)	1.109	1.106	1.093	1.089
RF (Mid subcruise wt, nm)	7613	7632	7725	7757
L/D (Mid supercruise wt)	8.46	8.47	8.37	8.36
TSFC (Mid supercruise wt, lb/hr/lb)	1.287	1.287	1.286	1.286
RF (Mid supercruise wt, nm)	9046	9060	8960	8950

Table 23.—MFTF3093 Results, 1993 Propulsion Ground rules, McDonnell Douglas HSCT

	Adv TO, Dry Throughout	Std TO, Dry Throughout	Adv TO, Transonic AB	Std TO, Transonic AB
Sized Airplane				
MTOGW (lb)		744524		
Landing Weight (lb)		397735		
OEW (lb)		325887		
SLS F_G (ISA + 18 °F, lb)		47920		
Effective Wing Area (ft^2)		9824		
Span (ft)		157		
Nozzle Weight (lb)		5039		
Total Pod Weight (lb)		17379		
Nozzle MFA (%)		90		
Nozzle Suppression (dB)		16.6		
FAR 25 Field Length (ft)		11000		
Wing Loading (lb/ft^2)		75.79		
Thrust Loading		.2575		
Design Mission				
Block Fuel (lb)		347727		
Block Time (hr)		5.29		
Reserve Fuel (lb)		10347		
Total Fuel (lb)		357137		
L/D (Mid subcruise wt)		14.73		
TSFC (Mid subcruise wt, lb/hr/lb)		1.100		
RF (Mid subcruise wt, nm)		7465		
EI (Mid subcruise wt, lb/1000 lb)		5.93		
Subcruise NO_X (lb)		381		
Begin Supercruise Altitude (ft)		57118		
End Supercruise Altitude (ft)		64292		
L/D (Mid supercruise wt)		8.95		
TSFC (Mid supercruise wt, lb/hr/lb)		1.288		
RF (Mid supercruise wt, nm)		9562		
EI (Mid supercruise wt, lb/1000 lb)		7.28		
Supercruise NO_X (lb)		1408		
Min PROC/Mach (ft/min)		1000/2.40		

Table 24.—MFTF3094 Results, 1994 Propulsion Ground rules, Boeing HSCT

	Adv TO, Dry Throughout	Std TO, Dry Throughout	Adv TO, Transonic AB	Std TO, Transonic AB
Sized Airplane				
MTOGW (lb)	752283	762237		
Landing Weight (lb)	405437	411295		
OEW (lb)	293283	298653		
SLS F_G (ISA + 18 °F, lb)	48867	49150		
Effective Wing Area (ft^2)	7903	7965		
Span (ft)	137	137		
Nozzle Weight (lb)	3769	4386		
Total Pod Weight (lb)	16943	17640		
Nozzle MFA (%)	38	85		
Nozzle Suppression (dB)	10.4	16.5		
FAR 25 Field Length (ft)	10247	10347		
Wing Loading (lb/ft^2)	95.95	96.33		
Thrust Loading	.2578	.2562		
Design Mission				
Block Fuel (lb)	348486	352590		
Block Time (hr)	4.62	4.63		
Reserve Fuel (lb)	47263	47753		
Total Fuel (lb)	394110	398694		
Begin Supercruise Altitude (ft)	53780	53713		
End Supercruise Altitude (ft)	62705	62596		
L/D (Mid supercruise wt)	8.35	8.35		
TSFC (Mid supercruise wt, lb/hr/lb)	1.316	1.316		
RF (Mid supercruise wt, nm)	8732	8733		
EI (Mid supercruise wt, lb/1000 lb)	5.68	5.68		
Supercruise NO_X (lb)	1246	1252		
Min PROC/Mach (ft/min)	500/2.40	500/2.40		
Climb Time (min)	66.5	67.8		
Approach Velocity (keas)	137.5	137.8		
Economic Mission				
TOGW (lb)	592653	599849		
Block Fuel (lb)	217431	219887		
Block Time (hr)	4.00	4.01		
L/D (Mid subcruise wt)	16.13	16.13		
TSFC (Mid subcruise wt, lb/hr/lb)	1.096	1.093		
RF (Mid subcruise wt, nm)	7711	7728		
L/D (Mid supercruise wt)	8.34	8.34		
TSFC (Mid supercruise wt, lb/hr/lb)	1.319	1.319		
RF (Mid supercruise wt, nm)	8704	8705		

Table 25.—MFTF3094 Results, 1994 Propulsion Ground rules, McDonnell Douglas HSCT

	Adv TO, Dry Throughout	Std TO, Dry Throughout	Adv TO, Transonic AB	Std TO, Transonic AB
Sized Airplane				
MTOGW (lb)	747574	765338		
Landing Weight (lb)	395604	406138		
OEW (lb)	323515	333833		
SLS F_G (ISA + 18 °F, lb)	49690	50507		
Effective Wing Area (ft^2)	9773	10047		
Span (ft)	156	159		
Nozzle Weight (lb)	3899	4626		
Total Pod Weight (lb)	17305	18264		
Nozzle MFA (%)	51	89		
Nozzle Suppression (dB)	12.9	16.8		
FAR 25 Field Length (ft)	11000	11000		
Wing Loading (lb/ft^2)	77.01	76.67		
Thrust Loading	.2641	.2623		
Design Mission				
Block Fuel (lb)	352963	360209		
Block Time (hr)	5.26	5.27		
Reserve Fuel (lb)	10590	10805		
Total Fuel (lb)	362559	370005		
L/D (Mid subcruise wt)	14.72	14.77		
TSFC (Mid subcruise wt, lb/hr/lb)	1.105	1.103		
RF (Mid subcruise wt, nm)	7427	7464		
EI (Mid subcruise wt, lb/1000 lb)	6.50	6.46		
Subcruise NO_X (lb)	425	430		
Begin Supercruise Altitude (ft)	56109	56045		
End Supercruise Altitude (ft)	63779	63679		
L/D (Mid supercruise wt)	8.93	8.96		
TSFC (Mid supercruise wt, lb/hr/lb)	1.331	1.331		
RF (Mid supercruise wt, nm)	9234	9272		
EI (Mid supercruise wt, lb/1000 lb)	5.18	5.18		
Supercruise NO_X (lb)	1061	1080		
Min PROC/Mach (ft/min)	1000/2.40	1000/2.40		

Table 26.—MFTF3193 Results, 1993 Propulsion Ground rules, Boeing HSCT

	Adv TO, Dry Throughout	Std TO, Dry Throughout	Adv TO, Transonic AB	Std TO, Transonic AB
Sized Airplane				
MTOGW (lb)	744152	756351		
Landing Weight (lb)	406954	413783		
OEW (lb)	295812	301951		
SLS F_G (ISA + 18 °F, lb)	49700	50233		
Effective Wing Area (ft^2)	7713	7798		
Span (ft)	135	136		
Nozzle Weight (lb)	4114	4950		
Total Pod Weight (lb)	17569	18556		
Nozzle MFA (%)	30	84		
Nozzle Suppression (dB)	8.8	16.5		
FAR 25 Field Length (ft)	9953	10061		
Wing Loading (lb/ft^2)	96.48	96.99		
Thrust Loading	.2671	.2657		
Design Mission				
Block Fuel (lb)	338870	344258		
Block Time (hr)	4.62	4.63		
Reserve Fuel (lb)	46253	46942		
Total Fuel (lb)	383450	389509		
Begin Supercruise Altitude (ft)	55583	55525		
End Supercruise Altitude (ft)	64213	64125		
L/D (Mid supercruise wt)	8.48	8.49		
TSFC (Mid supercruise wt, lb/hr/lb)	1.283	1.283		
RF (Mid supercruise wt, nm)	9097	9108		
EI (Mid supercruise wt, lb/1000 lb)	5.16	5.16		
Supercruise NO_X (lb)	1110	1121		
Min PROC/Mach (ft/min)	500/2.40	500/2.40		
Climb Time (min)	61.7	62.9		
Approach Velocity (keas)	137.9	138.3		
Economic Mission				
TOGW (lb)	586619	596651		
Block Fuel (lb)	212447	215804		
Block Time (hr)	4.01	4.01		
L/D (Mid subcruise wt)	16.13	16.12		
TSFC (Mid subcruise wt, lb/hr/lb)	1.102	1.099		
RF (Mid subcruise wt, nm)	7662	7680		
L/D (Mid supercruise wt)	8.48	8.49		
TSFC (Mid supercruise wt, lb/hr/lb)	1.286	1.286		
RF (Mid supercruise wt, nm)	9075	9086		

Table 27.—MFTF3293 Results, 1993 Propulsion Ground rules, Boeing HSCT

	Adv TO, Dry Throughout	Std TO, Dry Throughout	Adv TO, Transonic AB	Std TO, Transonic AB
Sized Airplane				
MTOGW (lb)	752782	766331		
Landing Weight (lb)	411121	418805		
OEW (lb)	299438	306352		
SLS F_G (ISA + 18 °F, lb)	49300	49933		
Effective Wing Area (ft^2)	7783	7875		
Span (ft)	136	137		
Nozzle Weight (lb)	4096	5030		
Total Pod Weight (lb)	18126	19249		
Nozzle MFA (%)	34	89		
Nozzle Suppression (dB)	9.5	16.8		
FAR 25 Field Length (ft)	10166	10278		
Wing Loading (lb/ft^2)	96.72	97.31		
Thrust Loading	.2620	.2606		
Design Mission				
Block Fuel (lb)	343340	349227		
Block Time (hr)	4.62	4.63		
Reserve Fuel (lb)	46793	47563		
Total Fuel (lb)	388454	395089		
Begin Supercruise Altitude (ft)	55319	55280		
End Supercruise Altitude (ft)	64022	63942		
L/D (Mid supercruise wt)	8.47	8.49		
TSFC (Mid supercruise wt, lb/hr/lb)	1.286	1.286		
RF (Mid supercruise wt, nm)	9064	9081		
EI (Mid supercruise wt, lb/1000 lb)	5.12	5.12		
Supercruise NO_X (lb)	1113	1126		
Min PROC/Mach (ft/min)	500/2.40	500/2.40		
Climb Time (min)	62.3	63.3		
Approach Velocity (keas)	138.1	138.5		
Economic Mission				
TOGW (lb)	593411	604734		
Block Fuel (lb)	215206	218995		
Block Time (hr)	4.01	4.02		
L/D (Mid subcruise wt)	16.12	16.12		
TSFC (Mid subcruise wt, lb/hr/lb)	1.100	1.097		
RF (Mid subcruise wt, nm)	7676	7692		
L/D (Mid supercruise wt)	8.47	8.48		
TSFC (Mid supercruise wt, lb/hr/lb)	1.289	1.289		
RF (Mid supercruise wt, nm)	9043	9054		

Table 28.—MFTF2093 Results, 1993 Propulsion Ground rules, Boeing HSCT

	Adv TO, Dry Throughout	Std TO, Dry Throughout	Adv TO, Transonic AB	Std TO, Transonic AB
Sized Airplane				
MTOGW (lb)	769157	776979	762432	769805
Landing Weight (lb)	420658	424899	414083	418162
OEW (lb)	307775	311584	302290	305970
SLS F_G (ISA + 18 °F, lb)	53750	54050	50133	50417
Effective Wing Area (ft^2)	7895	7950	7878	7928
Span (ft)	137	137	137	137
Nozzle Weight (lb)	4826	5343	4486	4997
Total Pod Weight (lb)	18952	19553	18012	18604
Nozzle MFA (%)	30	64	30	66
Nozzle Suppression (dB)	5.9	14.5	7.8	14.8
FAR 25 Field Length (ft)	9691	9764	10224	10299
Wing Loading (lb/ft^2)	97.42	97.73	96.78	97.10
Thrust Loading	.2795	.2783	.2630	.2620
Design Mission				
Block Fuel (lb)	350131	353722	349871	353174
Block Time (hr)	4.65	4.66	4.62	4.62
Reserve Fuel (lb)	47993	48424	46904	47302
Total Fuel (lb)	396491	400505	395252	398946
Begin Supercruise Altitude (ft)	55257	55207	54311	54280
End Supercruise Altitude (ft)	63633	63552	62170	62091
L/D (Mid supercruise wt)	8.46	8.47	8.34	8.34
TSFC (Mid supercruise wt, lb/hr/lb)	1.278	1.278	1.277	1.277
RF (Mid supercruise wt, nm)	9112	9123	8988	8991
EI (Mid supercruise wt, lb/1000 lb)	8.03	8.03	8.04	8.04
Supercruise NO_X (lb)	1736	1742	1612	1618
Min PROC/Mach (ft/min)	500/2.40	500/2.40	500/2.40	500/2.40
Climb Time (min)	67.0	68.2	75.3	76.2
Approach Velocity (keas)	138.6	138.8	138.1	138.4
Economic Mission				
TOGW (lb)	608099	614393	597741	603740
Block Fuel (lb)	220327	222486	216628	218636
Block Time (hr)	4.03	4.03	3.98	3.98
L/D (Mid subcruise wt)	16.12	16.11	16.12	16.12
TSFC (Mid subcruise wt, lb/hr/lb)	1.110	1.108	1.087	1.085
RF (Mid subcruise wt, nm)	7601	7613	7763	7779
L/D (Mid supercruise wt)	8.46	8.47	8.31	8.32
TSFC (Mid supercruise wt, lb/hr/lb)	1.282	1.282	1.280	1.280
RF (Mid supercruise wt, nm)	9086	9097	8940	8948

Table 29.—MFTF2093 Results, 1993 Propulsion Ground rules, McDonnell Douglas HSCT

	Adv TO, Dry Throughout	Std TO, Dry Throughout	Adv TO, Transonic AB	Std TO, Transonic AB
Sized Airplane				
MTOGW (lb)		763057		
Landing Weight (lb)		408198		
OEW (lb)		336110		
SLS F_G (ISA + 18 °F, lb)		51825		
Effective Wing Area (ft^2)		9732		
Span (ft)		156		
Nozzle Weight (lb)		5266		
Total Pod Weight (lb)		18862		
Nozzle MFA (%)		72		
Nozzle Suppression (dB)		14.7		
FAR 25 Field Length (ft)		11000		
Wing Loading (lb/ft^2)		78.41		
Thrust Loading		.2717		
Design Mission				
Block Fuel (lb)		355820		
Block Time (hr)		5.30		
Reserve Fuel (lb)		10588		
Total Fuel (lb)		365448		
L/D (Mid subcruise wt)		14.69		
TSFC (Mid subcruise wt, lb/hr/lb)		1.098		
RF (Mid subcruise wt, nm)		7460		
EI (Mid subcruise wt, lb/1000 lb)		5.90		
Subcruise NO_X (lb)		389		
Begin Supercruise Altitude (ft)		56462		
End Supercruise Altitude (ft)		63628		
L/D (Mid supercruise wt)		8.95		
TSFC (Mid supercruise wt, lb/hr/lb)		1.284		
RF (Mid supercruise wt, nm)		9594		
EI (Mid supercruise wt, lb/1000 lb)		7.31		
Supercruise NO_X (lb)		1430		
Min PROC/Mach (ft/min)		1000/2.40		

Table 30.—MFTF2094 Results, 1994 Propulsion Ground rules, Boeing HSCT

	Adv TO, Dry Throughout	Std TO, Dry Throughout	Adv TO, Transonic AB	Std TO, Transonic AB
Sized Airplane				
MTOGW (lb)	775769	781013		
Landing Weight (lb)	417771	420712		
OEW (lb)	305059	307704		
SLS F_G (ISA + 18 °F, lb)	50117	50367		
Effective Wing Area (ft^2)	8023	8058		
Span (ft)	138	138		
Nozzle Weight (lb)	4186	4540		
Total Pod Weight (lb)	18054	18481		
Nozzle MFA (%)	30	70		
Nozzle Suppression (dB)	7.8	15.2		
FAR 25 Field Length (ft)	10129	10170		
Wing Loading (lb/ft^2)	96.69	96.92		
Thrust Loading	.2584	.2580		
Design Mission				
Block Fuel (lb)	359620	361931		
Block Time (hr)	4.70	4.70		
Reserve Fuel (lb)	47822	48118		
Total Fuel (lb)	405820	408419		
Begin Supercruise Altitude (ft)	53578	53569		
End Supercruise Altitude (ft)	61854	61826		
L/D (Mid supercruise wt)	8.30	8.30		
TSFC (Mid supercruise wt, lb/hr/lb)	1.304	1.304		
RF (Mid supercruise wt, nm)	8760	8761		
EI (Mid supercruise wt, lb/1000 lb)	5.77	5.77		
Supercruise NO_X (lb)	1196	1201		
Min PROC/Mach (ft/min)	500/1.19	500/1.19		
Climb Time (min)	80.9	81.3		
Approach Velocity (keas)	138.1	138.2		
Economic Mission				
TOGW (lb)	606550	610909		
Block Fuel (lb)	222148	223626		
Block Time (hr)	4.05	4.05		
L/D (Mid subcruise wt)	16.13	16.13		
TSFC (Mid subcruise wt, lb/hr/lb)	1.078	1.077		
RF (Mid subcruise wt, nm)	7830	7836		
L/D (Mid supercruise wt)	8.29	8.30		
TSFC (Mid supercruise wt, lb/hr/lb)	1.307	1.307		
RF (Mid supercruise wt, nm)	8732	8743		

Table 31.—MFTF2094 Results, 1994 Propulsion Ground rules, McDonnell Douglas HSCT

	Adv TO, Dry Throughout	Std TO, Dry Throughout	Adv TO, Transonic AB	Std TO, Transonic AB
Sized Airplane				
MTOGW (lb)	768431	780480		
Landing Weight (lb)	408544	415578		
OEW (lb)	336305	343188		
SLS F_G (ISA + 18 °F, lb)	51430	51897		
Effective Wing Area (ft^2)	9895	10086		
Span (ft)	157	159		
Nozzle Weight (lb)	4334	4821		
Total Pod Weight (lb)	18585	19208		
Nozzle MFA (%)	39	76		
Nozzle Suppression (dB)	10.7	15.7		
FAR 25 Field Length (ft)	11000	11000		
Wing Loading (lb/ft^2)	77.66	77.38		
Thrust Loading	.2977	.2660		
Design Mission				
Block Fuel (lb)	360844	365868		
Block Time (hr)	5.28	5.28		
Reserve Fuel (lb)	10739	10889		
Total Fuel (lb)	370626	375792		
L/D (Mid subcruise wt)	14.73	14.78		
TSFC (Mid subcruise wt, lb/hr/lb)	1.094	1.093		
RF (Mid subcruise wt, nm)	7508	7542		
EI (Mid subcruise wt, lb/1000 lb)	5.99	5.95		
Subcruise NO_X (lb)	397	400		
Begin Supercruise Altitude (ft)	55549	55458		
End Supercruise Altitude (ft)	63238	63121		
L/D (Mid supercruise wt)	8.92	8.94		
TSFC (Mid supercruise wt, lb/hr/lb)	1.318	1.318		
RF (Mid supercruise wt, nm)	9320	9339		
EI (Mid supercruise wt, lb/1000 lb)	5.35	5.35		
Supercruise NO_X (lb)	1096	1109		
Min PROC/Mach (ft/min)	1000/2.40	1000/2.40		

Table 32.—MFTF2193 Results, 1993 Propulsion Ground rules, Boeing HSCT

	Adv TO, Dry Throughout	Std TO, Dry Throughout	Adv TO, Transonic AB	Std TO, Transonic AB
Sized Airplane				
MTOGW (lb)	775058	783545		
Landing Weight (lb)	423458	428068		
OEW (lb)	310276	314430		
SLS F_G (ISA + 18 °F, lb)	53233	53517		
Effective Wing Area (ft^2)	7943	8000		
Span (ft)	137	138		
Nozzle Weight (lb)	4780	5364		
Total Pod Weight (lb)	19353	20018		
Nozzle MFA (%)	30	69		
Nozzle Suppression (dB)	6.2	15.0		
FAR 25 Field Length (ft)	9867	9958		
Wing Loading (lb/ft^2)	97.58	97.94		
Thrust Loading	.2747	.2732		
Design Mission				
Block Fuel (lb)	353272	357157		
Block Time (hr)	4.66	4.67		
Reserve Fuel (lb)	48291	48748		
Total Fuel (lb)	399891	404225		
Begin Supercruise Altitude (ft)	55139	55065		
End Supercruise Altitude (ft)	63561	63456		
L/D (Mid supercruise wt)	8.46	8.46		
TSFC (Mid supercruise wt, lb/hr/lb)	1.279	1.279		
RF (Mid supercruise wt, nm)	9102	9106		
EI (Mid supercruise wt, lb/1000 lb)	5.14	5.14		
Supercruise NO_X (lb)	1116	1120		
Min PROC/Mach (ft/min)	500/2.40	500/2.40		
Climb Time (min)	68.1	69.4		
Approach Velocity (keas)	138.7	139.0		
Economic Mission				
TOGW (lb)	612369	619251		
Block Fuel (lb)	221932	224314		
Block Time (hr)	4.03	4.04		
L/D (Mid subcruise wt)	16.12	16.12		
TSFC (Mid subcruise wt, lb/hr/lb)	1.104	1.101		
RF (Mid subcruise wt, nm)	7643	7662		
L/D (Mid supercruise wt)	8.46	8.46		
TSFC (Mid supercruise wt, lb/hr/lb)	1.283	1.283		
RF (Mid supercruise wt, nm)	9079	9084		

Table 33.—MFTF2293 Results, 1993 Propulsion Ground rules, Boeing HSCT

	Adv TO, Dry Throughout	Std TO, Dry Throughout	Adv TO, Transonic AB	Std TO, Transonic AB
Sized Airplane				
MTOGW (lb)	781170	790483		
Landing Weight (lb)	427963	431918		
OEW (lb)	314236	317808		
SLS F_G (ISA + 18 °F, lb)	53617	53333		
Effective Wing Area (ft^2)	7973	8050		
Span (ft)	137	138		
Nozzle Weight (lb)	4780	5350		
Total Pod Weight (lb)	20115	20599		
Nozzle MFA (%)	30	71		
Nozzle Suppression (dB)	6.1	15.1		
FAR 25 Field Length (ft)	9907	10099		
Wing Loading (lb/ft^2)	97.98	98.20		
Thrust Loading	.2745	.2699		
Design Mission				
Block Fuel (lb)	354911	360261		
Block Time (hr)	4.64	4.67		
Reserve Fuel (lb)	48837	49219		
Total Fuel (lb)	402044	407784		
Begin Supercruise Altitude (ft)	55276	55078		
End Supercruise Altitude (ft)	63853	63527		
L/D (Mid supercruise wt)	8.50	8.48		
TSFC (Mid supercruise wt, lb/hr/lb)	1.279	1.279		
RF (Mid supercruise wt, nm)	9149	9130		
EI (Mid supercruise wt, lb/1000 lb)	5.12	5.12		
Supercruise NO_X (lb)	1133	1117		
Min PROC/Mach (ft/min)	500/2.40	500/2.40		
Climb Time (min)	65.1	70.4		
Approach Velocity (keas)	139.0	139.1		
Economic Mission				
TOGW (lb)	618460	624867		
Block Fuel (lb)	223574	226178		
Block Time (hr)	4.03	4.04		
L/D (Mid subcruise wt)	16.12	16.12		
TSFC (Mid subcruise wt, lb/hr/lb)	1.104	1.098		
RF (Mid subcruise wt, nm)	7642	7687		
L/D (Mid supercruise wt)	8.50	8.48		
TSFC (Mid supercruise wt, lb/hr/lb)	1.282	1.282		
RF (Mid supercruise wt, nm)	9125	9106		

Table 34.—MFTF1093 Results, 1993 Propulsion Ground rules, Boeing HSCT

	Adv TO, Dry Throughout	Std TO, Dry Throughout	Adv TO, Transonic AB	Std TO, Transonic AB
Sized Airplane				
MTOGW (lb)	848853	854460	835693	842248
Landing Weight (lb)	457572	460465	455194	459057
OEW (lb)	339788	342409	338230	341698
SLS F_G (ISA + 18 °F, lb)	59350	59400	58917	59350
Effective Wing Area (ft^2)	8545	8583	8388	8428
Span (ft)	142	143	141	141
Nozzle Weight (lb)	5882	6282	5837	6277
Total Pod Weight (lb)	22589	23005	22944	23516
Nozzle MFA (%)	30	55	30	55
Nozzle Suppression (dB)	3.9	13.1	3.9	13.0
FAR 25 Field Length (ft)	10230	10311	10176	10211
Wing Loading (lb/ft^2)	99.34	99.55	99.63	99.93
Thrust Loading	.2798	.2781	.2820	.2819
Design Mission				
Block Fuel (lb)	392992	395708	382198	384902
Block Time (hr)	4.80	4.81	4.61	4.61
Reserve Fuel (lb)	52894	53166	52073	52470
Total Fuel (lb)	444174	447161	432572	435660
Begin Supercruise Altitude (ft)	54753	54700	54412	54415
End Supercruise Altitude (ft)	62386	62267	62356	62355
L/D (Mid supercruise wt)	8.44	8.44	8.45	8.46
TSFC (Mid supercruise wt, lb/hr/lb)	1.284	1.284	1.284	1.284
RF (Mid supercruise wt, nm)	9046	9046	9058	9069
EI (Mid supercruise wt, lb/1000 lb)	8.53	8.53	8.53	8.53
Supercruise NO_X (lb)	1780	1775	1870	1884
Min PROC/Mach (ft/min)	500/2.40	500/2.40	500/2.40	500/2.40
Climb Time (min)	92.8	94.3	74.3	74.2
Approach Velocity (keas)	139.9	140.1	140.2	140.4
Economic Mission				
TOGW (lb)	670909	675461	661308	666913
Block Fuel (lb)	247254	248984	239829	241650
Block Time (hr)	4.12	4.13	3.97	3.97
L/D (Mid subcruise wt)	16.10	16.10	16.09	16.08
TSFC (Mid subcruise wt, lb/hr/lb)	1.114	1.111	1.118	1.117
RF (Mid subcruise wt, nm)	7568	7591	7540	7542
L/D (Mid supercruise wt)	8.44	8.43	8.44	8.45
TSFC (Mid supercruise wt, lb/hr/lb)	1.289	1.288	1.288	1.288
RF (Mid supercruise wt, nm)	9015	9007	9019	9029

Table 35.—MFTF1093 Results, 1993 Propulsion Ground rules, McDonnell Douglas HSCT

	Adv TO, Dry Throughout	Std TO, Dry Throughout	Adv TO, Transonic AB	Std TO, Transonic AB
Sized Airplane				
MTOGW (lb)		825610		
Landing Weight (lb)		441370		
OEW (lb)		368402		
SLS F_G (ISA + 18 °F, lb)		57483		
Effective Wing Area (ft^2)		10364		
Span (ft)		161		
Nozzle Weight (lb)		5970		
Total Pod Weight (lb)		22126		
Nozzle MFA (%)		51		
Nozzle Suppression (dB)		11.1		
FAR 25 Field Length (ft)		11000		
Wing Loading (lb/ft^2)		79.66		
Thrust Loading		.2785		
Design Mission				
Block Fuel (lb)		385226		
Block Time (hr)		5.33		
Reserve Fuel (lb)		11468		
Total Fuel (lb)		395708		
L/D (Mid subcruise wt)		14.80		
TSFC (Mid subcruise wt, lb/hr/lb)		1.110		
RF (Mid subcruise wt, nm)		7432		
EI (Mid subcruise wt, lb/1000 lb)		5.81		
Subcruise NO_X (lb)		415		
Begin Supercruise Altitude (ft)		55862		
End Supercruise Altitude (ft)		62868		
L/D (Mid supercruise wt)		9.07		
TSFC (Mid supercruise wt, lb/hr/lb)		1.293		
RF (Mid supercruise wt, nm)		9657		
EI (Mid supercruise wt, lb/1000 lb)		8.28		
Supercruise NO_X (lb)		1694		
Min PROC/Mach (ft/min)		1000/2.40		

Table 36.—MFTF1094 Results, 1994 Propulsion Ground rules, Boeing HSCT

	Adv TO, Dry Throughout	Std TO, Dry Throughout	Adv TO, Transonic AB	Std TO, Transonic AB
Sized Airplane				
MTOGW (lb)	840372	842971		
Landing Weight (lb)	451218	452278		
OEW (lb)	334102	335053		
SLS F_G (ISA + 18 °F, lb)	58383	58300		
Effective Wing Area (ft^2)	8508	8528		
Span (ft)	142	142		
Nozzle Weight (lb)	5223	5376		
Total Pod Weight (lb)	21686	21814		
Nozzle MFA (%)	30	53		
Nozzle Suppression (dB)	4.1	12.8		
FAR 25 Field Length (ft)	9946	9998		
Wing Loading (lb/ft^2)	98.77	98.85		
Thrust Loading	.2779	.2766		
Design Mission				
Block Fuel (lb)	390854	392390		
Block Time (hr)	4.74	4.75		
Reserve Fuel (lb)	52226	52335		
Total Fuel (lb)	441381	443028		
Begin Supercruise Altitude (ft)	53302	53250		
End Supercruise Altitude (ft)	61241	61122		
L/D (Mid supercruise wt)	8.33	8.32		
TSFC (Mid supercruise wt, lb/hr/lb)	1.318	1.318		
RF (Mid supercruise wt, nm)	8700	8690		
EI (Mid supercruise wt, lb/1000 lb)	6.01	6.01		
Supercruise NO_X (lb)	1310	1306		
Min PROC/Mach (ft/min)	500/1.20	500/1.07		
Climb Time (min)	87.5	88.9		
Approach Velocity (keas)	139.6	139.6		
Economic Mission				
TOGW (lb)	660679	662566		
Block Fuel (lb)	243478	244343		
Block Time (hr)	4.08	4.08		
L/D (Mid subcruise wt)	16.11	16.11		
TSFC (Mid subcruise wt, lb/hr/lb)	1.096	1.094		
RF (Mid subcruise wt, nm)	7693	7708		
L/D (Mid supercruise wt)	8.30	8.29		
TSFC (Mid supercruise wt, lb/hr/lb)	1.321	1.321		
RF (Mid supercruise wt, nm)	8650	8638		

Table 37.—MFTF1094 Results, 1994 Propulsion Ground rules, McDonnell Douglas HSCT

	Adv TO, Dry Throughout	Std TO, Dry Throughout	Adv TO, Transonic AB	Std TO, Transonic AB
Sized Airplane				
MTOGW (lb)	824335	831195		
Landing Weight (lb)	436635	440547		
OEW (lb)	363564	367389		
SLS F_G (ISA + 18 °F, lb)	57947	58192		
Effective Wing Area (ft^2)	10294	10407		
Span (ft)	160	161		
Nozzle Weight (lb)	5182	5430		
Total Pod Weight (lb)	21516	21848		
Nozzle MFA (%)	30	57		
Nozzle Suppression (dB)	7.7	13.5		
FAR 25 Field Length (ft)	11000	11000		
Wing Loading (lb/ft^2)	80.08	79.87		
Thrust Loading	.2812	.2800		
Design Mission				
Block Fuel (lb)	388709	391661		
Block Time (hr)	5.30	5.30		
Reserve Fuel (lb)	11570	11659		
Total Fuel (lb)	399270	402306		
L/D (Mid subcruise wt)	14.78	14.80		
TSFC (Mid subcruise wt, lb/hr/lb)	1.096	1.095		
RF (Mid subcruise wt, nm)	7515	7534		
EI (Mid subcruise wt, lb/1000 lb)	5.59	5.59		
Subcruise NO_X (lb)	394	396		
Begin Supercruise Altitude (ft)	54700	54652		
End Supercruise Altitude (ft)	62267	62184		
L/D (Mid supercruise wt)	8.99	9.00		
TSFC (Mid supercruise wt, lb/hr/lb)	1.341	1.341		
RF (Mid supercruise wt, nm)	9228	9237		
EI (Mid supercruise wt, lb/1000 lb)	5.85	5.85		
Supercruise NO_X (lb)	1269	1276		
Min PROC/Mach (ft/min)	1000/2.40	1000/2.40		

Table 38.—MFTF1193 Results, 1993 Propulsion Ground rules, Boeing HSCT

	Adv TO, Dry Throughout	Std TO, Dry Throughout	Adv TO, Transonic AB	Std TO, Transonic AB
Sized Airplane				
MTOGW (lb)	852451	857833		
Landing Weight (lb)	460382	463245		
OEW (lb)	342248	344839		
SLS F_G (ISA + 18 °F, lb)	59483	59583		
Effective Wing Area (ft^2)	8558	8593		
Span (ft)	142	143		
Nozzle Weight (lb)	5870	6257		
Total Pod Weight (lb)	23090	23508		
Nozzle MFA (%)	30	54		
Nozzle Suppression (dB)	3.9	12.8		
FAR 25 Field Length (ft)	10012	10080		
Wing Loading (lb/ft^2)	99.61	99.83		
Thrust Loading	.2791	.2778		
Design Mission				
Block Fuel (lb)	393798	396321		
Block Time (hr)	4.79	4.80		
Reserve Fuel (lb)	53244	53516		
Total Fuel (lb)	445313	448104		
Begin Supercruise Altitude (ft)	54804	54768		
End Supercruise Altitude (ft)	62428	62327		
L/D (Mid supercruise wt)	8.45	8.45		
TSFC (Mid supercruise wt, lb/hr/lb)	1.283	1.283		
RF (Mid supercruise wt, nm)	9069	9071		
EI (Mid supercruise wt, lb/1000 lb)	5.14	5.14		
Supercruise NO_X (lb)	1097	1095		
Min PROC/Mach (ft/min)	500/1.07	500/1.07		
Climb Time (min)	89.8	91.1		
Approach Velocity (keas)	140.1	140.3		
Economic Mission				
TOGW (lb)	674743	679292		
Block Fuel (lb)	248296	250035		
Block Time (hr)	4.11	4.12		
L/D (Mid subcruise wt)	16.11	16.09		
TSFC (Mid subcruise wt, lb/hr/lb)	1.116	1.113		
RF (Mid subcruise wt, nm)	7557	7571		
L/D (Mid supercruise wt)	8.44	8.44		
TSFC (Mid supercruise wt, lb/hr/lb)	1.287	1.287		
RF (Mid supercruise wt, nm)	9029	9030		

Table 39.—MFTF1293 Results, 1993 Propulsion Ground rules, Boeing HSCT

	Adv TO, Dry Throughout	Std TO, Dry Throughout	Adv TO, Transonic AB	Std TO, Transonic AB
Sized Airplane				
MTOGW (lb)	861224	868978		
Landing Weight (lb)	464079	469128		
OEW (lb)	345376	349879		
SLS F_G (ISA + 18 °F, lb)	58733	59617		
Effective Wing Area (ft^2)	8633	8675		
Span (ft)	143	143		
Nozzle Weight (lb)	5768	6253		
Total Pod Weight (lb)	23528	24293		
Nozzle MFA (%)	30	55		
Nozzle Suppression (dB)	3.9	13.0		
FAR 25 Field Length (ft)	10252	10233		
Wing Loading (lb/ft^2)	99.76	100.17		
Thrust Loading	.2728	.2744		
Design Mission				
Block Fuel (lb)	398871	401603		
Block Time (hr)	4.81	4.80		
Reserve Fuel (lb)	53813	54359		
Total Fuel (lb)	450958	454209		
Begin Supercruise Altitude (ft)	54679	54747		
End Supercruise Altitude (ft)	62222	62372		
L/D (Mid supercruise wt)	8.44	8.47		
TSFC (Mid supercruise wt, lb/hr/lb)	1.285	1.285		
RF (Mid supercruise wt, nm)	9047	9071		
EI (Mid supercruise wt, lb/1000 lb)	5.11	5.11		
Supercruise NO_X (lb)	1085	1108		
Min PROC/Mach (ft/min)	500/1.21	500/2.40		
Climb Time (min)	92.7	90.5		
Approach Velocity (keas)	140.2	140.5		
Economic Mission				
TOGW (lb)	681374	688315		
Block Fuel (lb)	251356	253321		
Block Time (hr)	4.13	4.12		
L/D (Mid subcruise wt)	16.09	16.08		
TSFC (Mid subcruise wt, lb/hr/lb)	1.112	1.115		
RF (Mid subcruise wt, nm)	7575	7555		
L/D (Mid supercruise wt)	8.43	8.45		
TSFC (Mid supercruise wt, lb/hr/lb)	1.289	1.289		
RF (Mid supercruise wt, nm)	9006	9028		

Table 40.—VCE701510 Results, 1993 Propulsion Ground rules, Boeing HSCT

	Adv TO, Dry Throughout	Std TO, Dry Throughout	Adv TO, Transonic AB	Std TO, Transonic AB
Sized Airplane				
MTOGW (lb)	714108	732155	718794	737021
Landing Weight (lb)	384193	394224	386288	395840
OEW (lb)	273193	282137	275022	283525
SLS F_G (ISA + 18 °F, lb)	44250	44933	44250	44567
Effective Wing Area (ft^2)	7610	7735	7648	7785
Span (ft)	134	135	135	136
Bare Engine Weight (lb)	6043	6142	6288	6336
Nozzle Weight (lb)	3341	4613	3341	4574
Total Pod Weight (lb)	13738	15179	13983	15296
Nozzle MFA (%)	52	127	52	127
Nozzle Suppression (dB)	12.3	19.1	12.3	19.1
FAR 25 Field Length (ft)	10299	10487	10382	10644
Wing Loading (lb/ft^2)	93.84	94.65	93.98	94.67
Thrust Loading	.2479	.2455	.2462	.2419
Design Mission				
Block Fuel (lb)	331726	339770	334316	343005
Block Time (hr)	4.52	4.53	4.50	4.52
Reserve Fuel (lb)	46110	47196	46375	47425
Total Fuel (lb)	376025	385128	378881	388606
Begin Supercruise Altitude (ft)	55250	55142	55123	54899
End Supercruise Altitude (ft)	64446	64283	64332	64001
L/D (Mid supercruise wt)	8.40	8.41	8.40	8.39
TSFC (Mid supercruise wt, lb/hr/lb)	1.326	1.326	1.326	1.326
RF (Mid supercruise wt, nm)	8720	8734	8717	8715
EI (Mid supercruise wt, lb/1000 lb)	8.54	8.53	8.54	8.54
Supercruise NO_X (lb)	1850	1876	1859	1864
Min PROC/Mach (ft/min)	500/2.40	500/2.40	500/2.40	500/2.40
Climb Time (min)	52.7	54.3	51.8	55.7
Approach Velocity (keas)	136.0	136.6	136.1	136.6
Economic Mission				
TOGW (lb)	555597	570460	559216	573730
Block Fuel (lb)	204632	209704	206221	211432
Block Time (hr)	3.94	3.95	3.93	3.94
L/D (Mid subcruise wt)	16.12	16.14	16.12	16.13
TSFC (Mid subcruise wt, lb/hr/lb)	1.095	1.094	1.094	1.091
RF (Mid subcruise wt, nm)	7706	7727	7713	7740
L/D (Mid supercruise wt)	8.40	8.41	8.40	8.39
TSFC (Mid supercruise wt, lb/hr/lb)	1.329	1.329	1.329	1.328
RF (Mid supercruise wt, nm)	8703	8716	8700	8695

Table 41.—VCE703010 Results, 1993 Propulsion Ground rules, Boeing HSCT

	Adv TO, Dry Throughout	Std TO, Dry Throughout	Adv TO, Transonic AB	Std TO, Transonic AB
Sized Airplane				
MTOGW (lb)	732242	749371	737154	754079
Landing Weight (lb)	394931	403216	396224	404400
OEW (lb)	281680	289101	282839	290154
SLS F_G (ISA + 18 °F, lb)	46033	45917	45400	45300
Effective Wing Area (ft^2)	7745	7878	7798	7930
Span (ft)	135	137	136	137
Bare Engine Weight (lb)	6403	6387	6582	6567
Nozzle Weight (lb)	3593	4721	3549	4655
Total Pod Weight (lb)	14841	15939	14906	15985
Nozzle MFA (%)	40	119	43	119
Nozzle Suppression (dB)	10.0	18.5	10.5	18.5
FAR 25 Field Length (ft)	10279	10606	10488	10812
Wing Loading (lb/ft^2)	94.54	95.12	94.53	95.09
Thrust Loading	.2515	.2451	.2464	.2403
Design Mission				
Block Fuel (lb)	339104	347944	342698	351443
Block Time (hr)	4.54	4.56	4.52	4.55
Reserve Fuel (lb)	48361	49225	48495	49356
Total Fuel (lb)	385671	395380	389425	399035
Begin Supercruise Altitude (ft)	54920	54659	54644	54425
End Supercruise Altitude (ft)	63842	63341	63429	62929
L/D (Mid supercruise wt)	8.38	8.36	8.35	8.33
TSFC (Mid supercruise wt, lb/hr/lb)	1.314	1.314	1.314	1.313
RF (Mid supercruise wt, nm)	8781	8761	8750	8731
EI (Mid supercruise wt, lb/1000 lb)	8.95	8.96	8.96	8.96
Supercruise NO_X (lb)	1919	1893	1889	1856
Min PROC/Mach (ft/min)	500/2.40	500/2.40	500/2.40	500/2.40
Climb Time (min)	58.0	64.6	60.4	67.3
Approach Velocity (keas)	136.5	136.9	136.5	136.9
Economic Mission				
TOGW (lb)	575724	588461	578526	591079
Block Fuel (lb)	213797	218487	215393	220006
Block Time (hr)	3.95	3.96	3.94	3.94
L/D (Mid subcruise wt)	16.13	16.14	16.13	16.14
TSFC (Mid subcruise wt, lb/hr/lb)	1.194	1.183	1.185	1.174
RF (Mid subcruise wt, nm)	7072	7145	7126	7195
L/D (Mid supercruise wt)	8.38	8.36	8.35	8.33
TSFC (Mid supercruise wt, lb/hr/lb)	1.317	1.316	1.317	1.316
RF (Mid supercruise wt, nm)	8760	8742	8730	8712

Table 42.—VCE706520 Results, 1993 Propulsion Ground rules, Boeing HSCT

	Adv TO, Dry Throughout	Std TO, Dry Throughout	Adv TO, Transonic AB	Std TO, Transonic AB
Sized Airplane				
MTOGW (lb)	778601	790722	783294	795525
Landing Weight (lb)	420824	427558	423385	430327
OEW (lb)	306244	312253	308552	314761
SLS F_G (ISA + 18 °F, lb)	52317	52833	52317	52883
Effective Wing Area (ft^2)	8045	8130	8080	8160
Span (ft)	138	139	138	139
Bare Engine Weight (lb)	7613	7692	7985	8076
Nozzle Weight (lb)	4264	5075	4264	5113
Total Pod Weight (lb)	18343	19300	18715	19728
Nozzle MFA (%)	30	81	30	82
Nozzle Suppression (dB)	6.2	16.1	6.2	16.1
FAR 25 Field Length (ft)	9971	10076	10047	10151
Wing Loading (lb/ft^2)	96.78	97.26	96.94	97.49
Thrust Loading	.2688	.2673	.2672	.2659
Design Mission				
Block Fuel (lb)	359592	364997	361724	367032
Block Time (hr)	4.61	4.61	4.54	4.55
Reserve Fuel (lb)	49689	50414	49942	50676
Total Fuel (lb)	407467	413579	409852	415874
Begin Supercruise Altitude (ft)	54104	54099	53960	53926
End Supercruise Altitude (ft)	61959	61853	61810	61721
L/D (Mid supercruise wt)	8.31	8.32	8.31	8.32
TSFC (Mid supercruise wt, lb/hr/lb)	1.299	1.299	1.299	1.299
RF (Mid supercruise wt, nm)	8804	8815	8805	8816
EI (Mid supercruise wt, lb/1000 lb)	10.73	10.73	10.74	10.73
Supercruise NO_X (lb)	2134	2136	2152	2172
Min PROC/Mach (ft/min)	500/2.40	500/2.40	500/2.40	500/2.40
Climb Time (min)	79.7	81.7	75.7	76.6
Approach Velocity (keas)	138.1	138.5	138.3	138.6
Economic Mission				
TOGW (lb)	607211	617185	611139	621338
Block Fuel (lb)	220347	223746	221764	225162
Block Time (hr)	3.98	3.99	3.94	3.94
L/D (Mid subcruise wt)	16.13	16.13	16.13	16.13
TSFC (Mid subcruise wt, lb/hr/lb)	1.037	1.036	1.036	1.035
RF (Mid subcruise wt, nm)	8150	8156	8155	8161
L/D (Mid supercruise wt)	8.30	8.31	8.29	8.31
TSFC (Mid supercruise wt, lb/hr/lb)	1.304	1.304	1.303	1.303
RF (Mid supercruise wt, nm)	8764	8771	8753	8771

Table 43.—VCE708020 Results, 1993 Propulsion Ground rules, Boeing HSCT

	Adv TO, Dry Throughout	Std TO, Dry Throughout	Adv TO, Transonic AB	Std TO, Transonic AB
Sized Airplane				
MTOGW (lb)	846074	856848		
Landing Weight (lb)	453224	459009		
OEW (lb)	330983	336131		
SLS F_G (ISA + 18 °F, lb)	57267	57667		
Effective Wing Area (ft^2)	8623	8695		
Span (ft)	143	144		
Bare Engine Weight (lb)	8606	8669		
Nozzle Weight (lb)	4906	5601		
Total Pod Weight (lb)	20929	21741		
Nozzle MFA (%)	30	72		
Nozzle Suppression (dB)	5.2	14.9		
FAR 25 Field Length (ft)	10090	10191		
Wing Loading (lb/ft^2)	98.12	98.54		
Thrust Loading	.2707	.2692		
Design Mission				
Block Fuel (lb)	396104	401116		
Block Time (hr)	4.66	4.67		
Reserve Fuel (lb)	57351	57988		
Total Fuel (lb)	450201	455827		
Begin Supercruise Altitude (ft)	54105	54103		
End Supercruise Altitude (ft)	61795	61686		
L/D (Mid supercruise wt)	8.37	8.38		
TSFC (Mid supercruise wt, lb/hr/lb)	1.302	1.302		
RF (Mid supercruise wt, nm)	8849	8859		
EI (Mid supercruise wt, lb/1000 lb)	11.07	11.07		
Supercruise NO_X (lb)	2298	2290		
Min PROC/Mach (ft/min)	500/2.40	500/2.40		
Climb Time (min)	86.6	89.0		
Approach Velocity (keas)	139.1	139.4		
Economic Mission				
TOGW (lb)	664291	672924		
Block Fuel (lb)	246861	249867		
Block Time (hr)	4.01	4.01		
L/D (Mid subcruise wt)	16.12	16.11		
TSFC (Mid subcruise wt, lb/hr/lb)	1.072	1.070		
RF (Mid subcruise wt, nm)	7872	7884		
L/D (Mid supercruise wt)	8.36	8.37		
TSFC (Mid supercruise wt, lb/hr/lb)	1.304	1.304		
RF (Mid supercruise wt, nm)	8825	8832		

Table 44.—F193 Results, 1993 Propulsion Ground rules, Boeing HSCT

	Adv TO, Dry, 10% Oversize			
Sized Airplane				
MTOGW (lb)	748373			
Landing Weight (lb)	402409			
OEW (lb)	293082			
SLS F_G (ISA + 18 °F, lb)	55569			
Effective Wing Area (ft^2)	7813			
Span (ft)	136			
Total Pod Weight (lb)	16286			
FAR 25 Field Length (ft)	8764			
Wing Loading (lb/ft^2)	95.79			
Thrust Loading	.2970			
Design Mission				
Block Fuel (lb)	347998			
Block Time (hr)	4.47			
Reserve Fuel (lb)	44448			
Total Fuel (lb)	390401			
Begin Supercruise Altitude (ft)	56059			
End Supercruise Altitude (ft)	65701			
L/D (Mid supercruise wt)	8.54			
TSFC (Mid supercruise wt, lb/hr/lb)	1.348			
RF (Mid supercruise wt, nm)	8719			
EI (Mid supercruise wt, lb/1000 lb)	7.51			
Supercruise NO_X (lb)	1853			
Min PROC/Mach (ft/min)	500/2.40			
Climb Time (min)	39.1			
Approach Velocity (keas)	137.4			
Economic Mission				
TOGW (lb)	582545			
Block Fuel (lb)	213831			
Block Time (hr)	3.94			
L/D (Mid subcruise wt)	16.14			
TSFC (Mid subcruise wt, lb/hr/lb)	1.026			
RF (Mid subcruise wt, nm)	8239			
L/D (Mid supercruise wt)	8.54			
TSFC (Mid supercruise wt, lb/hr/lb)	1.352			
RF (Mid supercruise wt, nm)	8698			

Table 45.—AIV222, AIV216, AIV209, AIV202 Results,
1993 Propulsion Ground rules, Boeing HSCT

	AIV222	AIV216	AIV209	AIV202
Sized Airplane				
MTOGW (lb)	778344	757651	751757	745472
Landing Weight (lb)	417097	406812	403385	400645
OEW (lb)	304563	296159	293107	290770
SLS F_G (ISA + 18 °F, lb)	43667	41267	39783	39033
Effective Wing Area (ft^2)	8063	7898	7858	7803
Span (ft)	138	137	136	136
Total Pod Weight (lb)	17023	16059	15668	15443
FAR 25 Field Length (ft)	9891	10132	10524	10859
Wing Loading (lb/ft^2)	96.53	95.93	95.67	95.54
Thrust Loading	.2244	.2179	.2117	.2094
Design Mission				
Block Fuel (lb)	368716	351902	349550	346158
Block Time (hr)	4.56	4.56	4.54	4.55
Reserve Fuel (lb)	47644	45762	45388	44985
Total Fuel (lb)	408891	396601	393760	389812
Begin Supercruise Altitude (ft)	54015	54010	54034	53960
End Supercruise Altitude (ft)	62103	62185	62340	62702
L/D (Mid supercruise wt)	8.31	8.29	8.29	8.29
TSFC (Mid supercruise wt, lb/hr/lb)	1.337	1.337	1.338	1.339
RF (Mid supercruise wt, nm)	8555	8532	8528	8520
EI (Mid supercruise wt, lb/1000 lb)	7.47	7.15	7.45	6.79
Supercruise NO_X (lb)	1519	1430	1503	1397
Min PROC/Mach (ft/min)	500/2.40	500/2.40	500/2.40	500/2.40
Climb Time (min)	77.9	77.0	73.4	71.1
Approach Velocity (keas)	138.0	137.5	137.3	137.2
Economic Mission				
TOGW (lb)	603471	585896	580931	575886
Block Fuel (lb)	225967	212120	210637	208435
Block Time (hr)	3.94	3.94	3.93	3.94
L/D (Mid subcruise wt)	15.50	15.54	15.56	15.57
TSFC (Mid subcruise wt, lb/hr/lb)	1.023	1.025	1.027	1.030
RF (Mid subcruise wt, nm)	7819	7829	7817	7806
L/D (Mid supercruise wt)	8.30	8.28	8.28	8.29
TSFC (Mid supercruise wt, lb/hr/lb)	1.340	1.340	1.341	1.342
RF (Mid supercruise wt, nm)	8529	8505	8503	8507

Table 46.—AIV196, AIV189, AIV181, AIV139 Results,
1993 Propulsion Ground rules, Boeing HSCT

	AIV196	AIV189	AIV181	AIV139
Sized Airplane				
MTOGW (lb)	739387	737166	728173	869077
Landing Weight (lb)	397224	396418	394366	456572
OEW (lb)	287585	286904	285221	337396
SLS F_G (ISA + 18 °F, lb)	37250	36883	36567	45417
Effective Wing Area (ft^2)	7763	7738	7635	8835
Span (ft)	136	135	134	145
Total Pod Weight (lb)	15052	15027	15111	20893
FAR 25 Field Length (ft)	10922	11000	11000	11000
Wing Loading (lb/ft^2)	95.25	95.27	95.37	98.37
Thrust Loading	.2015	.2001	.2009	.2090
Design Mission				
Block Fuel (lb)	343264	341909	335060	414091
Block Time (hr)	4.55	4.54	4.50	4.73
Reserve Fuel (lb)	44749	44624	44255	54286
Total Fuel (lb)	386912	385373	378062	466790
Begin Supercruise Altitude (ft)	54287	54652	54735	57599
End Supercruise Altitude (ft)	62878	63560	64534	66736
L/D (Mid supercruise wt)	8.32	8.37	8.44	8.62
TSFC (Mid supercruise wt, lb/hr/lb)	1.343	1.344	1.349	1.371
RF (Mid supercruise wt, nm)	8523	8571	8615	8656
EI (Mid supercruise wt, lb/1000 lb)	7.37	7.07	6.69	5.23
Supercruise NO_X (lb)	1516	1513	1469	1361
Min PROC/Mach (ft/min)	500/2.40	500/2.40	500/2.40	500/2.40
Climb Time (min)	69.9	63.0	54.2	65.5
Approach Velocity (keas)	137.0	137.0	137.1	139.3
Economic Mission				
TOGW (lb)	570974	570271	564790	669397
Block Fuel (lb)	206658	206736	203209	247961
Block Time (hr)	3.94	3.94	3.93	4.00
L/D (Mid subcruise wt)	15.59	15.57	15.56	15.46
TSFC (Mid subcruise wt, lb/hr/lb)	1.037	1.037	1.048	1.071
RF (Mid subcruise wt, nm)	7758	7754	7662	7452
L/D (Mid supercruise wt)	8.31	8.37	8.45	8.62
TSFC (Mid supercruise wt, lb/hr/lb)	1.345	1.347	1.351	1.373
RF (Mid supercruise wt, nm)	8504	8557	8610	8641

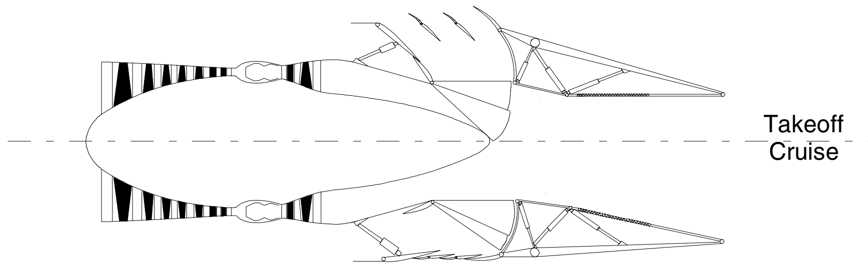

Figure 1.—Turbojet

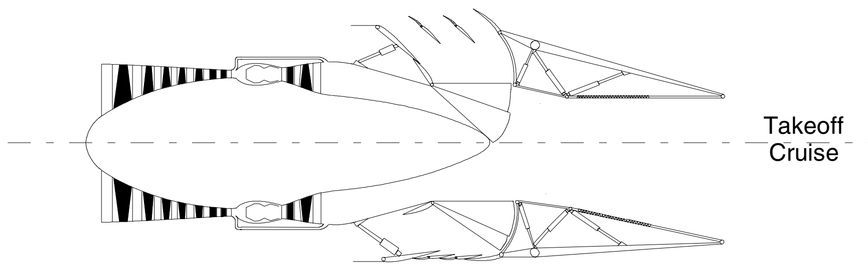

Figure 2.—Turbine Bypass Engine

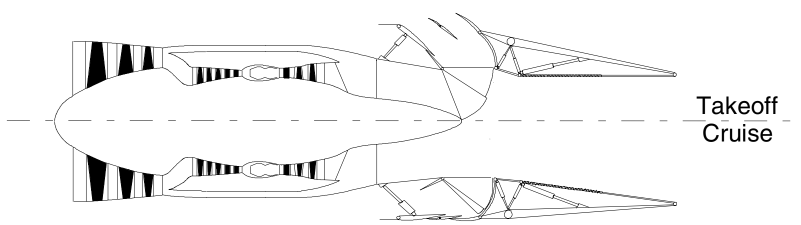

Figure 3.—Mixed Flow Turbofan

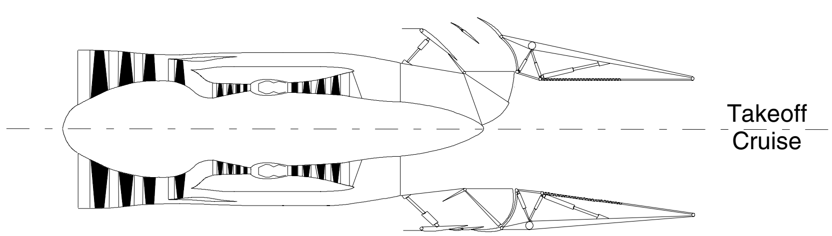

Figure 4.—Variable Cycle Engine

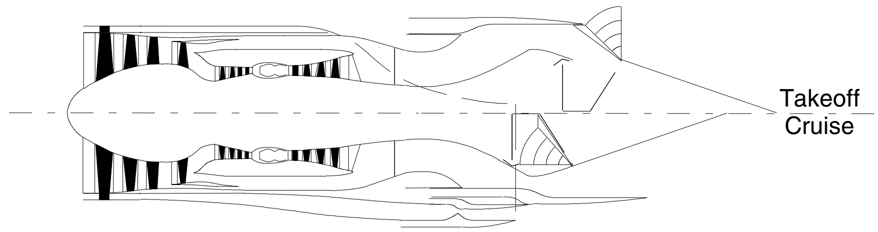

Figure 5.—Flade Engine

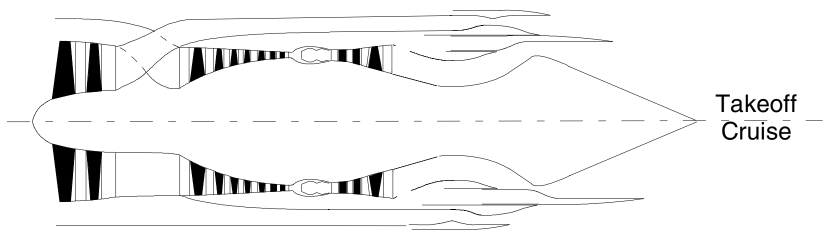

Figure 6.—Turbojet/Inverting Flow Valve Engine

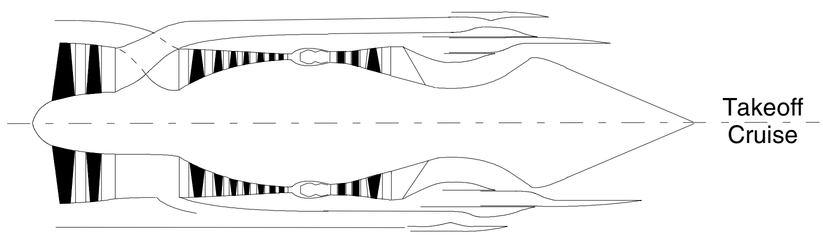

Figure 7.—Turbofan/Inverting Flow Valve Engine

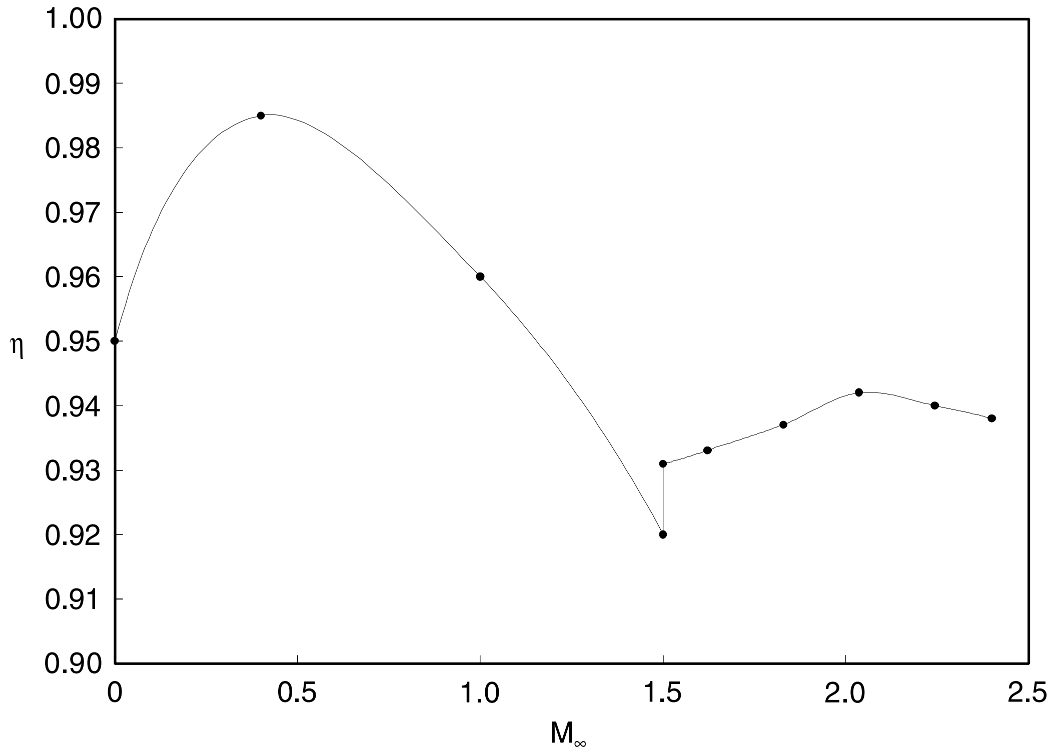

Figure 8.—Reference matched inlet recovery

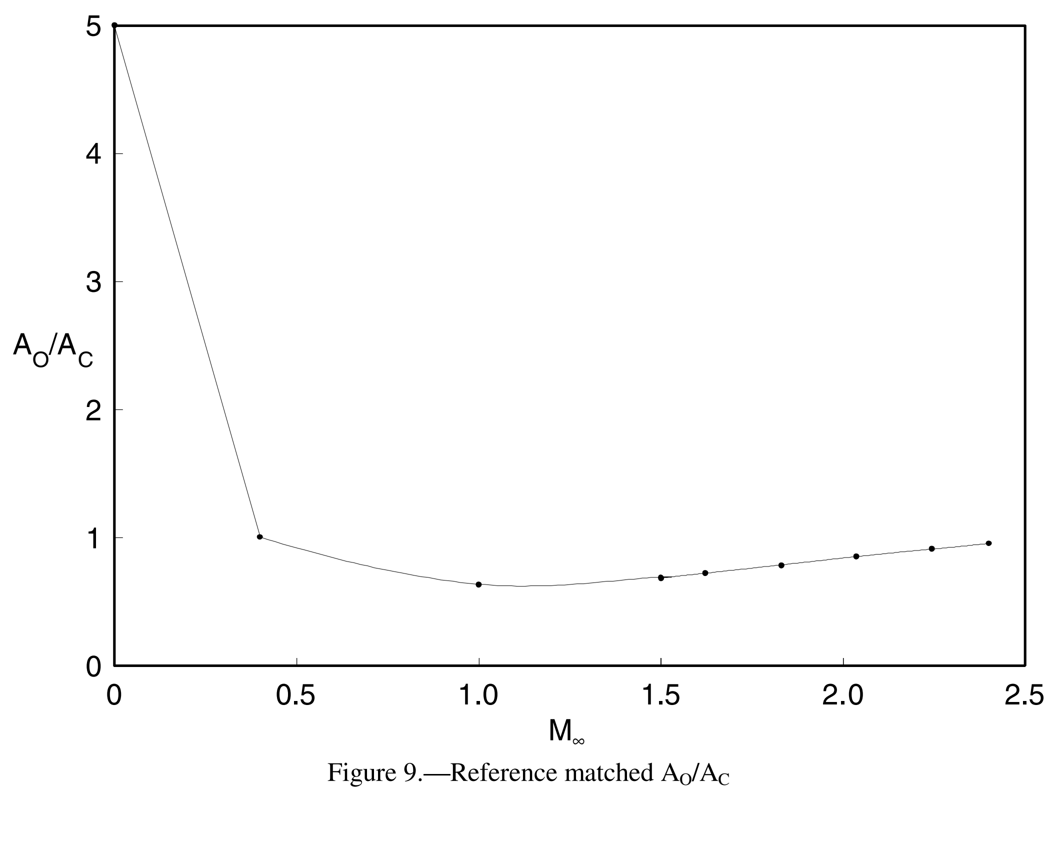

Figure 9.—Reference matched A_O/A_C

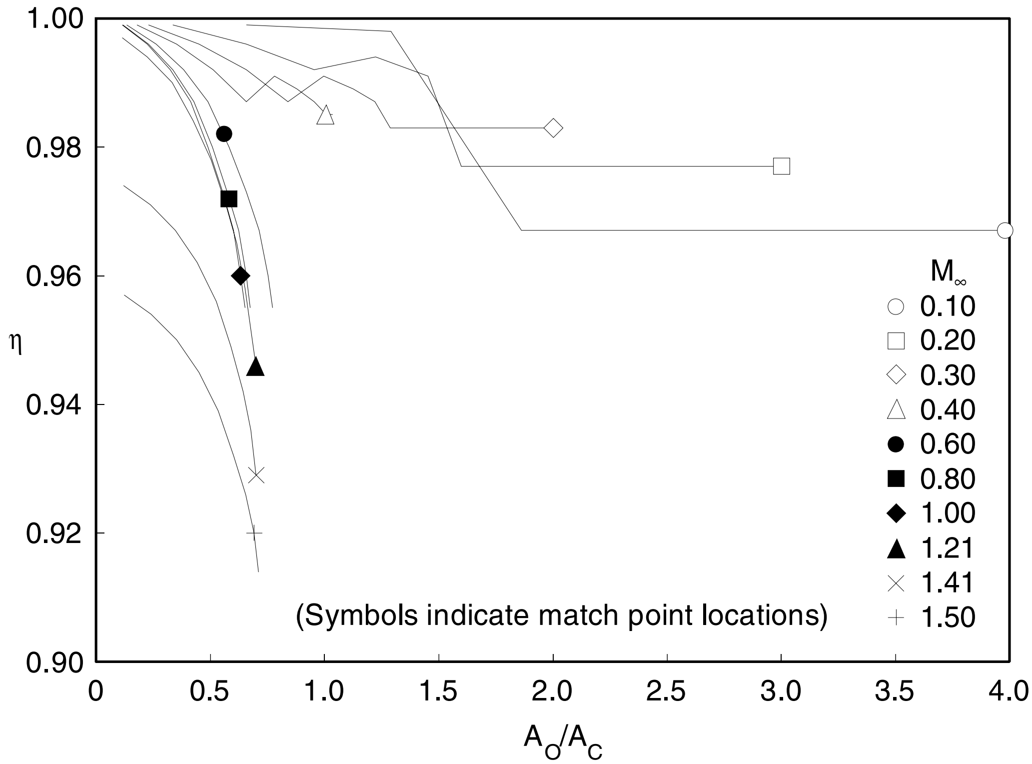

Figure 10.—Additional unmatched recoveries, 0.10 ≤ M_∞ ≤ 1.50

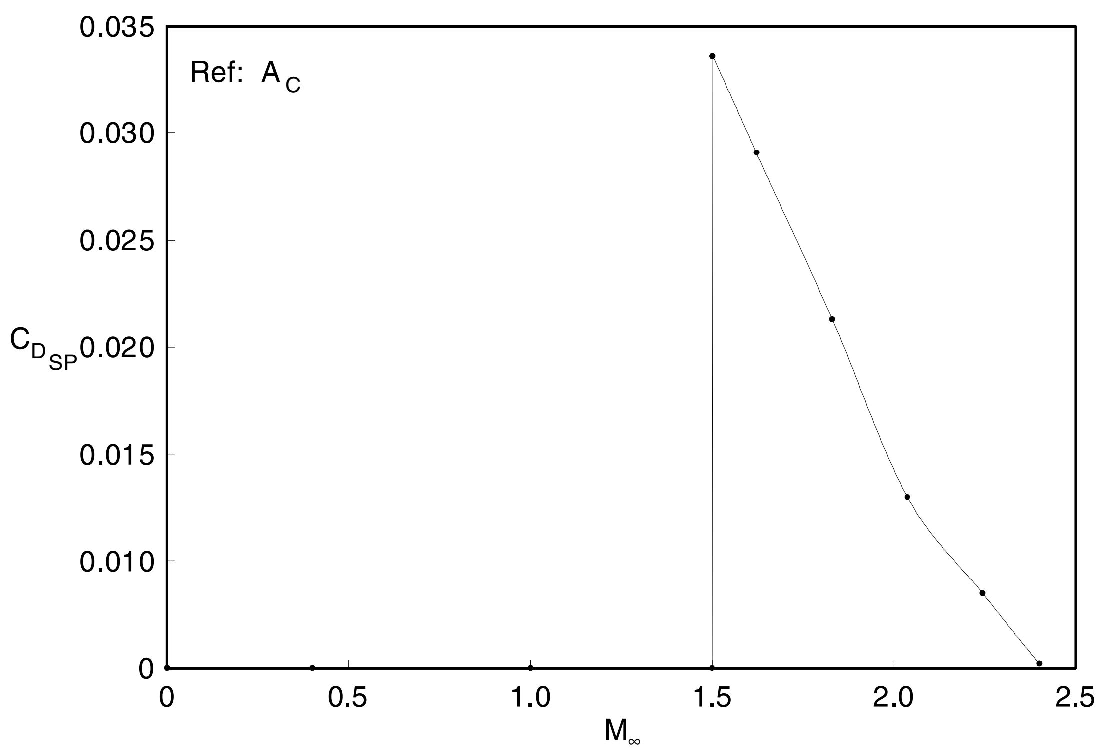

Figure 11.—Reference spillage drag

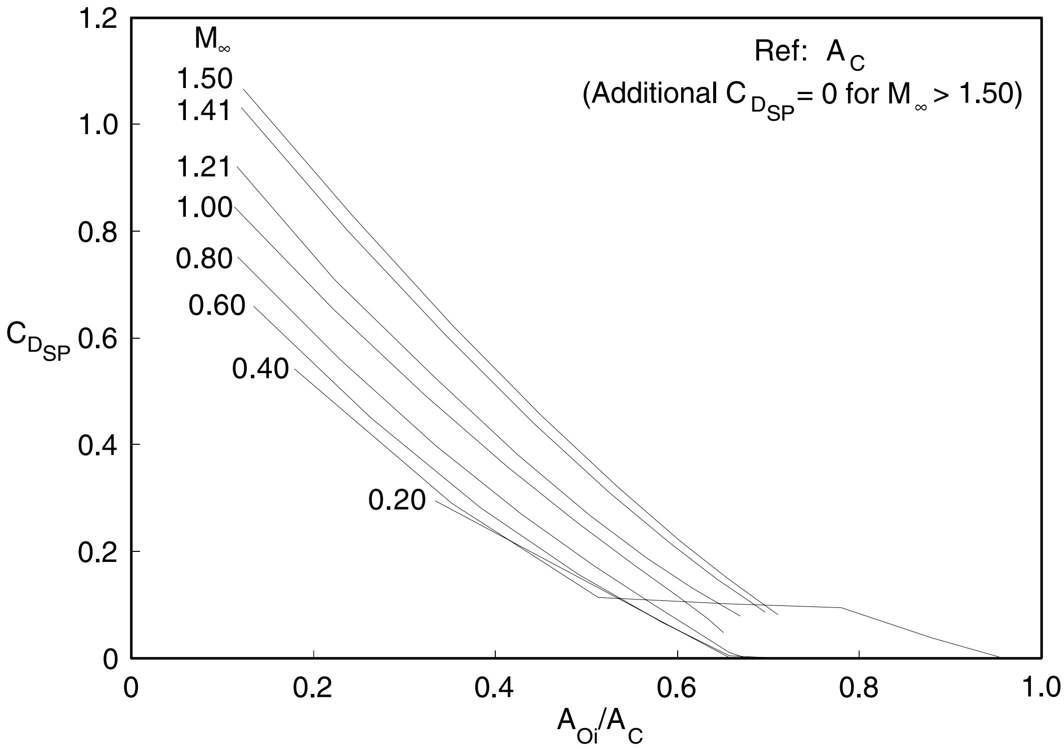

Figure 12.—Additional unmatched spillage drags

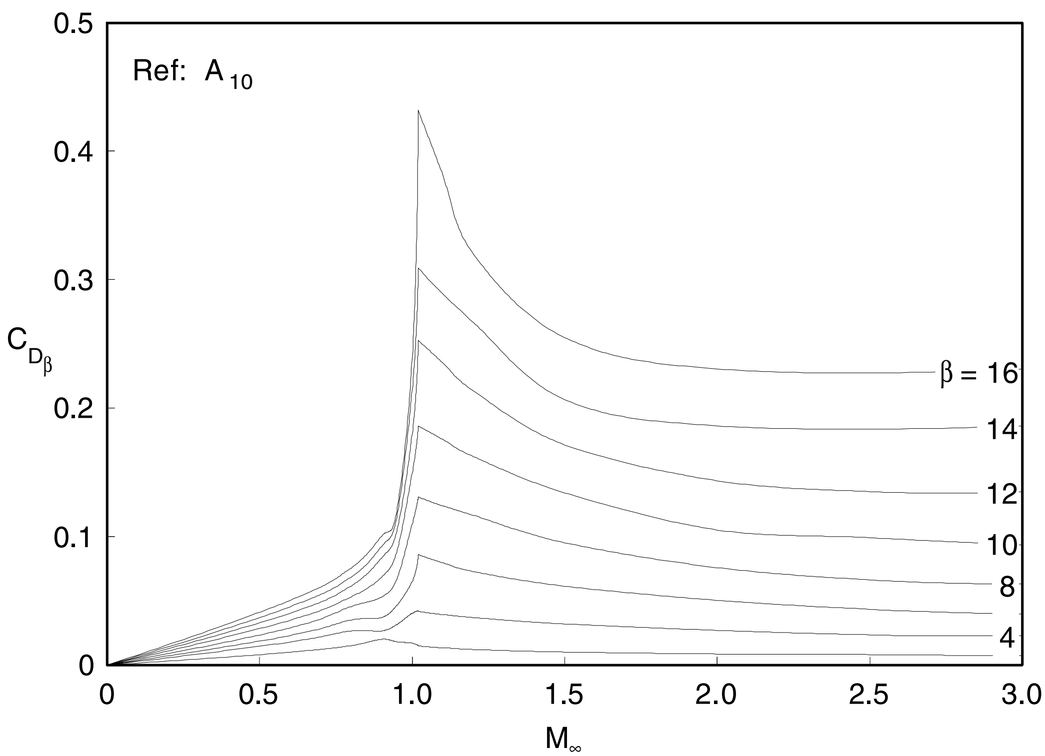

Figure 13.—2D nozzle boattail drag coefficients, $A_9/A_{10} = 0.25$

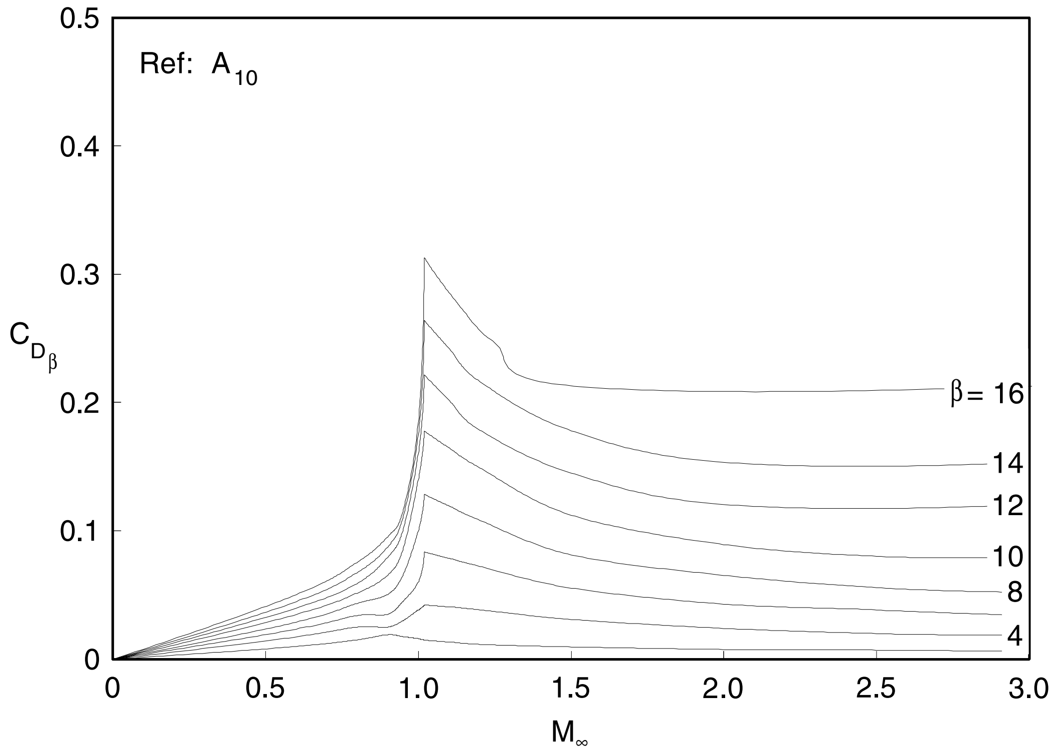

Figure 14.—2D nozzle boattail drag coefficients, $A_9/A_{10} = 0.50$

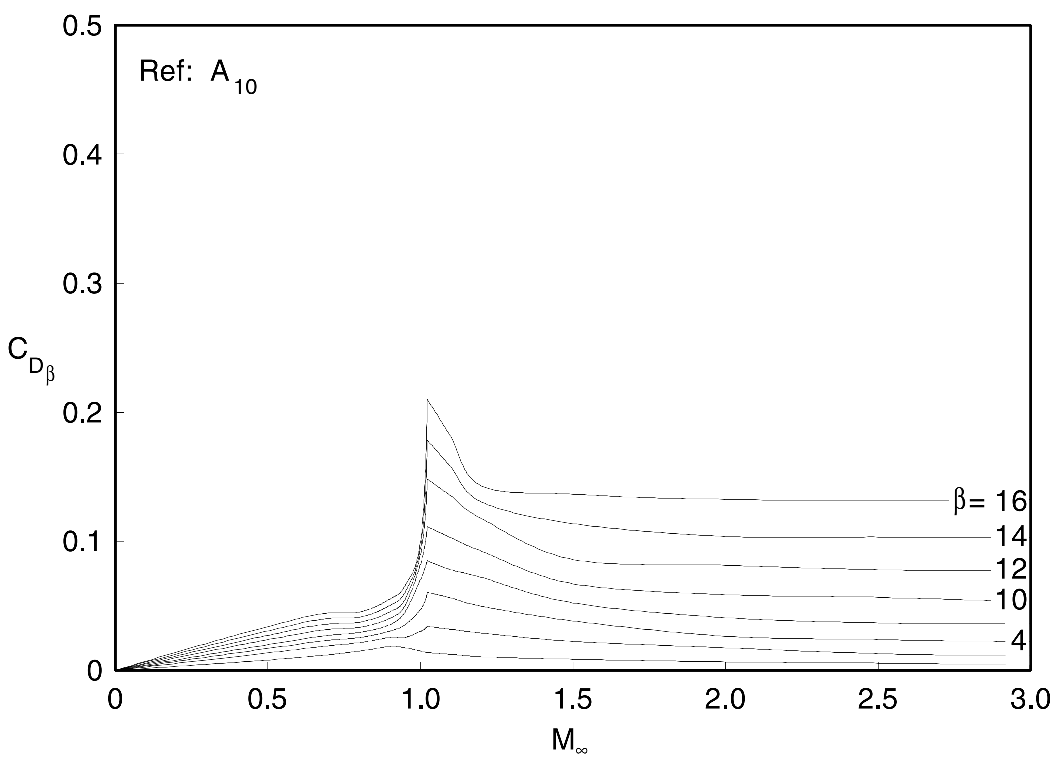

Figure 15.—2D nozzle boattail drag coefficients, $A_9/A_{10} = 0.75$

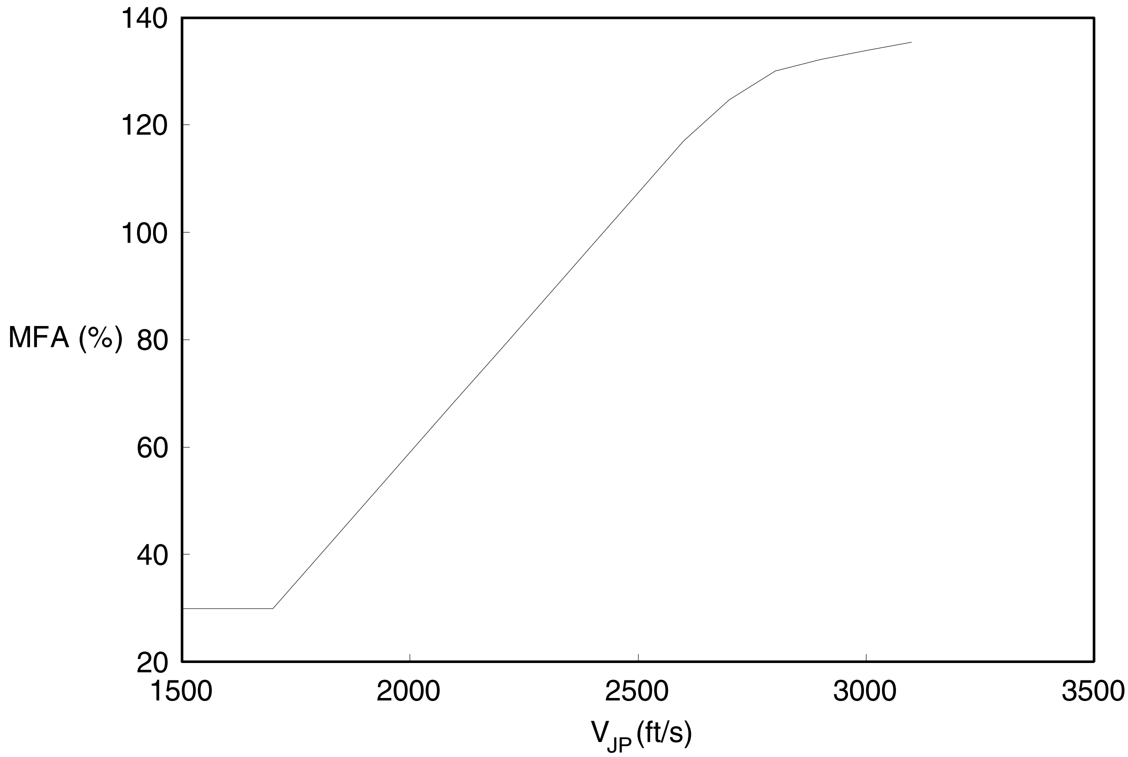

Figure 16.—1993, 1994 mixer-ejector nozzle MFA severity model

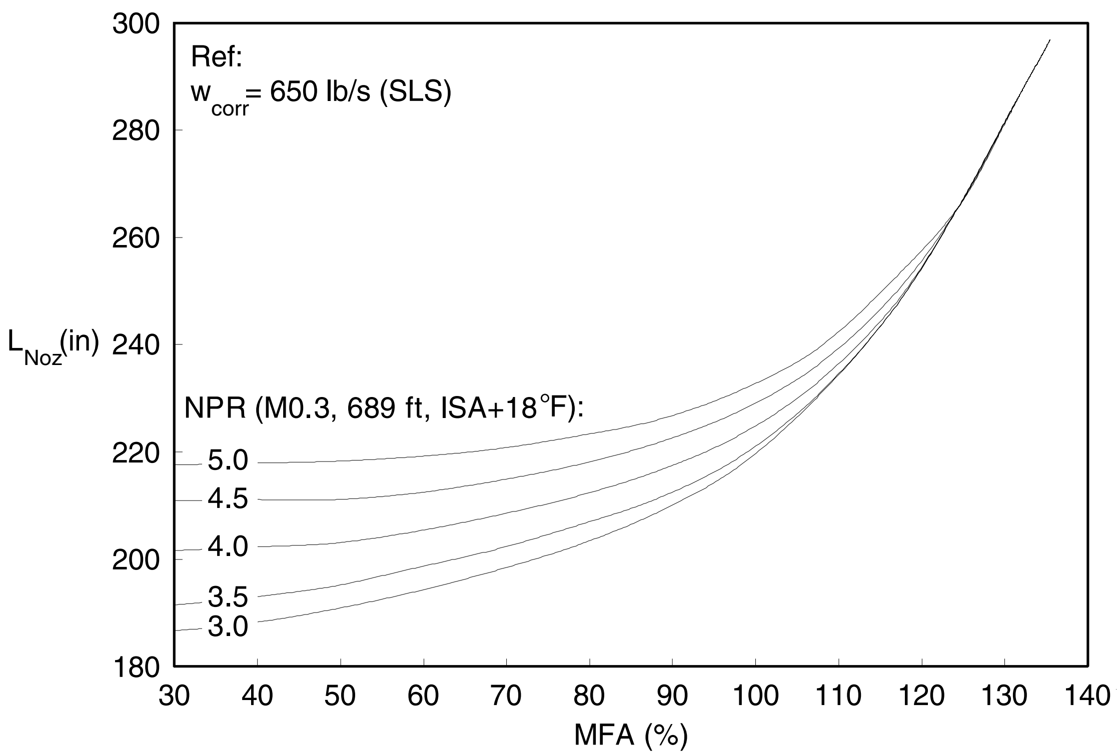

Figure 17.—1993 mixer-ejector nozzle length model

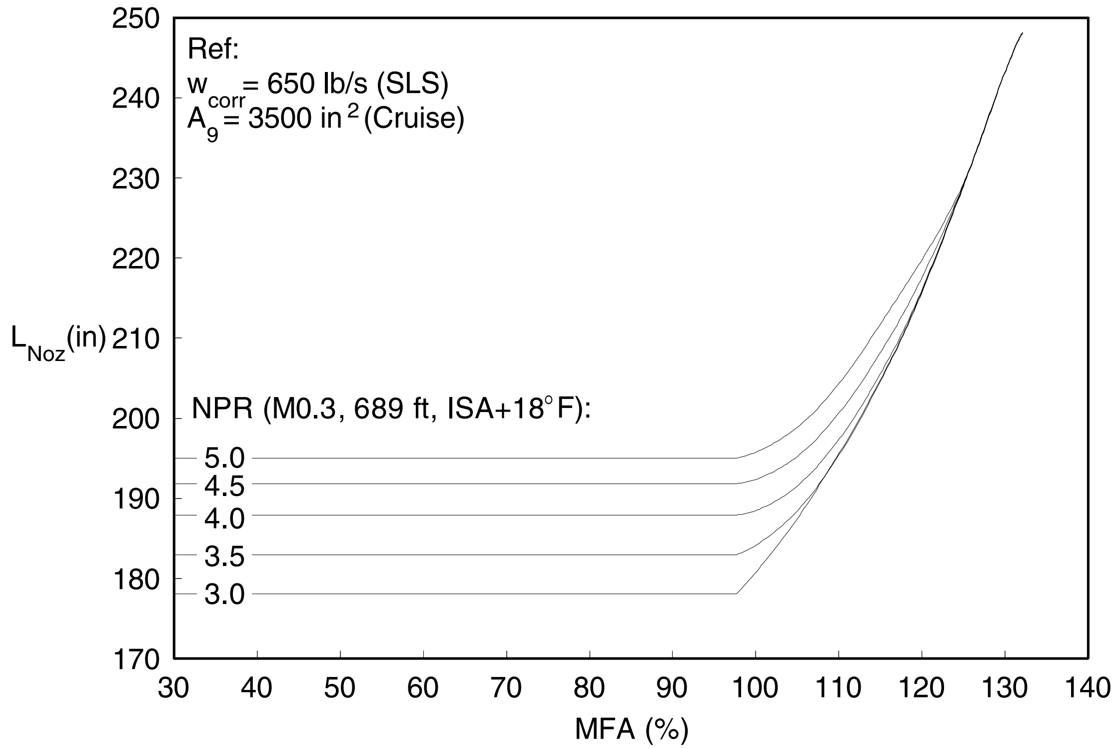

Figure 18.—1994 mixer-ejector nozzle length model

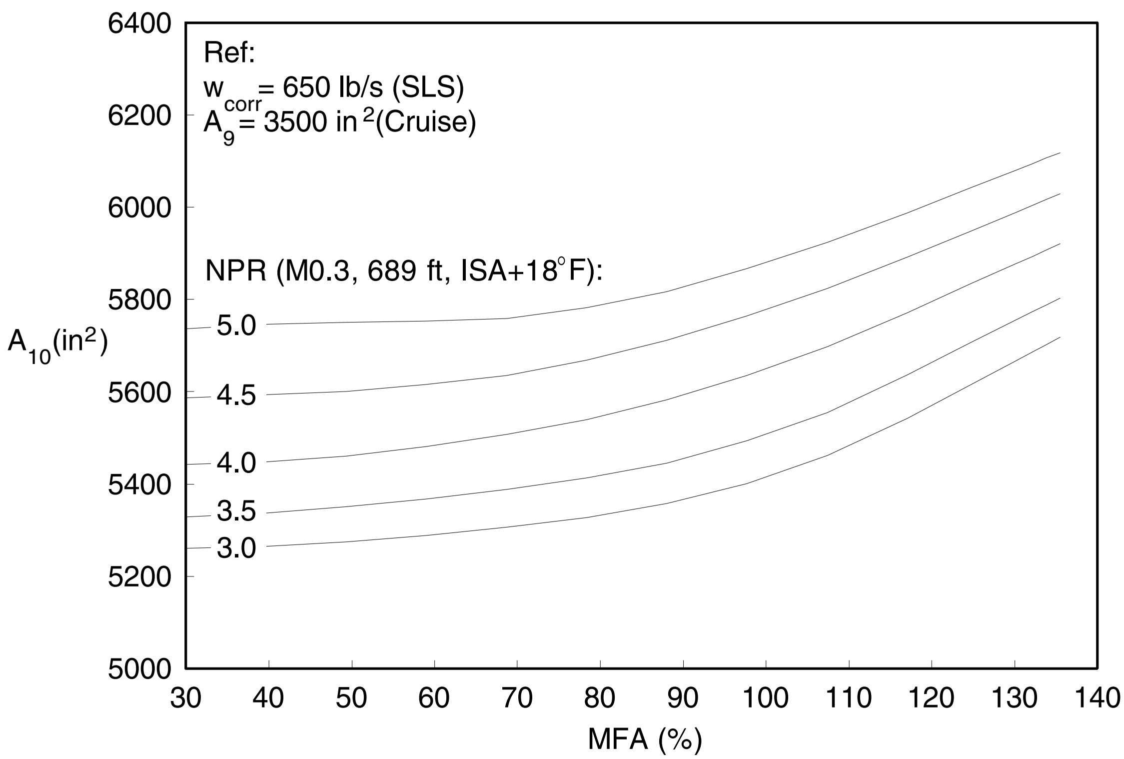

Figure 19.—1993, 1994 mixer-ejector nozzle A_{10} model

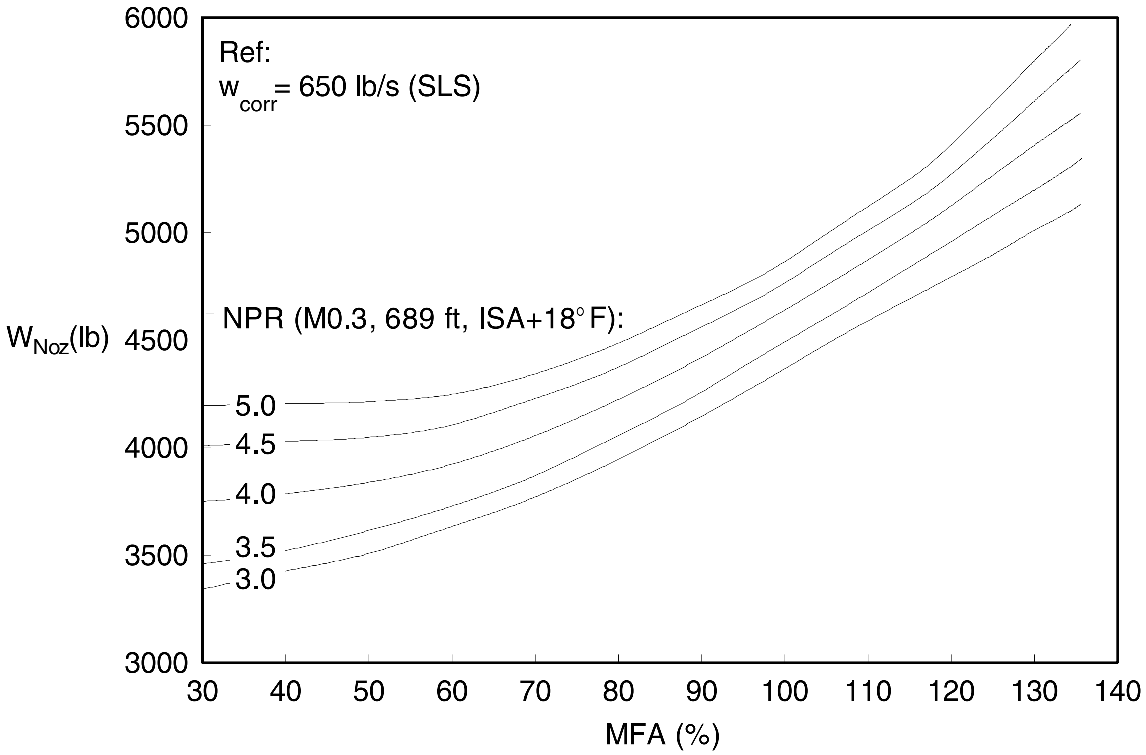

Figure 20.—1993 mixer-ejector nozzle weight model

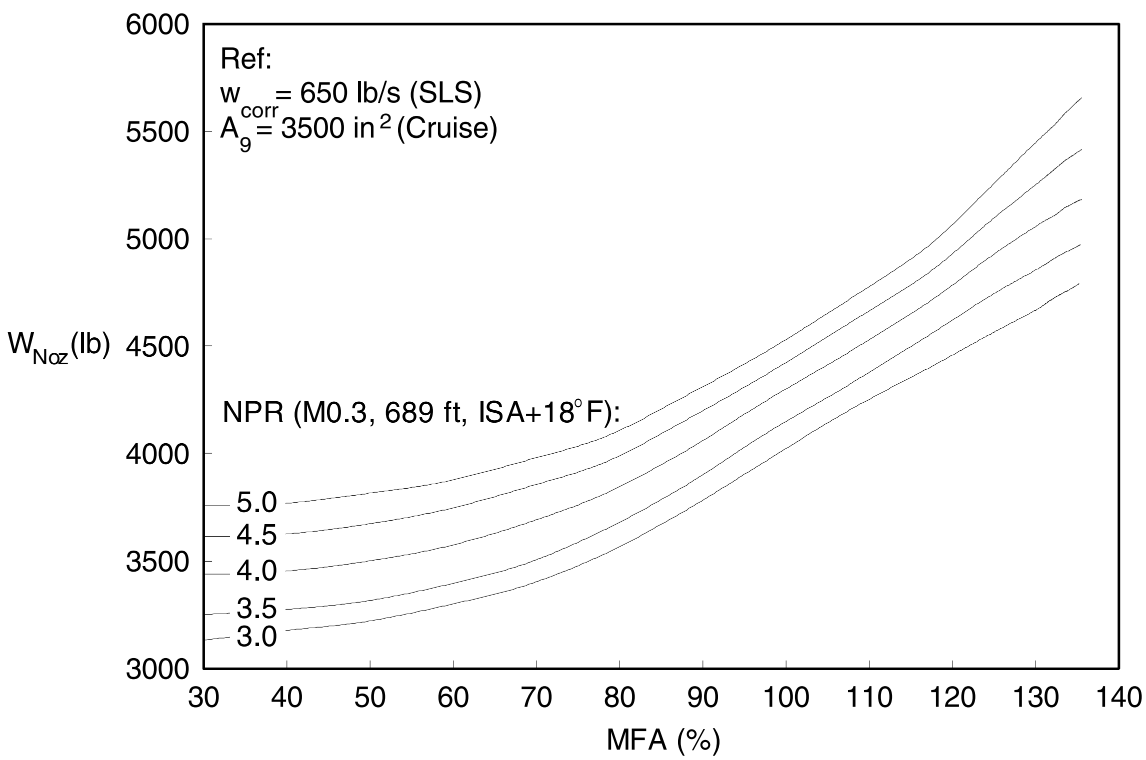

Figure 21.—1994 mixer-ejector nozzle weight model

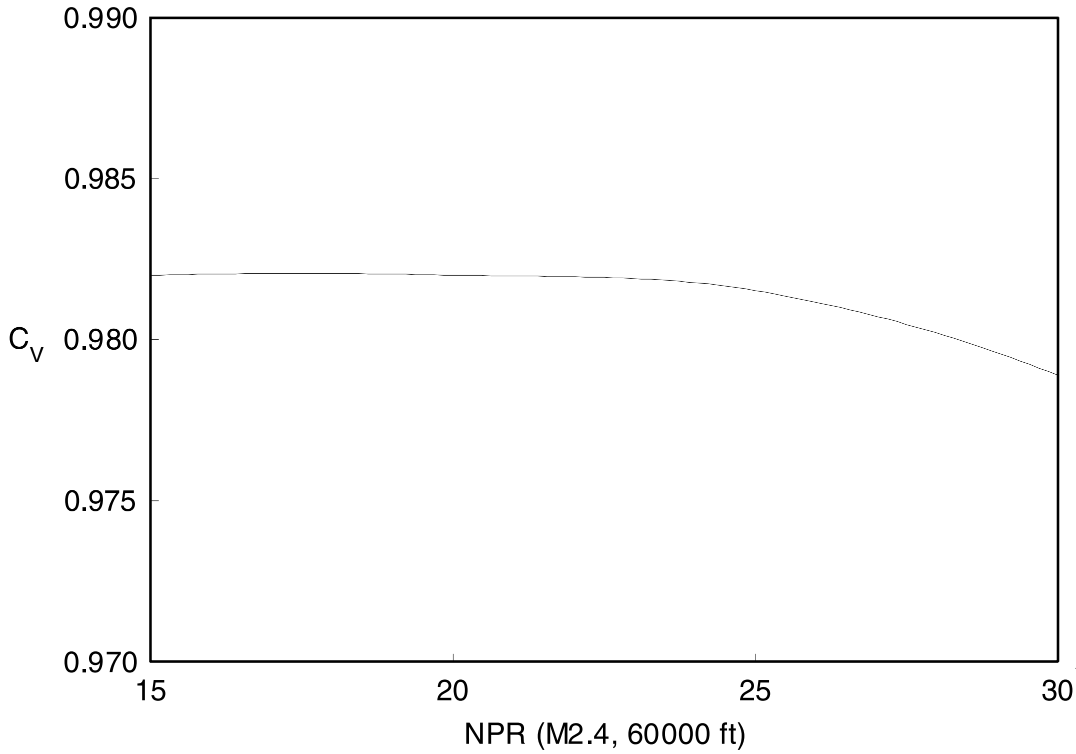

Figure 22.—1993, 1994 mixer-ejector nozzle thrust coefficient model (ejector stowed)

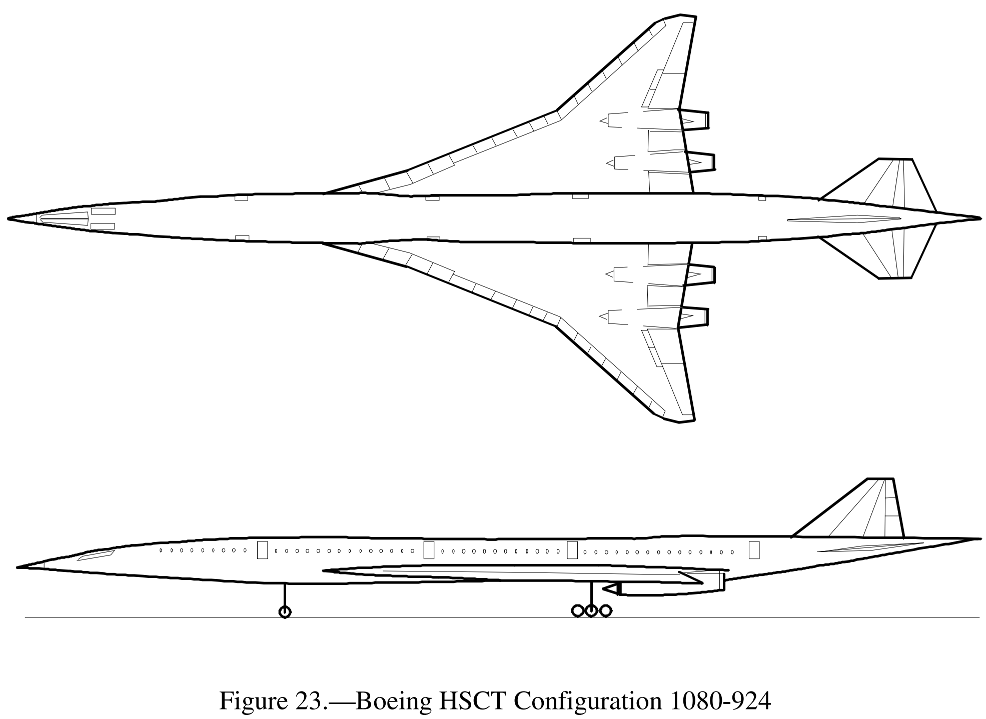

Figure 23.—Boeing HSCT Configuration 1080-924

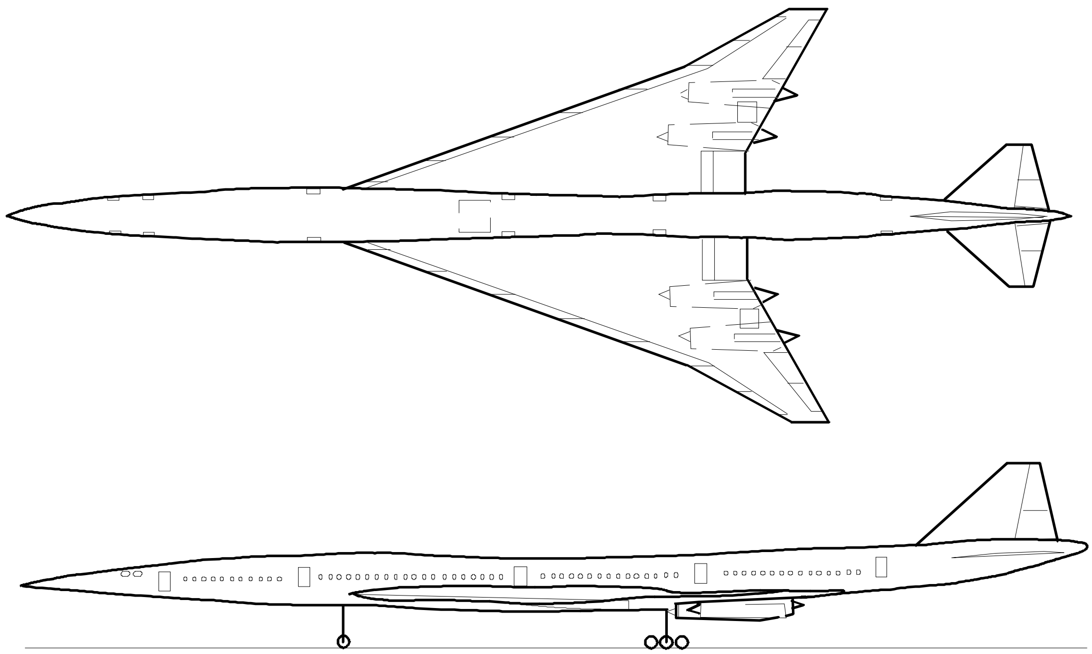

Figure 24.—McDonnell Douglas HSCT Configuration D-3235-2.4-7A

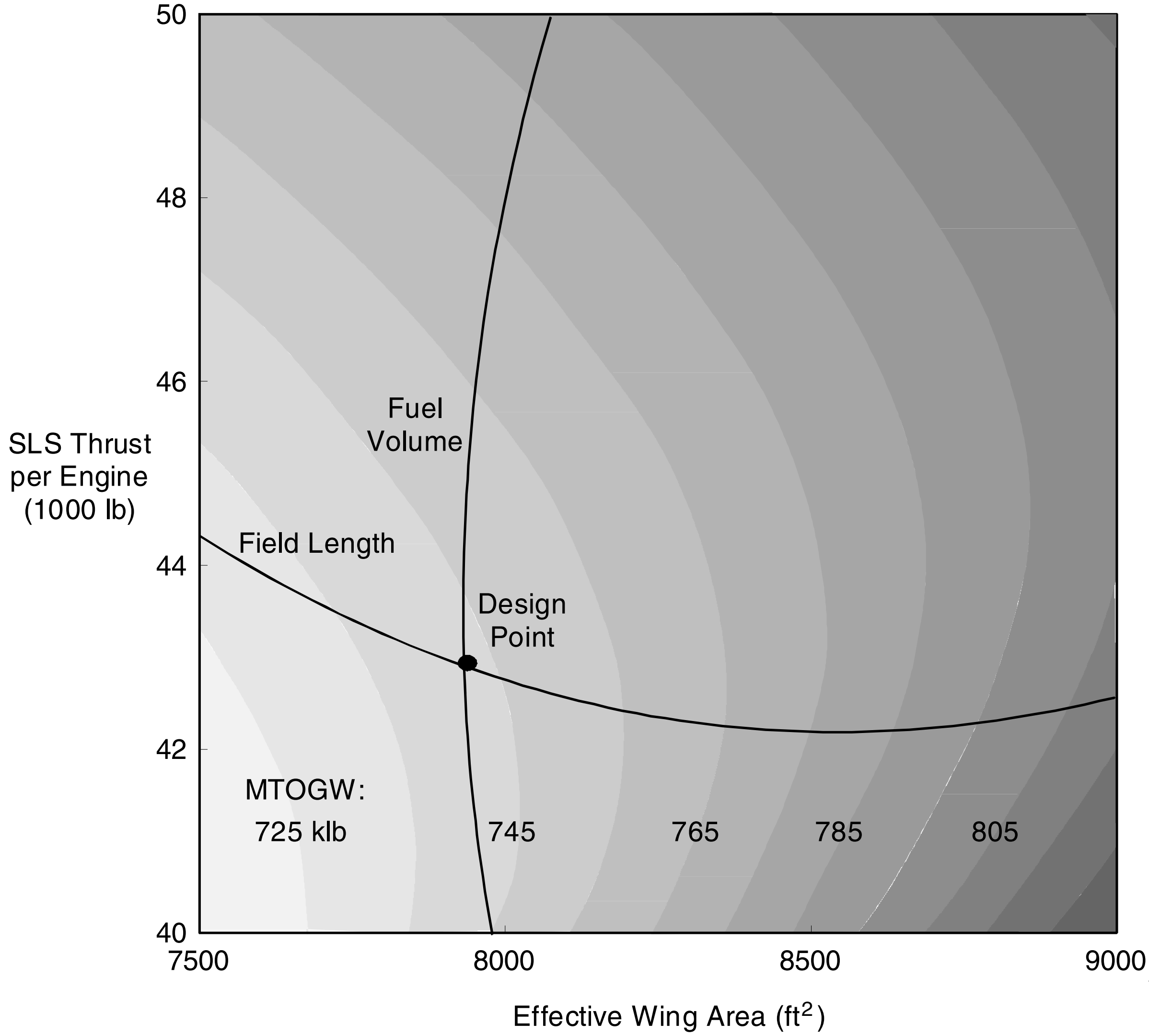

Figure 25.—Aircraft sizing “thumbprint” - 1993 TBE3010 on Boeing HSCT

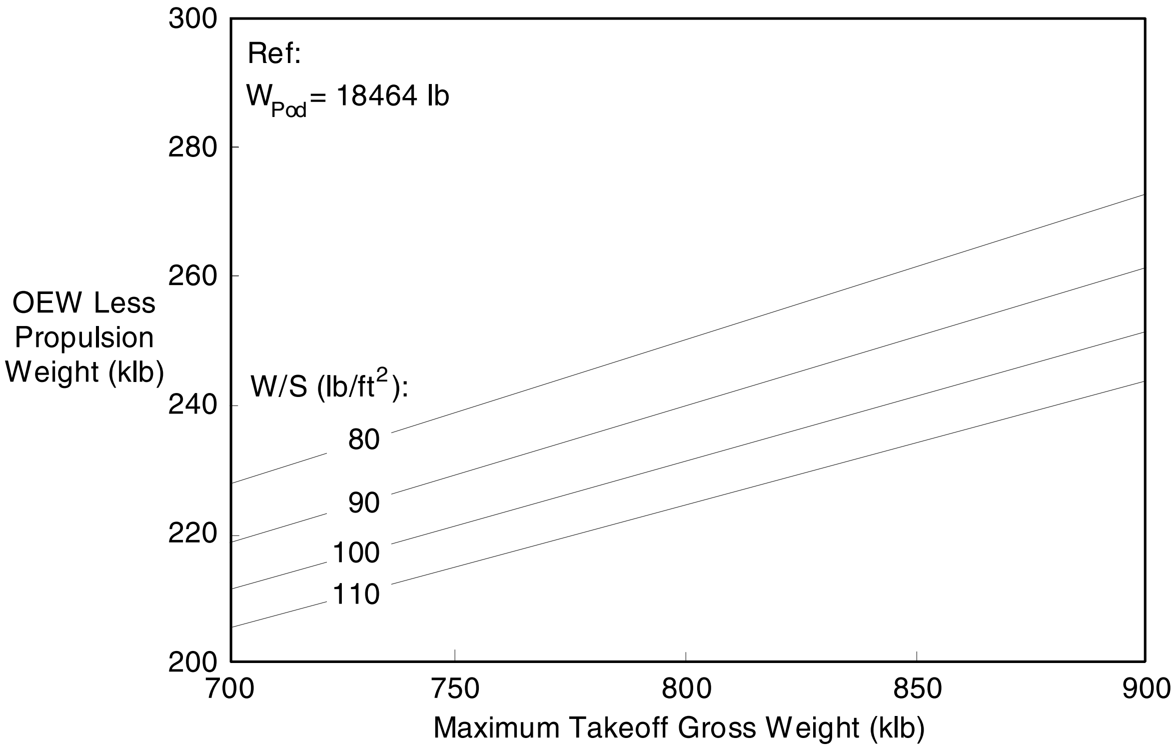

Figure 26.—Boeing HSCT operating empty weight scaling relationship

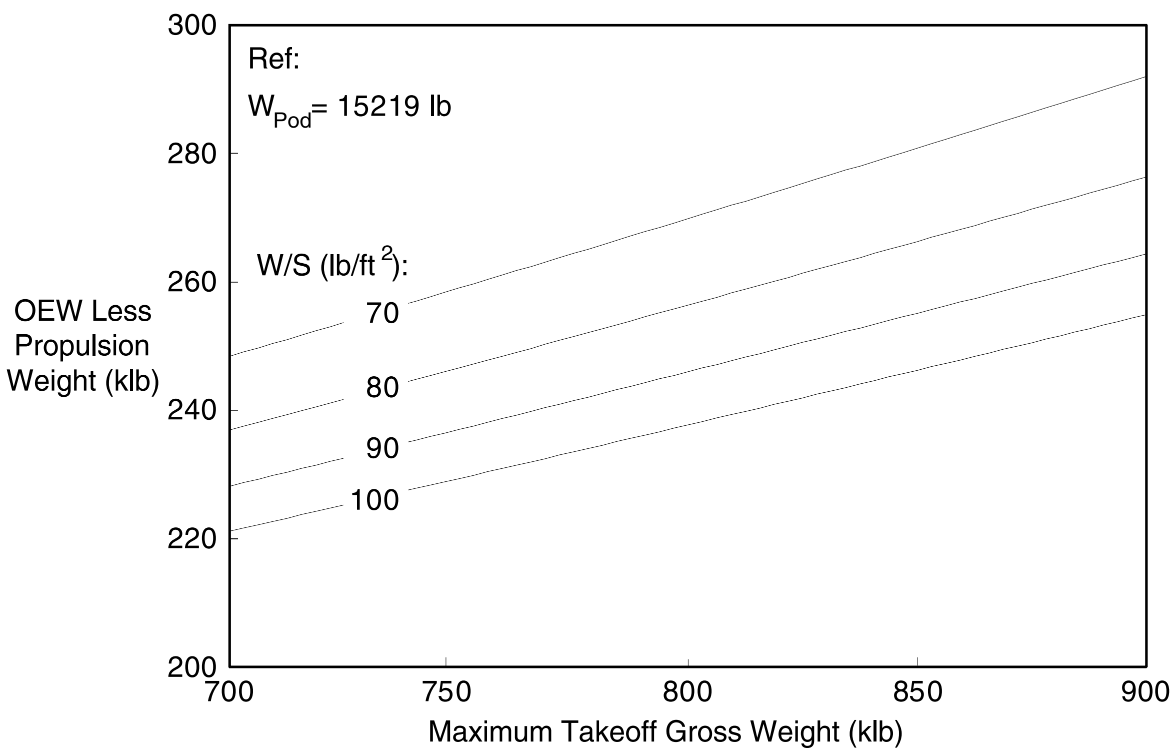

Figure 27.—McDonnell Douglas HSCT operating empty weight scaling relationship

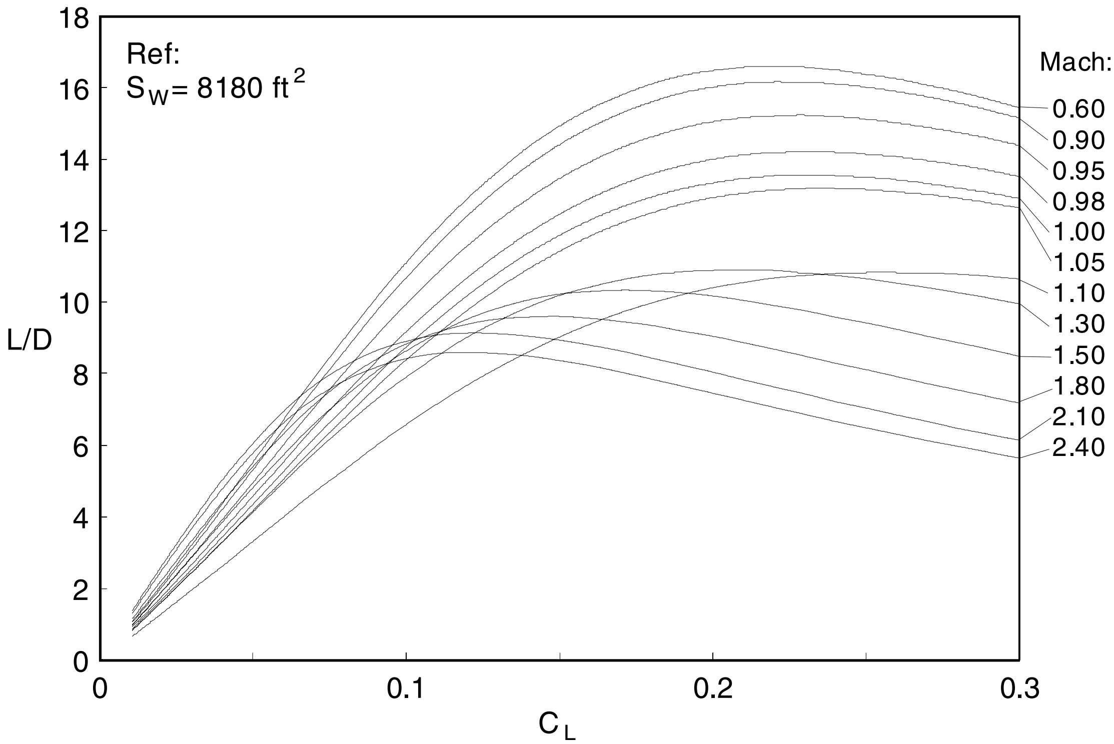

Figure 28.—Boeing HSCT aerodynamics

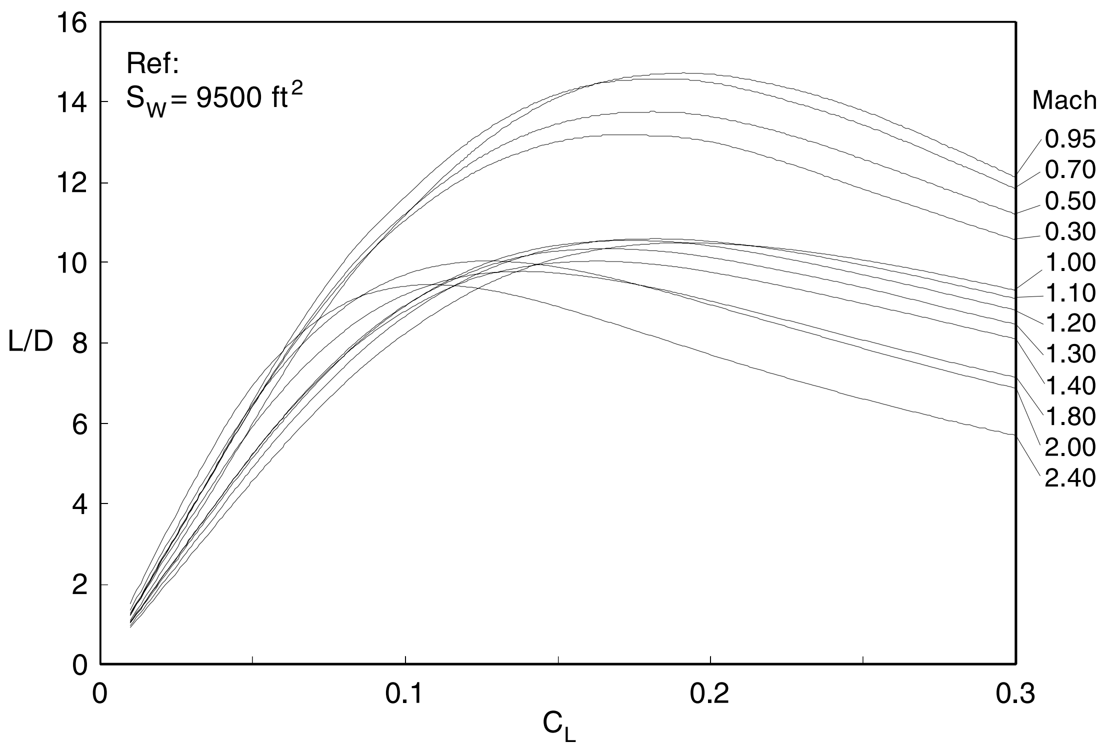

Figure 29.—McDonnell Douglas HSCT aerodynamics

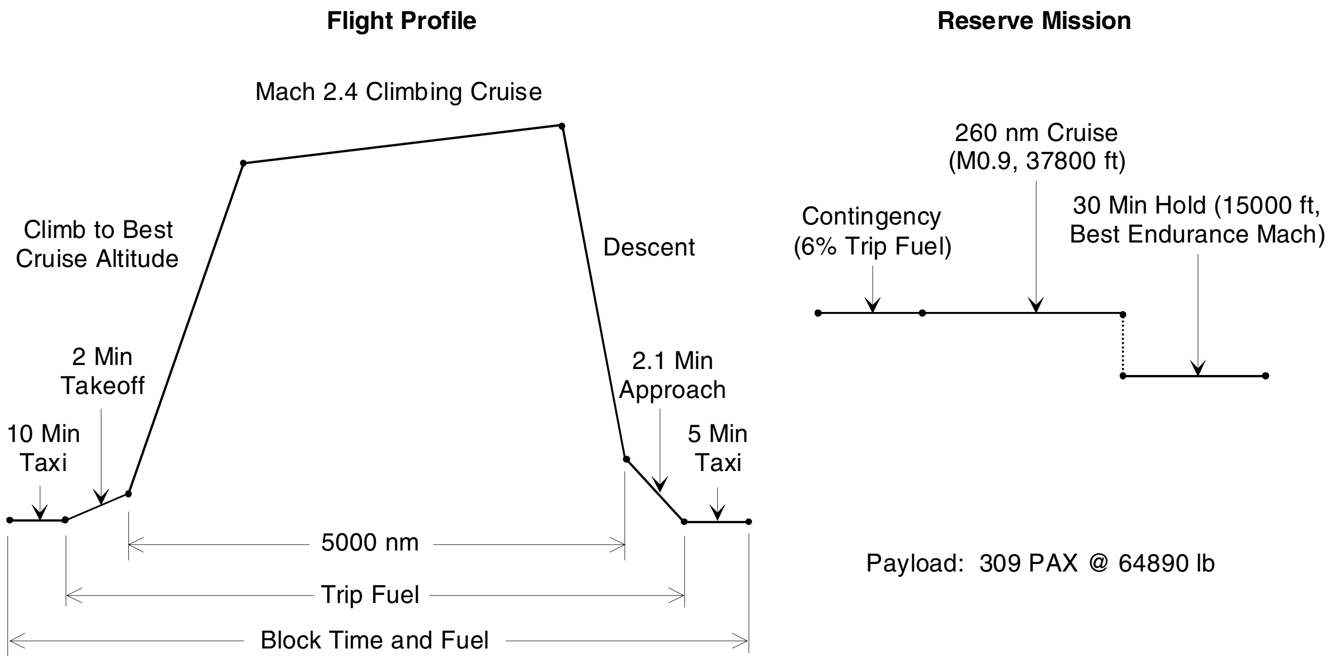

Figure 30.—Boeing HSCT design mission

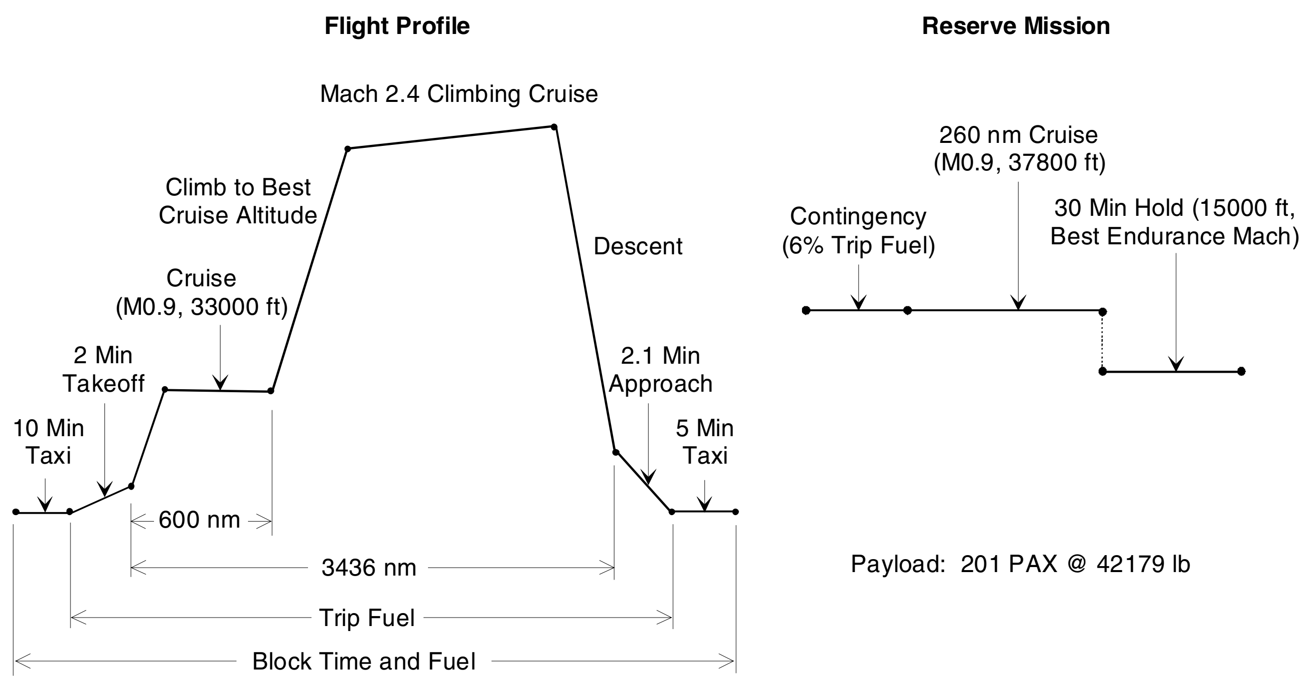

Figure 31.—Boeing HSCT economic mission

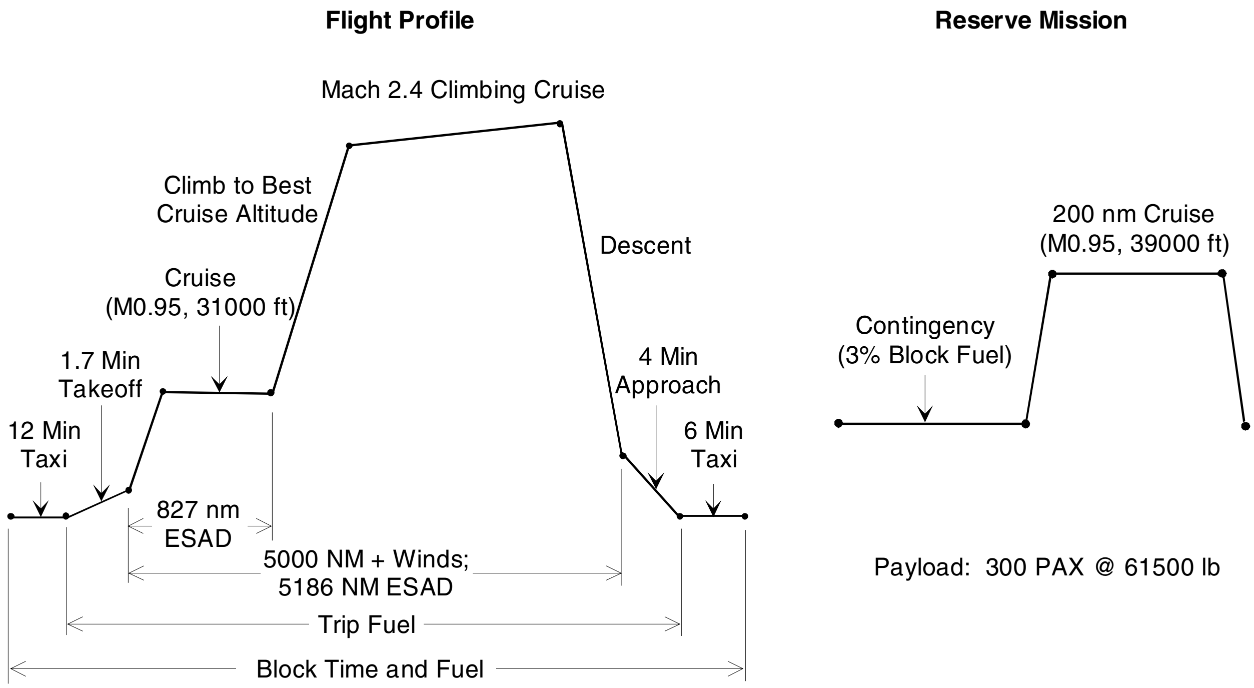

Figure 32.—McDonnell Douglas HSCT design mission

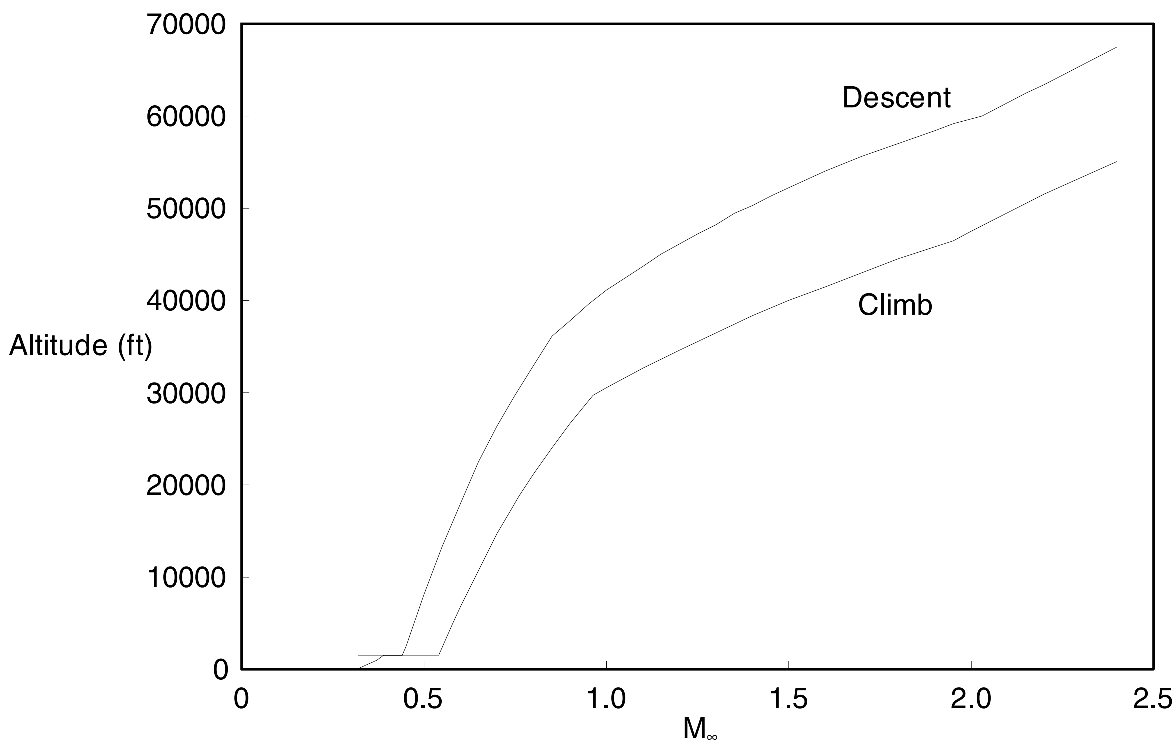

Figure 33.—Boeing HSCT climb and descent trajectories

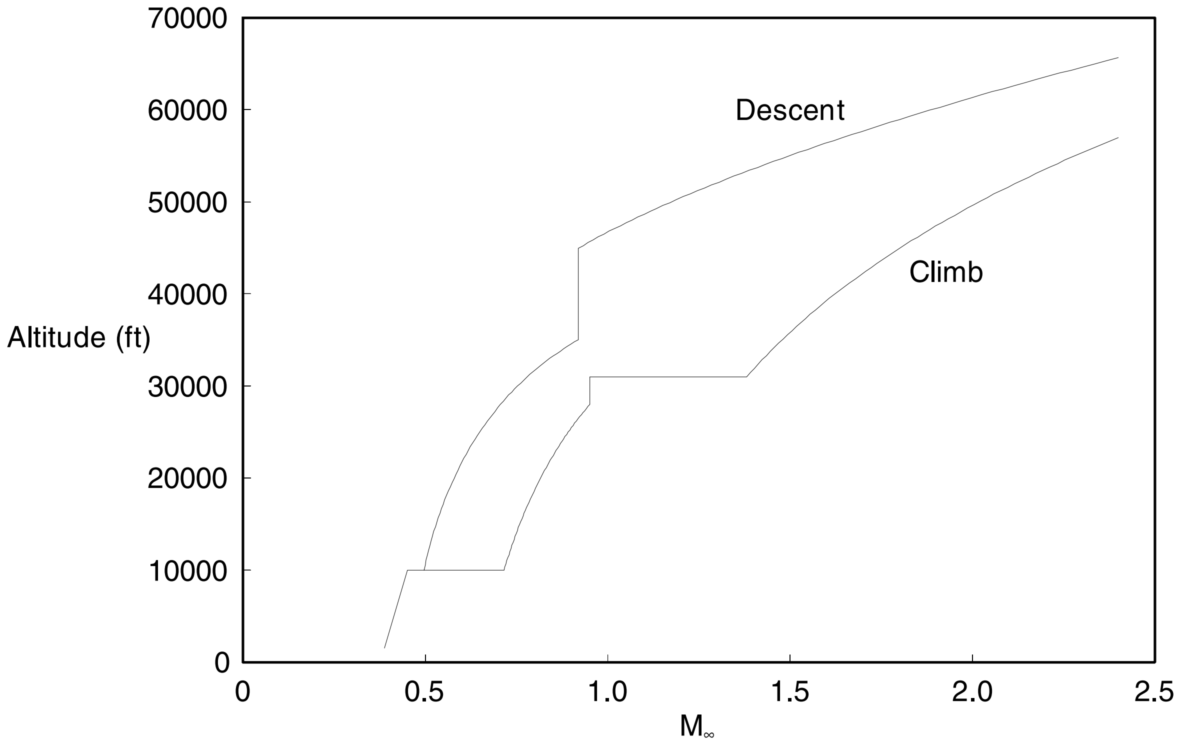

Figure 34.—McDonnell Douglas HSCT climb and descent trajectories

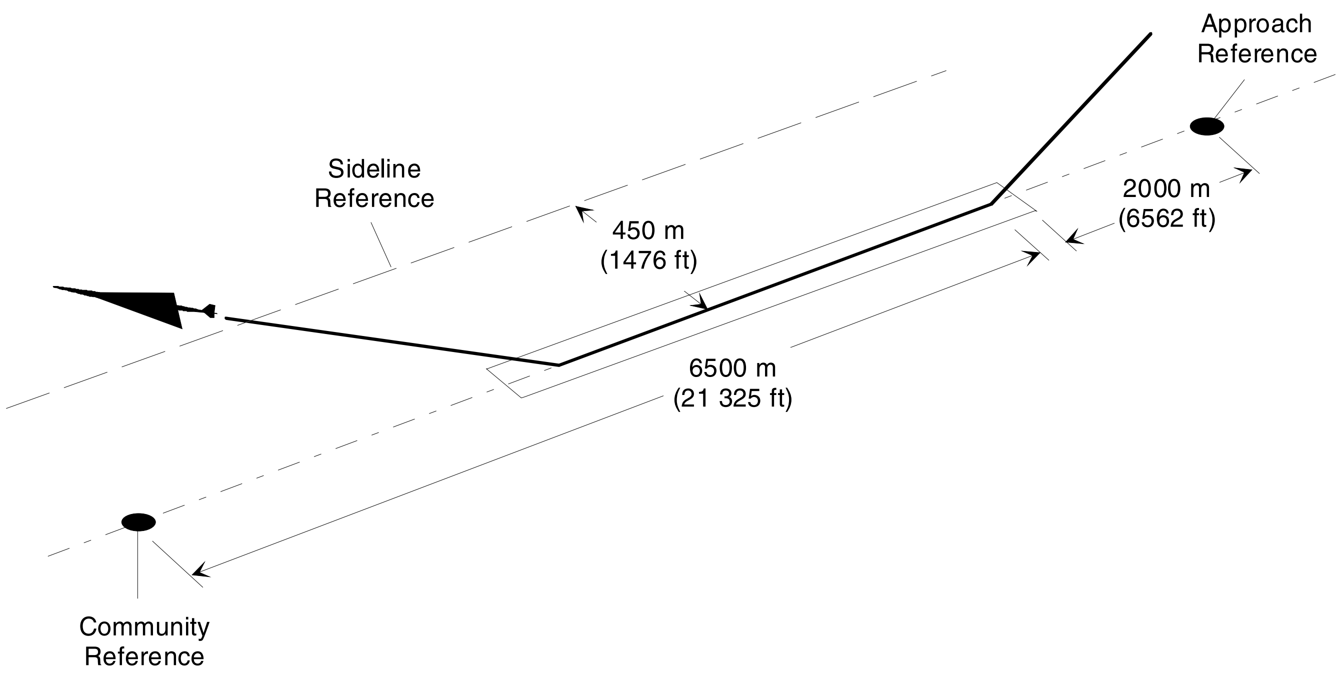

Figure 35.—Noise measurement arrangement

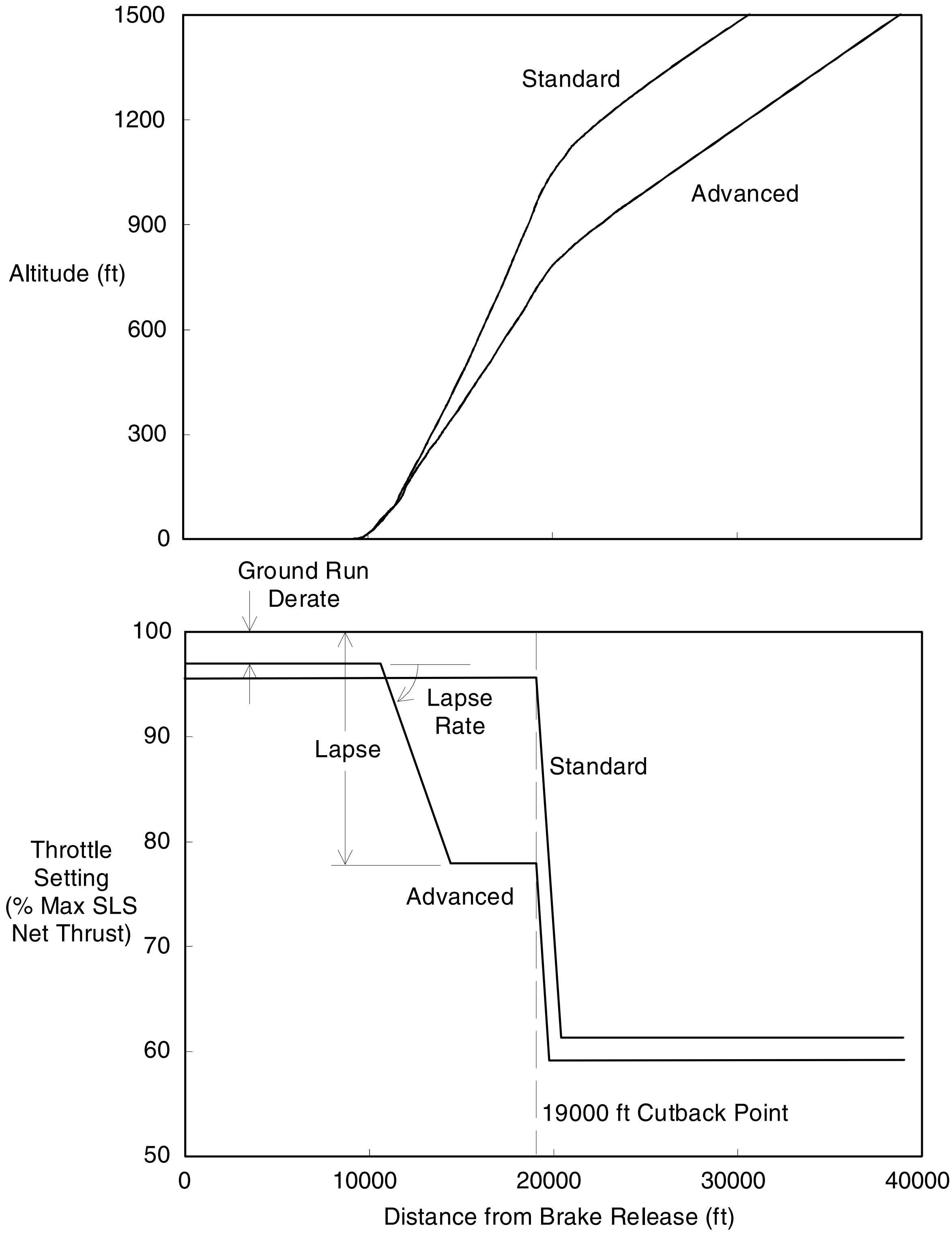

Figure 36.—Standard and advanced takeoff profiles for the 1993 TBE3010 Boeing HSCT

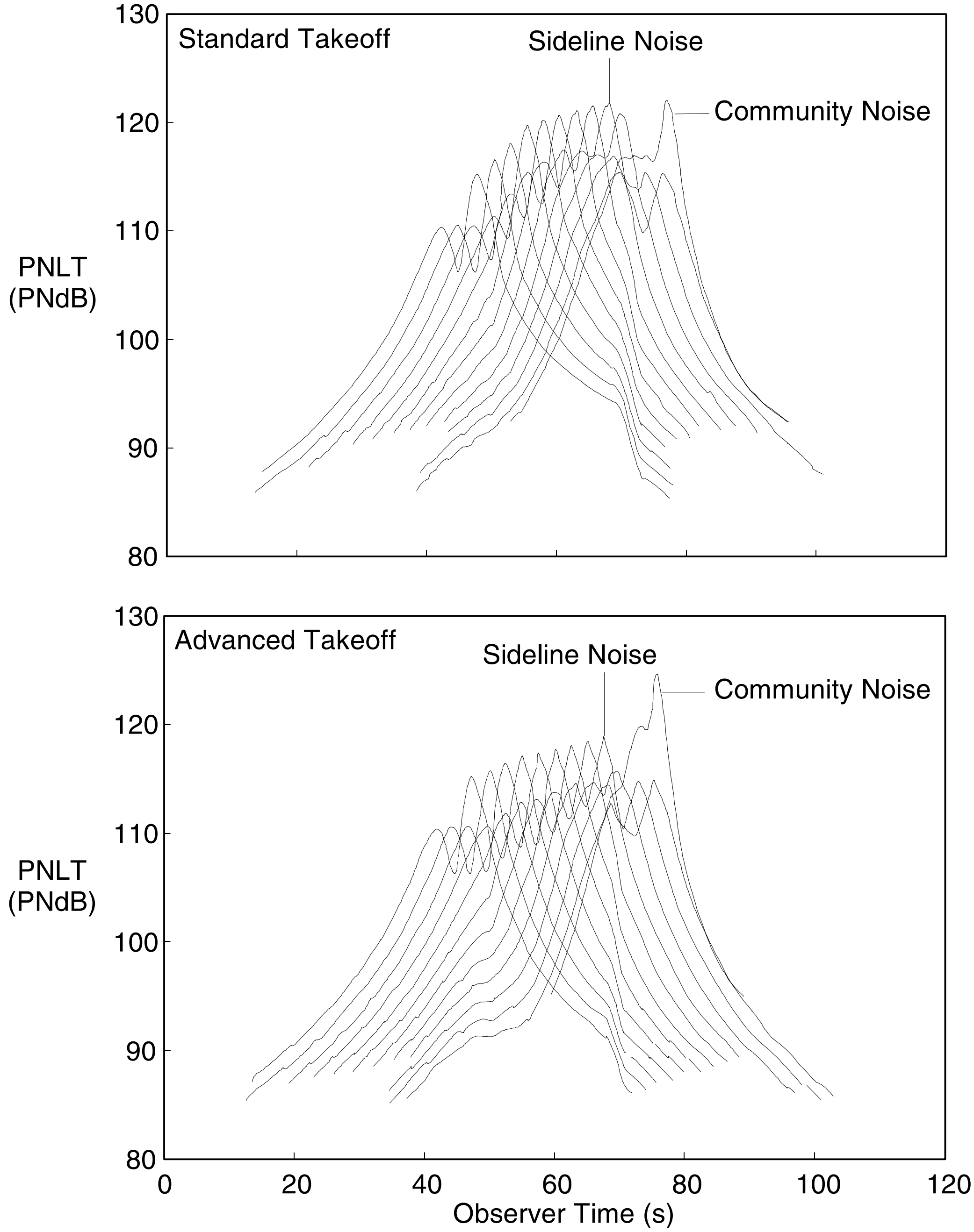

Figure 37: Takeoff noise traces for the 1993 TBE3010 Boeing HSCT

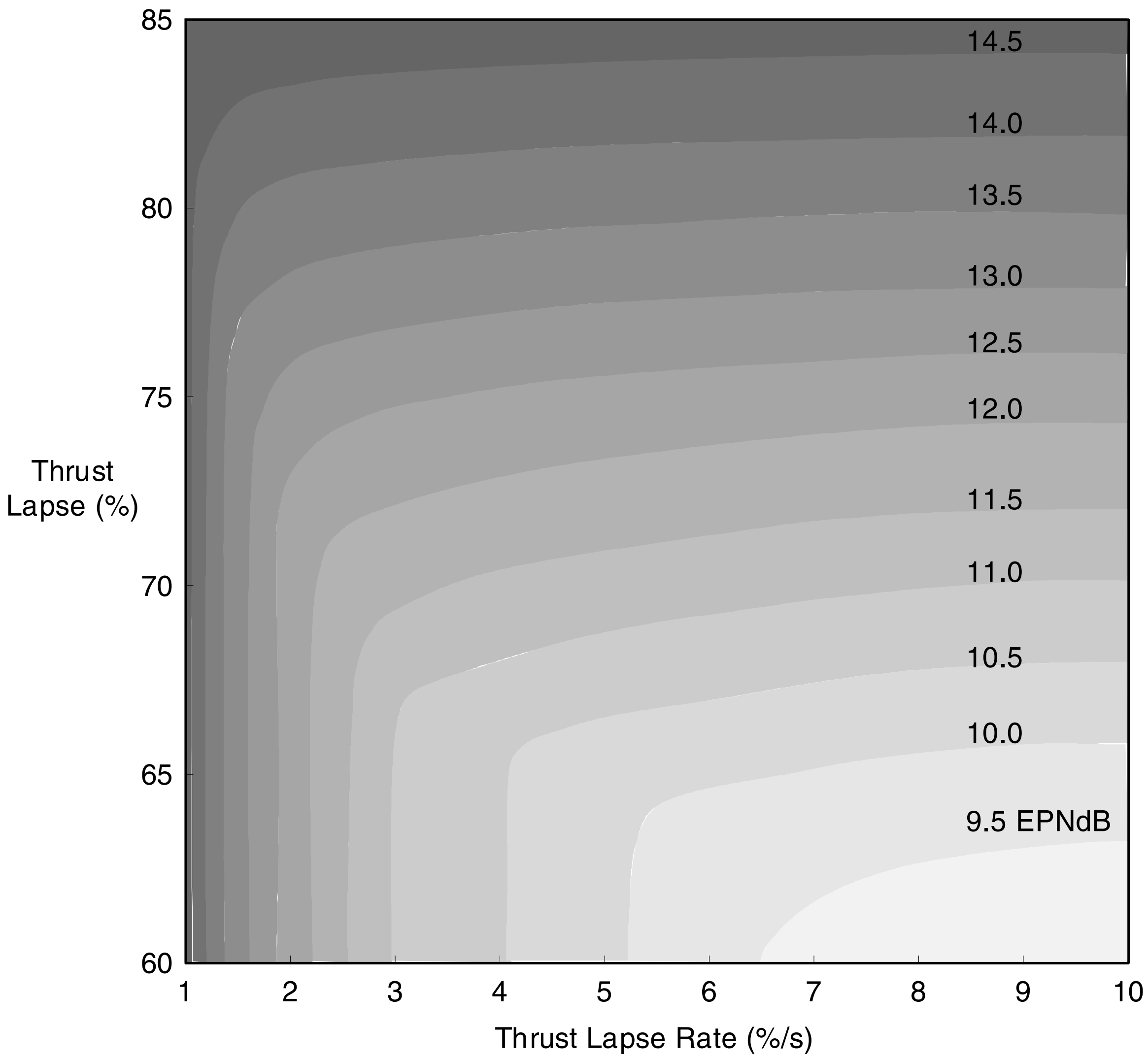

Figure 38.—Sideline noise suppression required - programmed lapse rate maneuver for the 1993 TBE3010 Boeing HSCT with three percent ground roll thrust derate

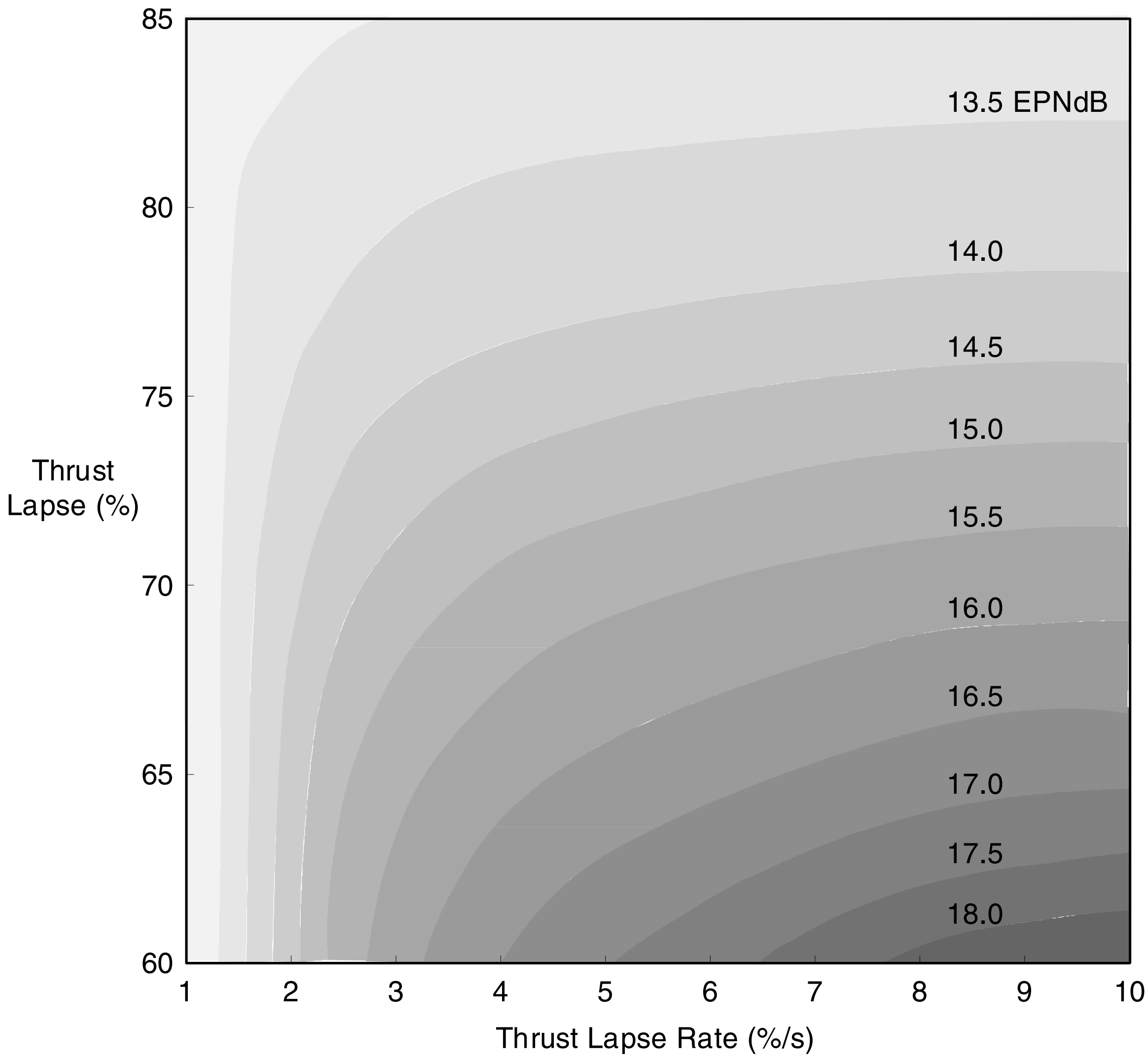

Figure 39.—Community noise suppression required - programmed lapse rate maneuver for the 1993 TBE3010 Boeing HSCT with three percent ground roll thrust derate

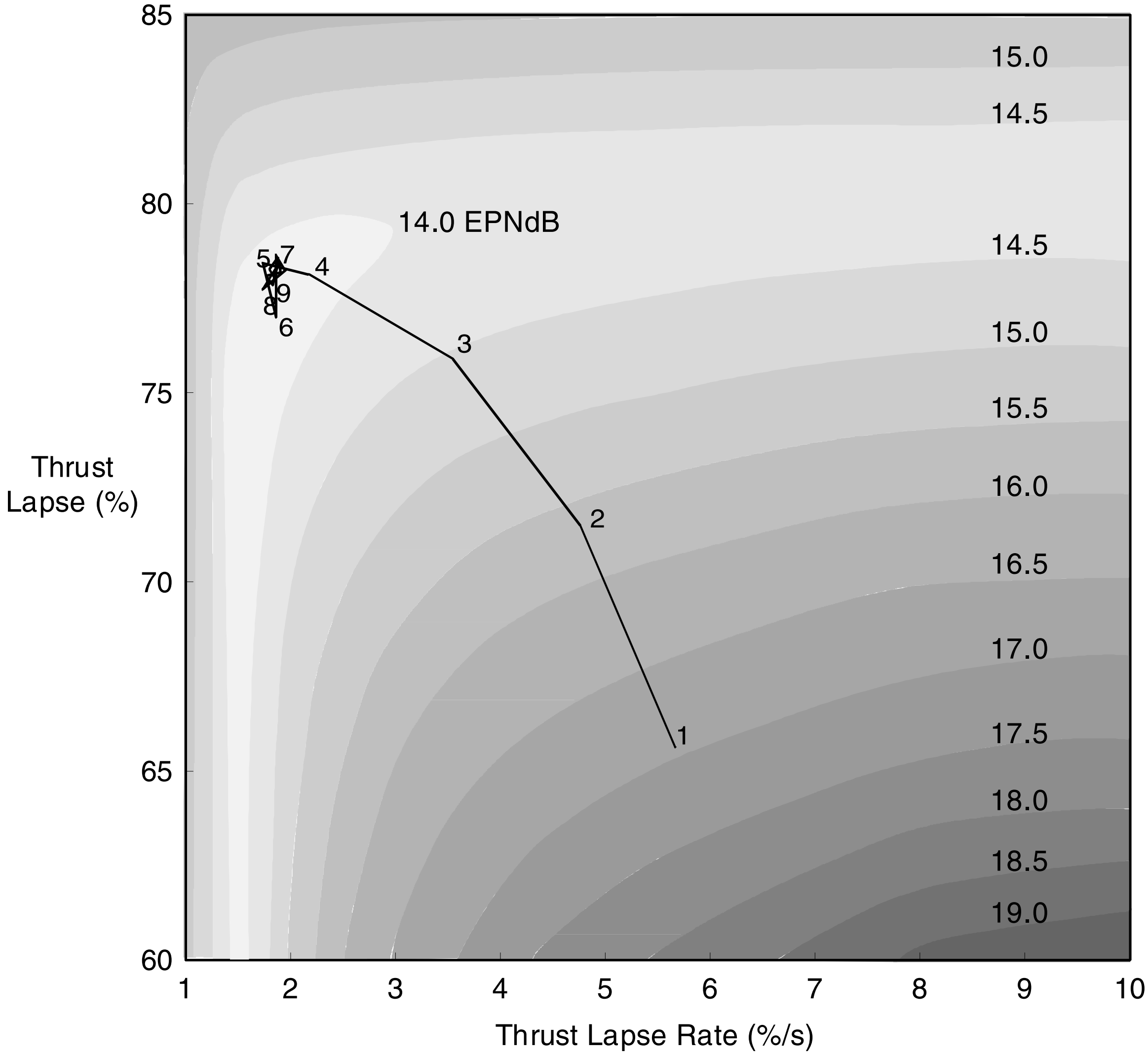

Figure 40.—Overall noise suppression required - programmed lapse rate maneuver for the 1993 TBE3010 Boeing HSCT with three percent ground roll thrust derate showing optimization path

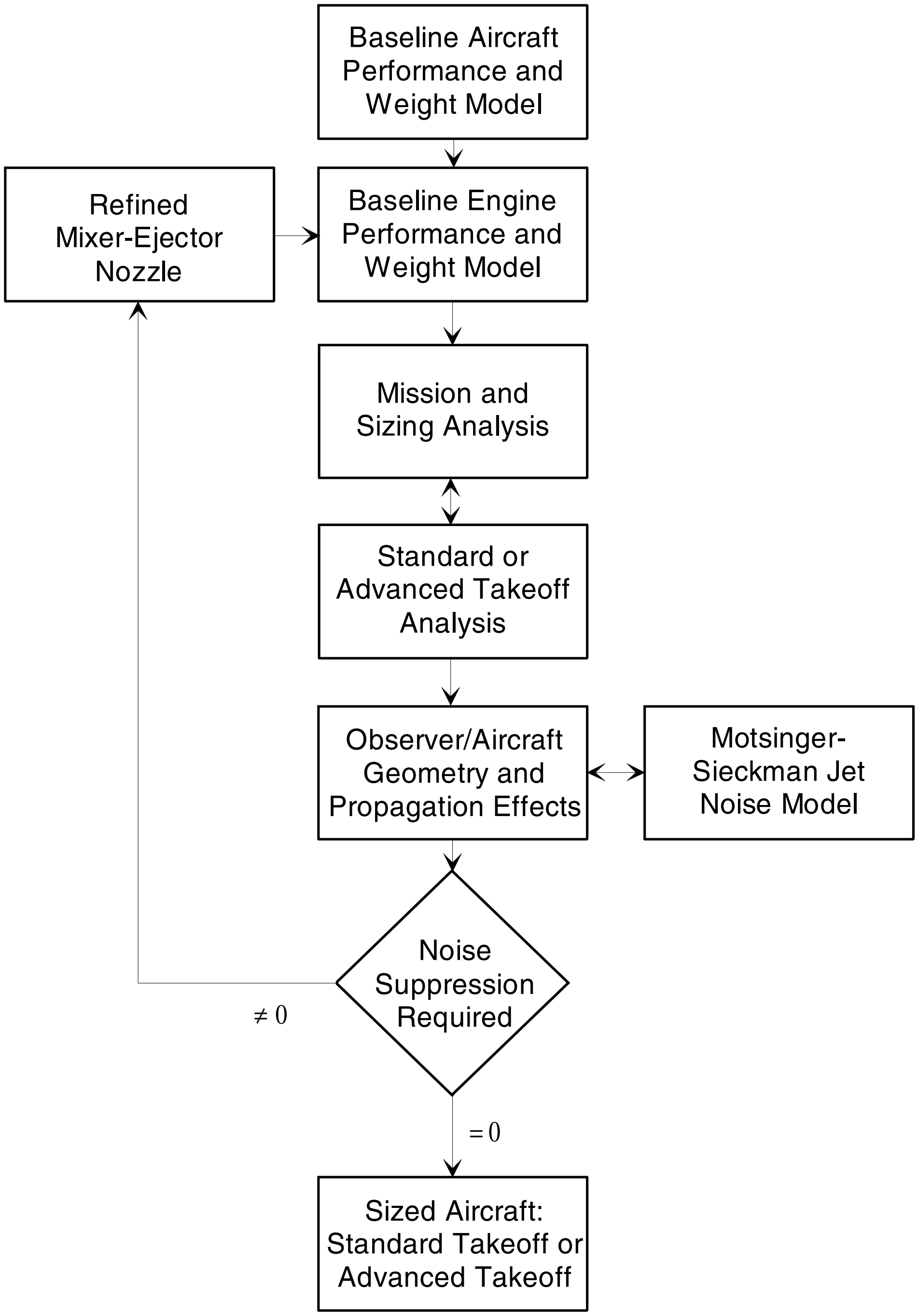

Figure 41.—Analysis flowpath for propulsion systems with mixer-ejector nozzles

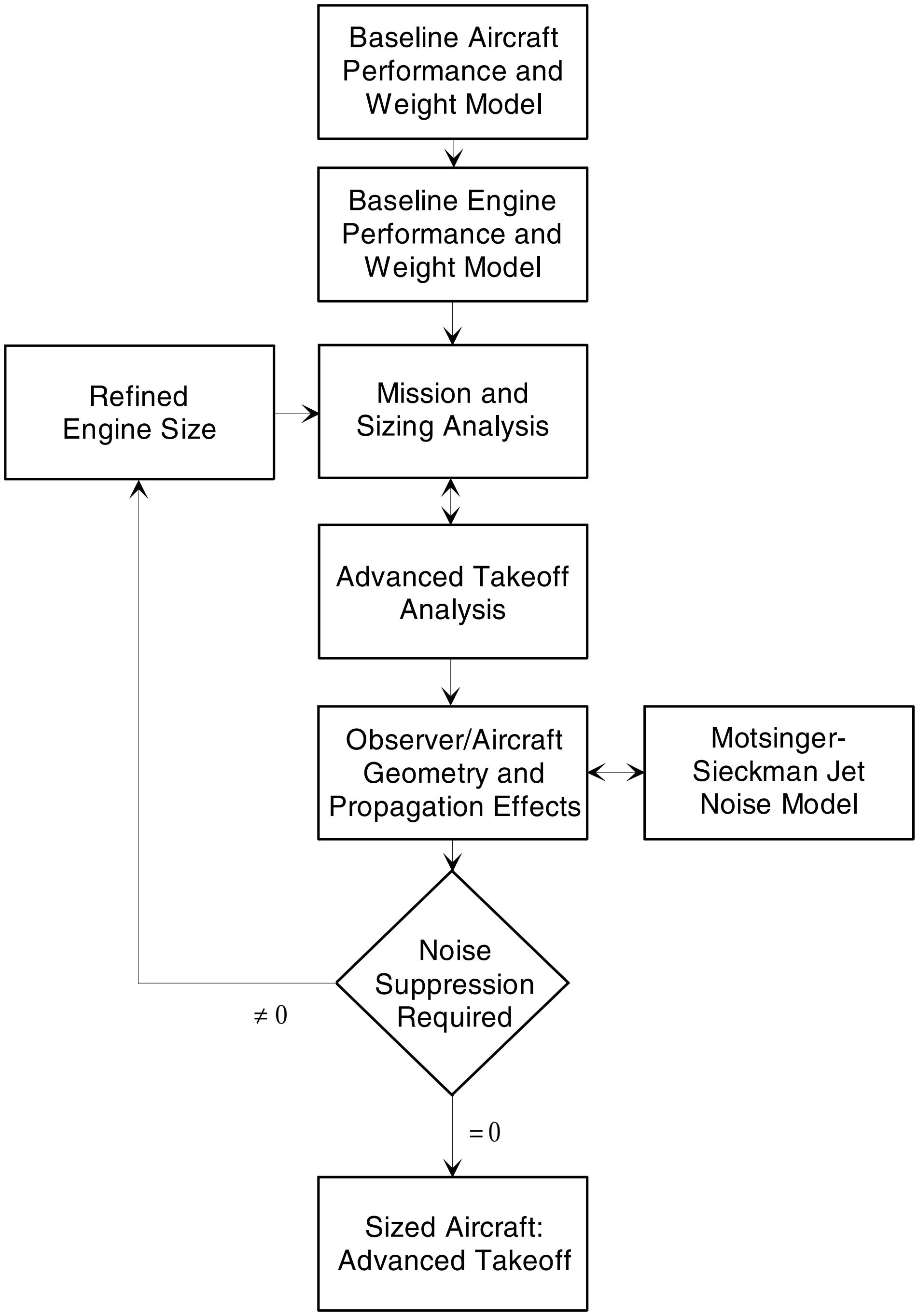

Figure 42.—Analysis flowpath for Flade propulsion systems

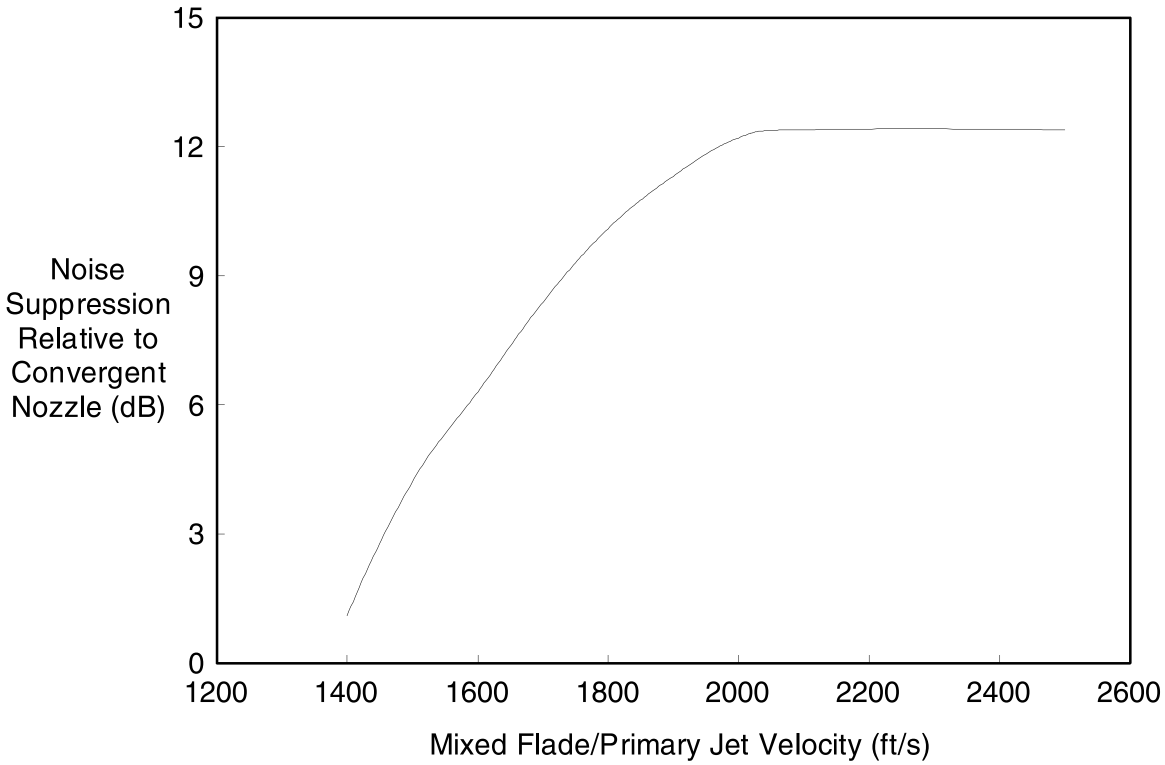

Figure 43.—Flade nozzle noise suppression capability

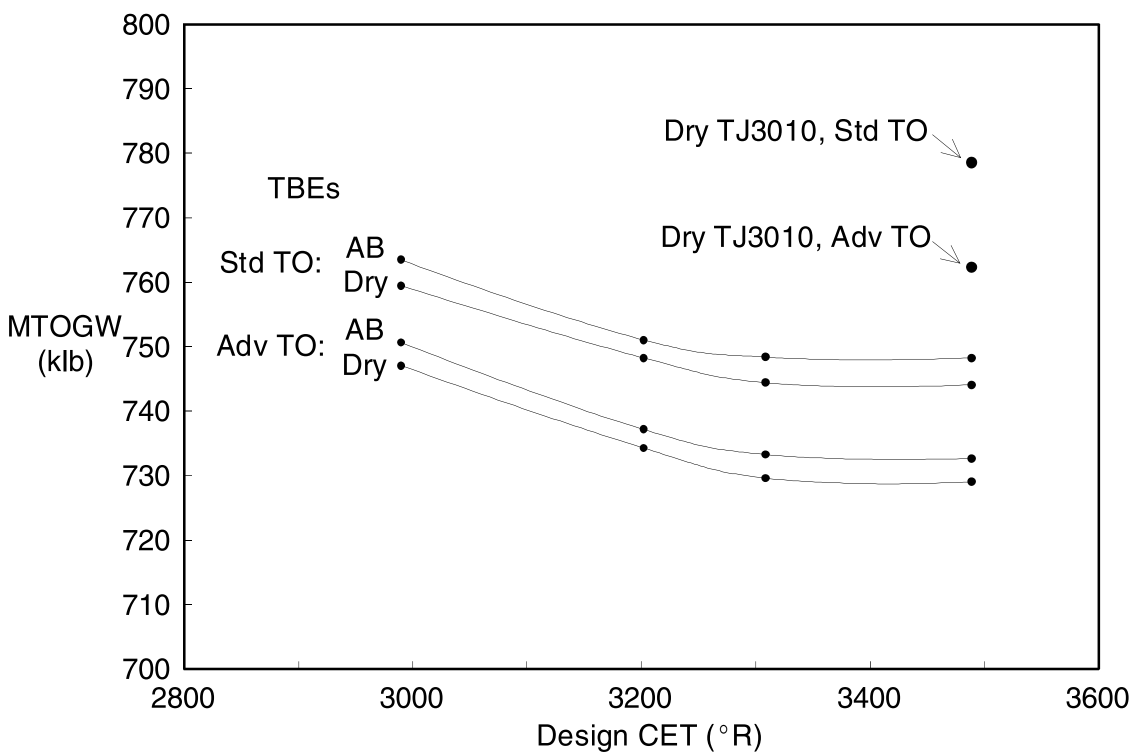

Figure 44.—1993 Turbojet and Turbine Bypass Engine Boeing HSCT gross weights: Influence of design combustor exit temperature and transonic afterburning

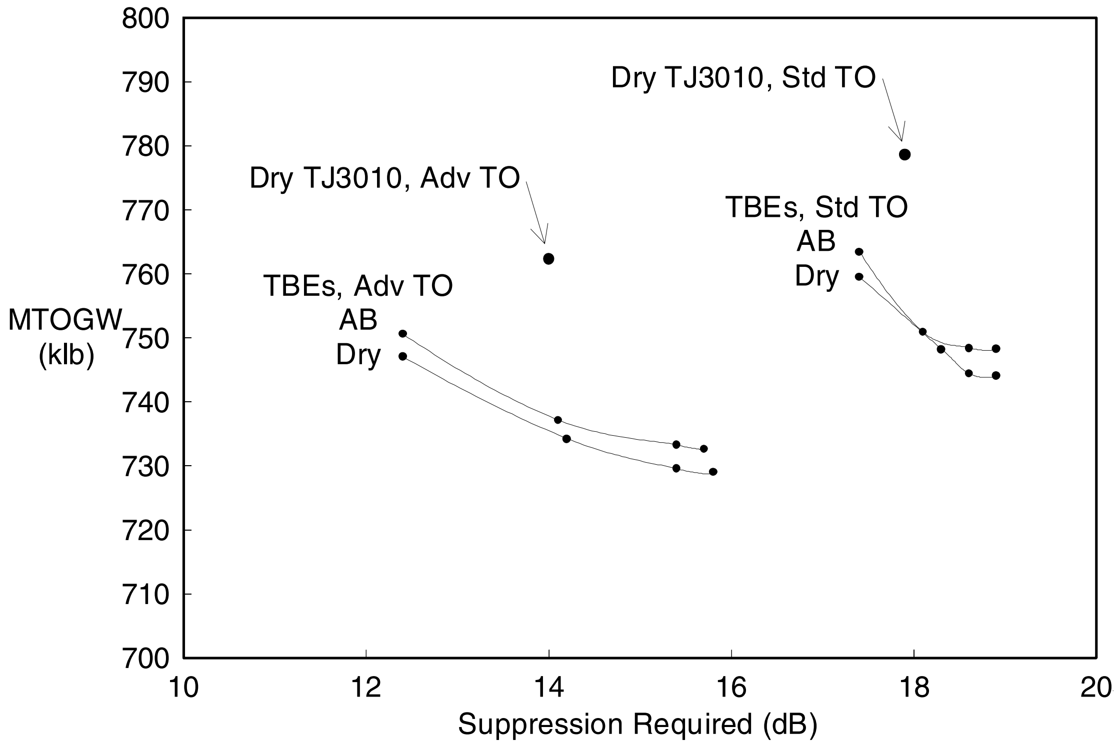

Figure 45.—1993 Turbojet and Turbine Bypass Engine Boeing HSCT gross weights: Influence of noise constraint and transonic afterburning

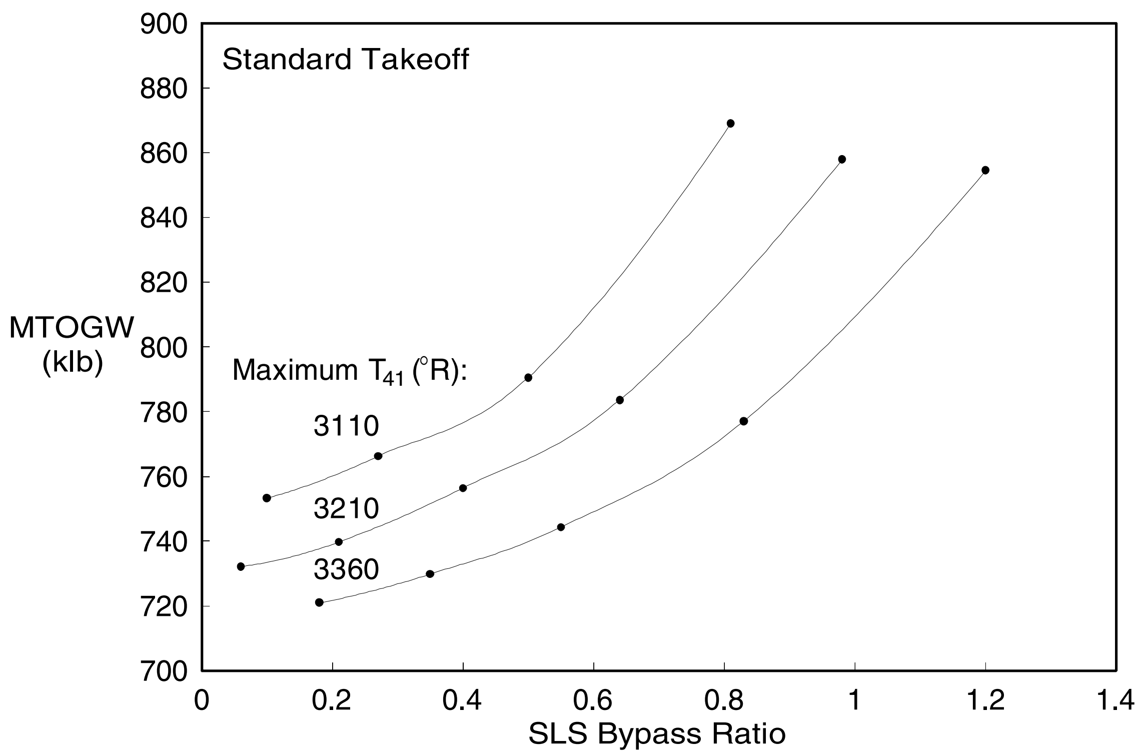

Figure 46.—1993 Dry Mixed Flow Turbofan Boeing HSCT gross weights: Influence of bypass ratio and maximum turbine inlet temperature

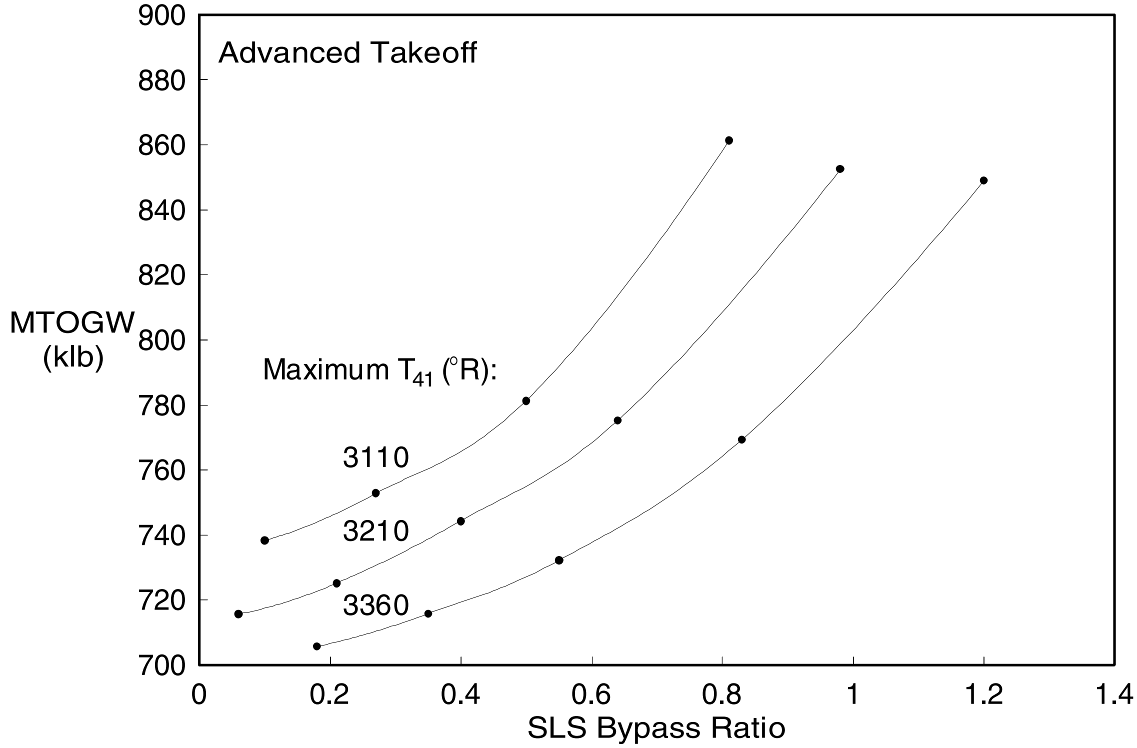

Figure 47.—1993 Dry Mixed Flow Turbofan Boeing HSCT gross weights: Influence of bypass ratio and maximum turbine inlet temperature

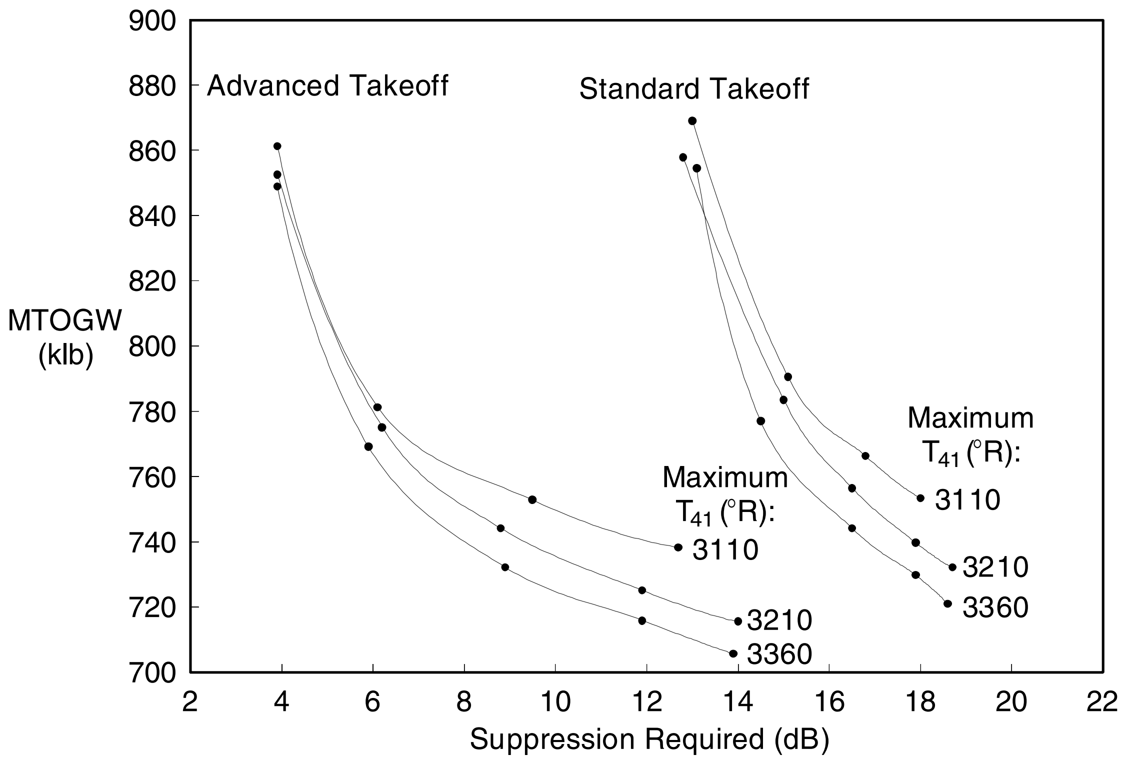

Figure 48.—1993 Dry Mixed Flow Turbofan Boeing HSCT gross weights: Influence of noise constraint and maximum turbine inlet temperature

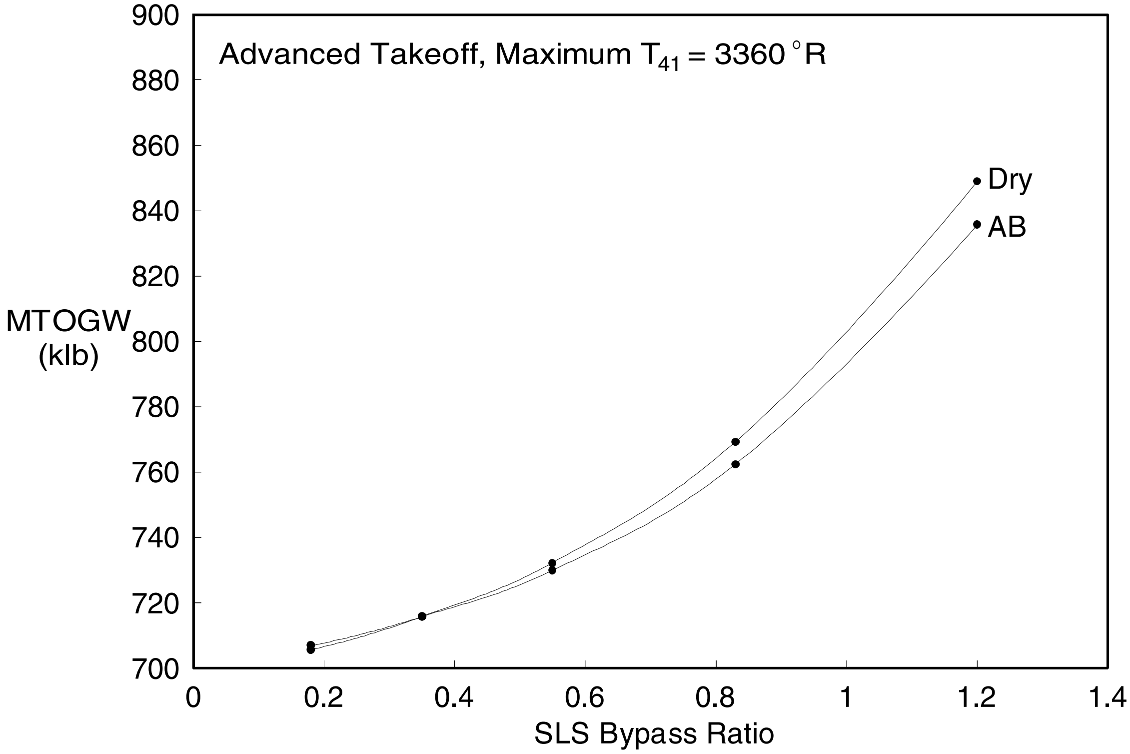

Figure 49.—1993 Mixed Flow Turbofan Boeing HSCT gross weights: Influence of bypass ratio and transonic afterburning

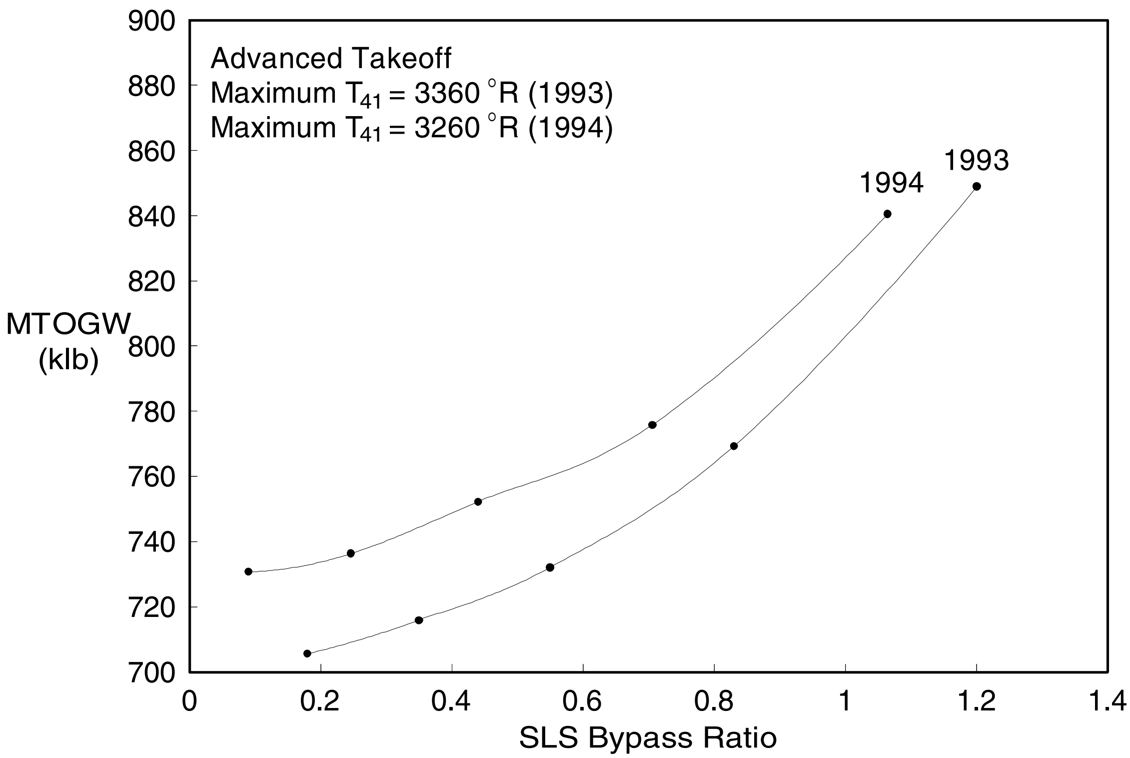

Figure 50.—Dry Mixed Flow Turbofan Boeing HSCT gross weights: Influence of bypass ratio and propulsion ground rules

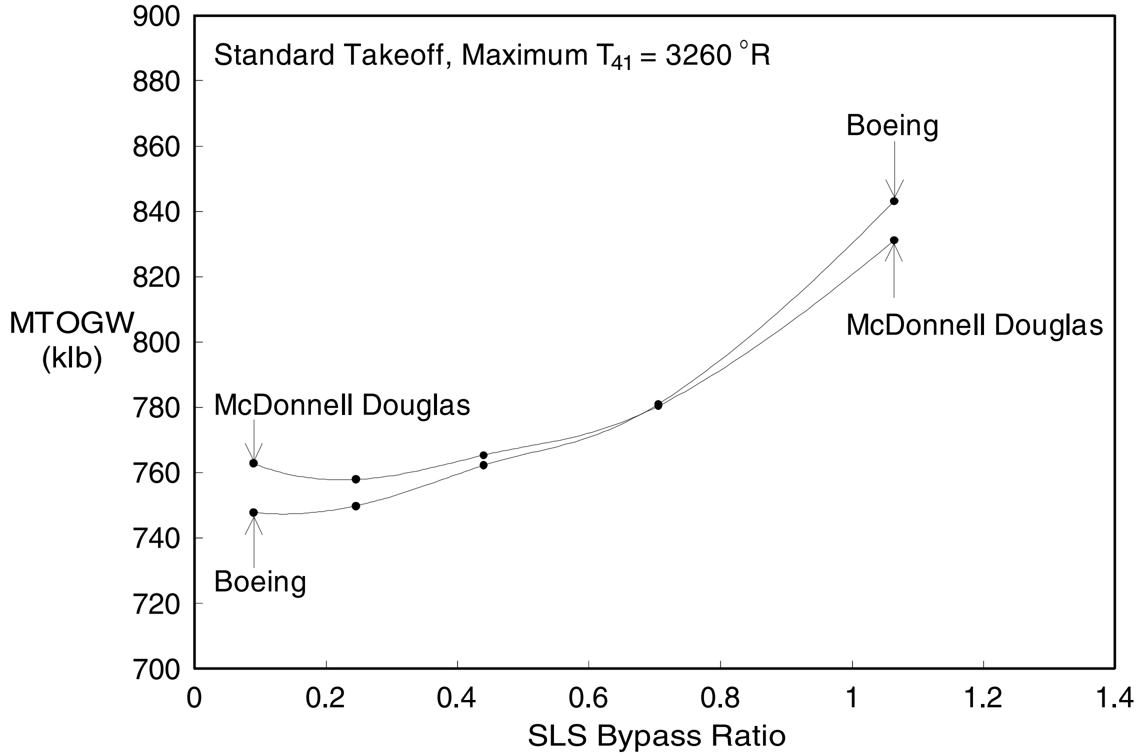

Figure 51.—1994 Dry Mixed Flow Turbofan gross weights: Influence of bypass ratio and aircraft

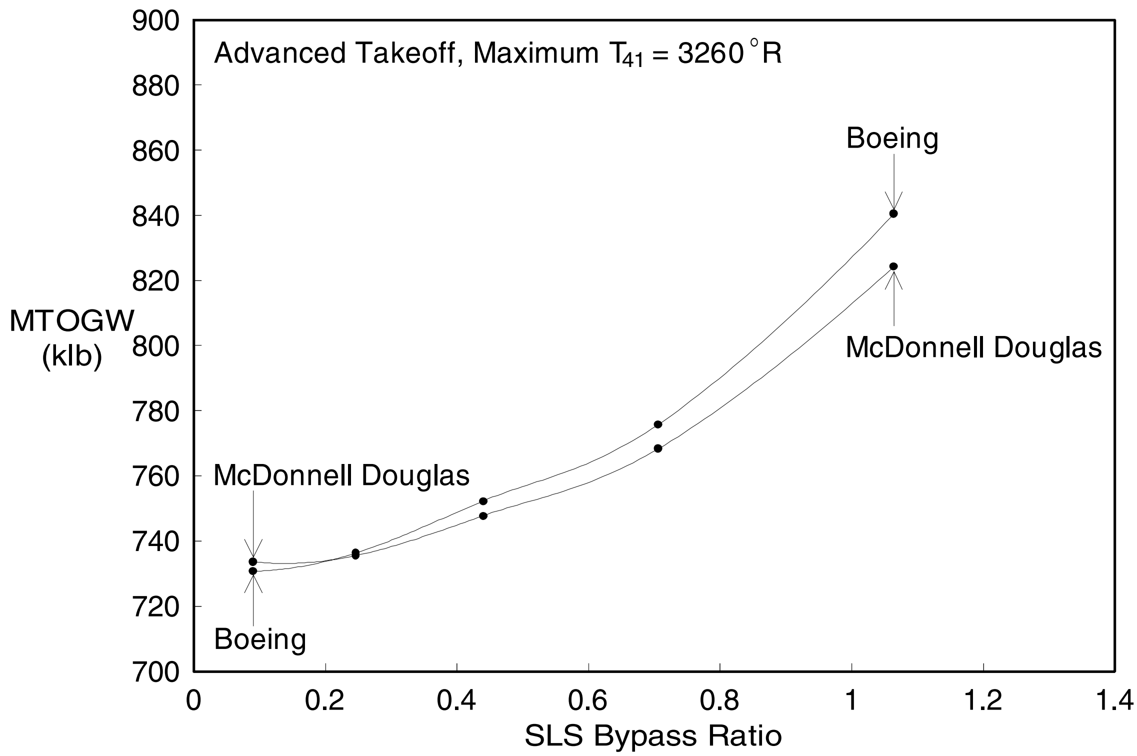

Figure 52.—1994 Dry Mixed Flow Turbofan gross weights: Influence of bypass ratio and aircraft

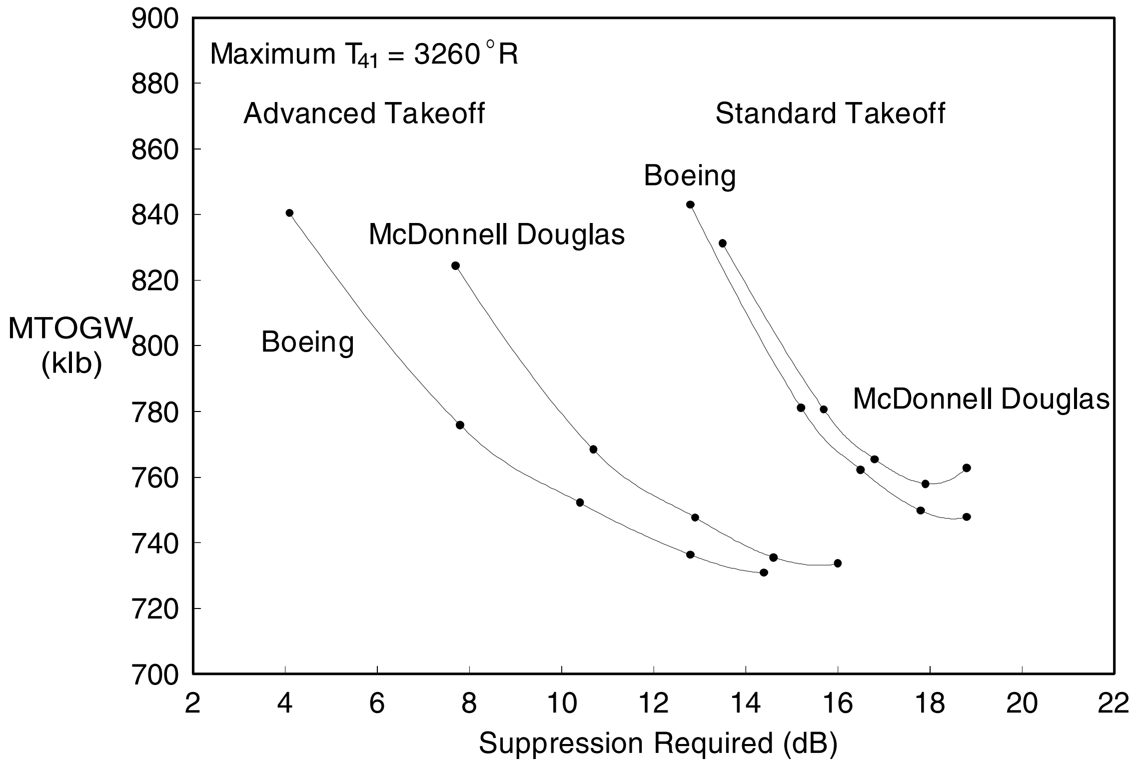

Figure 53.—1994 Dry Mixed Flow Turbofan gross weights: Influence of noise constraint, takeoff procedure, and aircraft

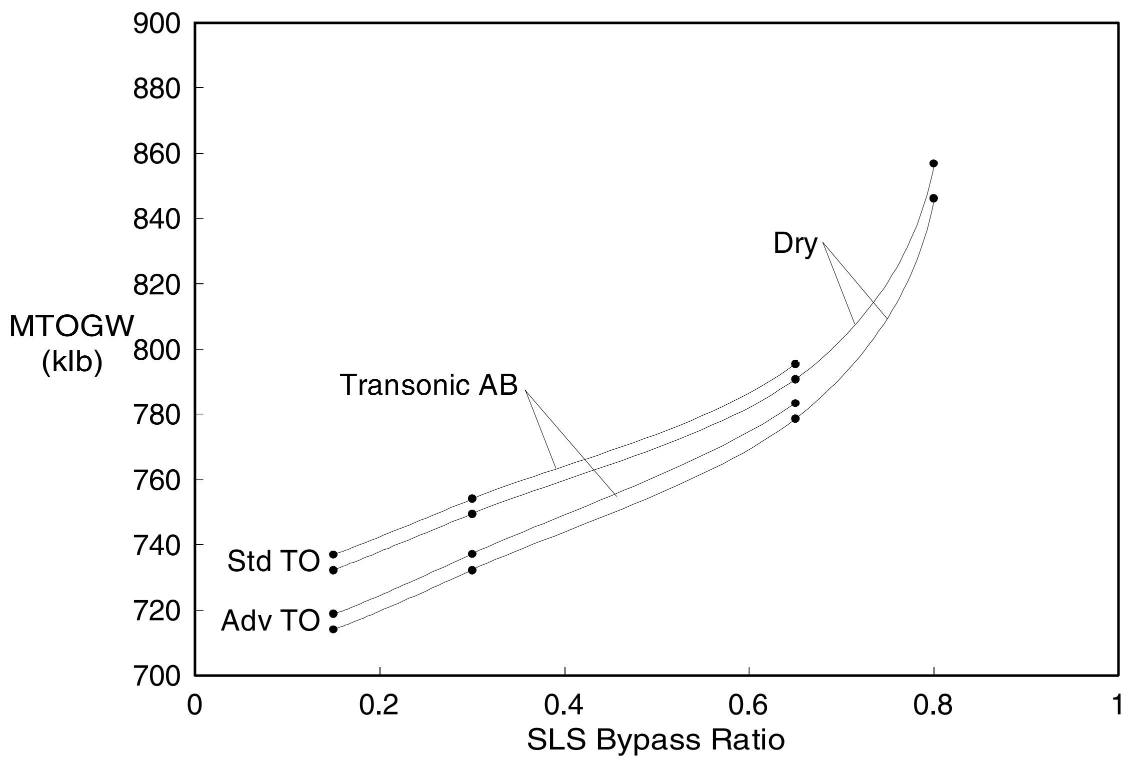

Figure 54.—1993 Variable Cycle Engine Boeing HSCT gross weights: Influence of bypass ratio and transonic afterburning

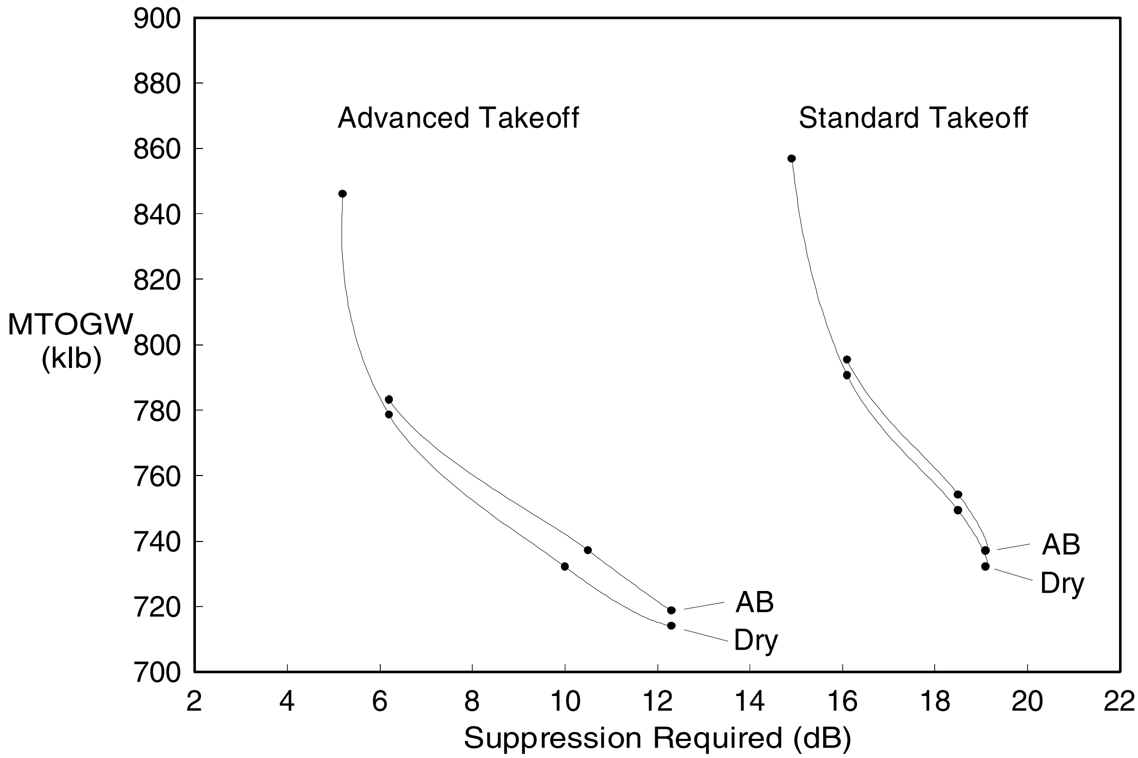

Figure 55.—1993 Variable Cycle Engine Boeing HSCT gross weights: Influence of noise constraint and transonic afterburning

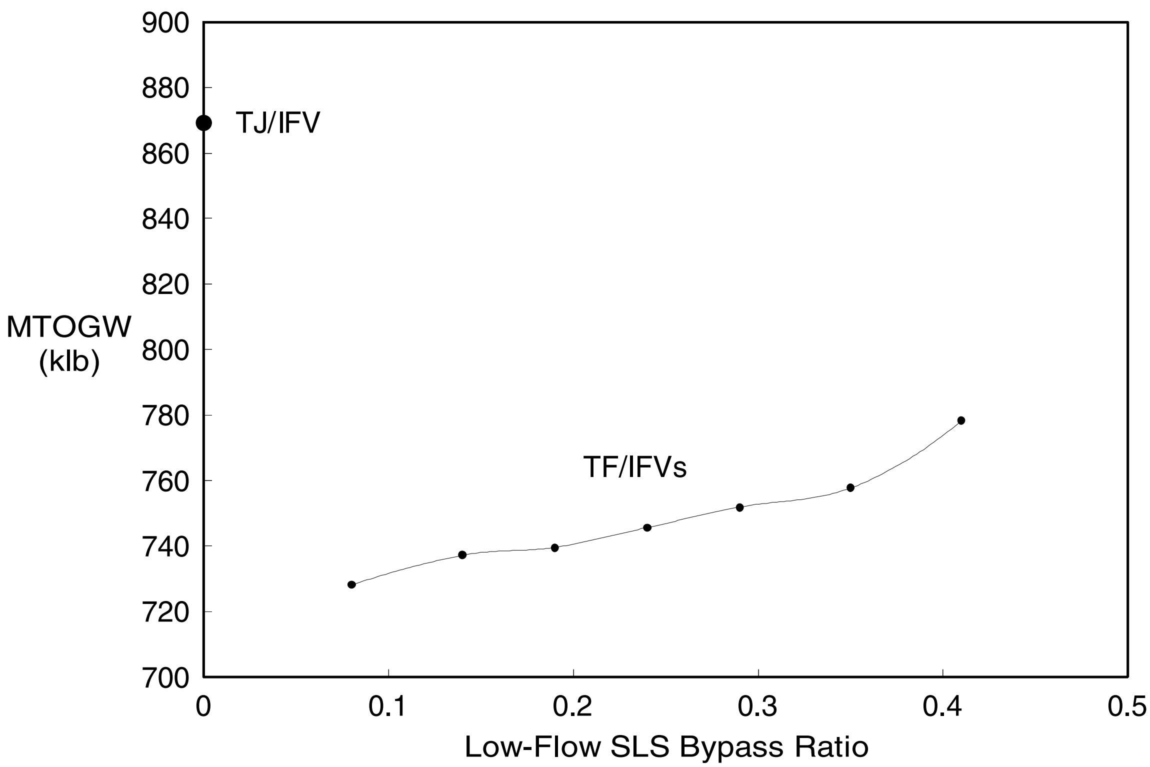

Figure 56.—1993 Inverting Flow Valve Boeing HSCT gross weights: Influence of low-flow mode bypass ratio

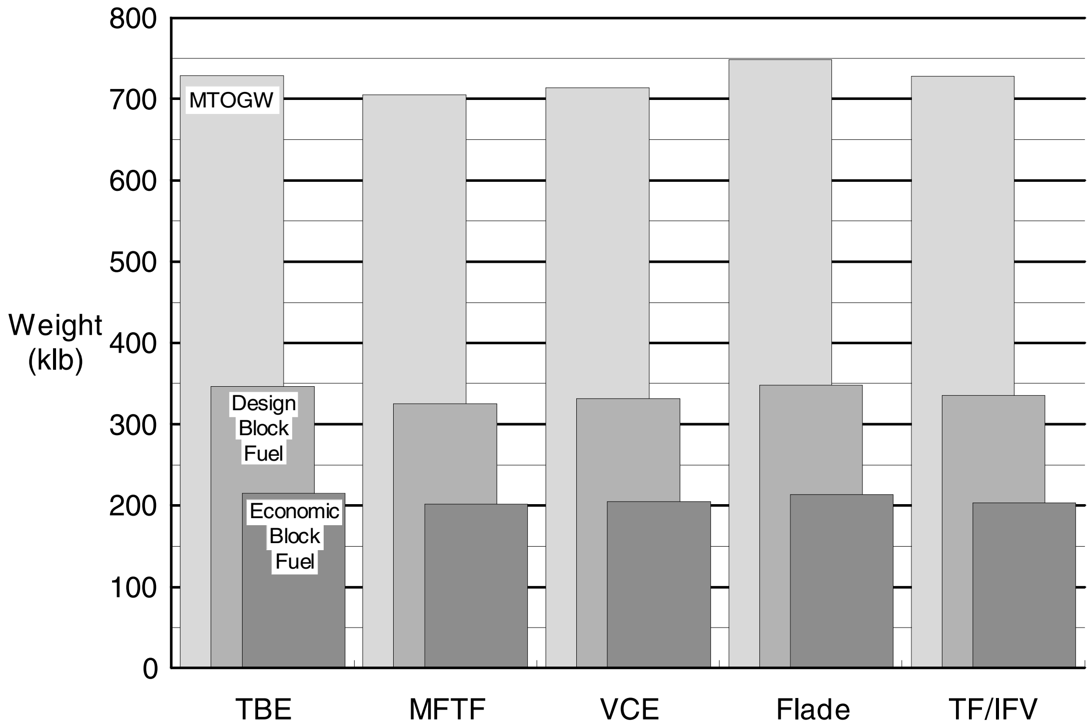

Figure 57.—Maximum takeoff gross weight, design mission block fuel, and economic mission block fuel comparison: 1993 cycle ground rules, advanced takeoff, Boeing HSCT

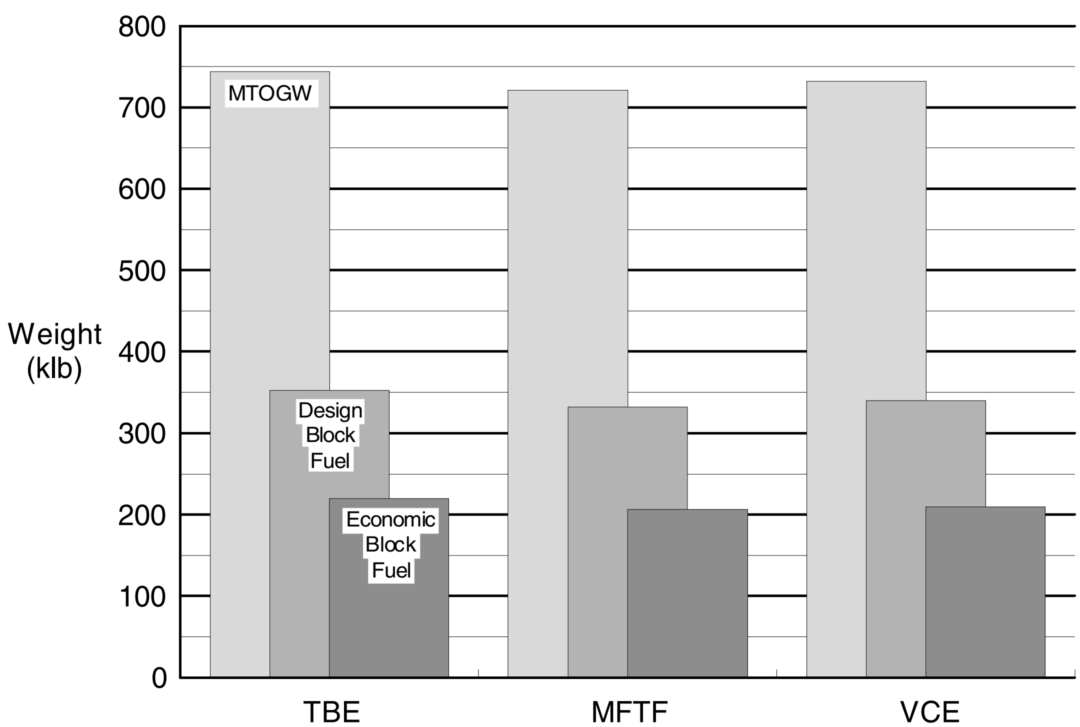

Figure 58.—Maximum takeoff gross weight, design mission block fuel, and economic mission block fuel comparison: 1993 cycle ground rules, standard takeoff, Boeing HSCT

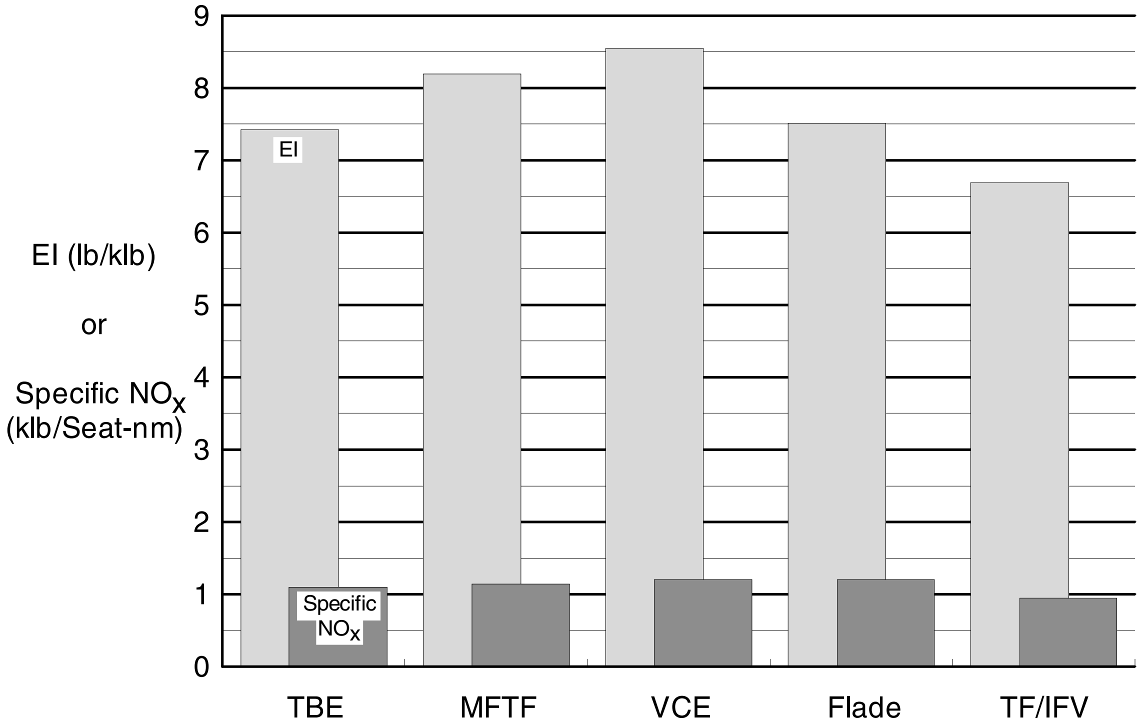

Figure 59.—Emissions index and specific NO_X comparison: 1993 cycle ground rules, advanced takeoff, Boeing HSCT

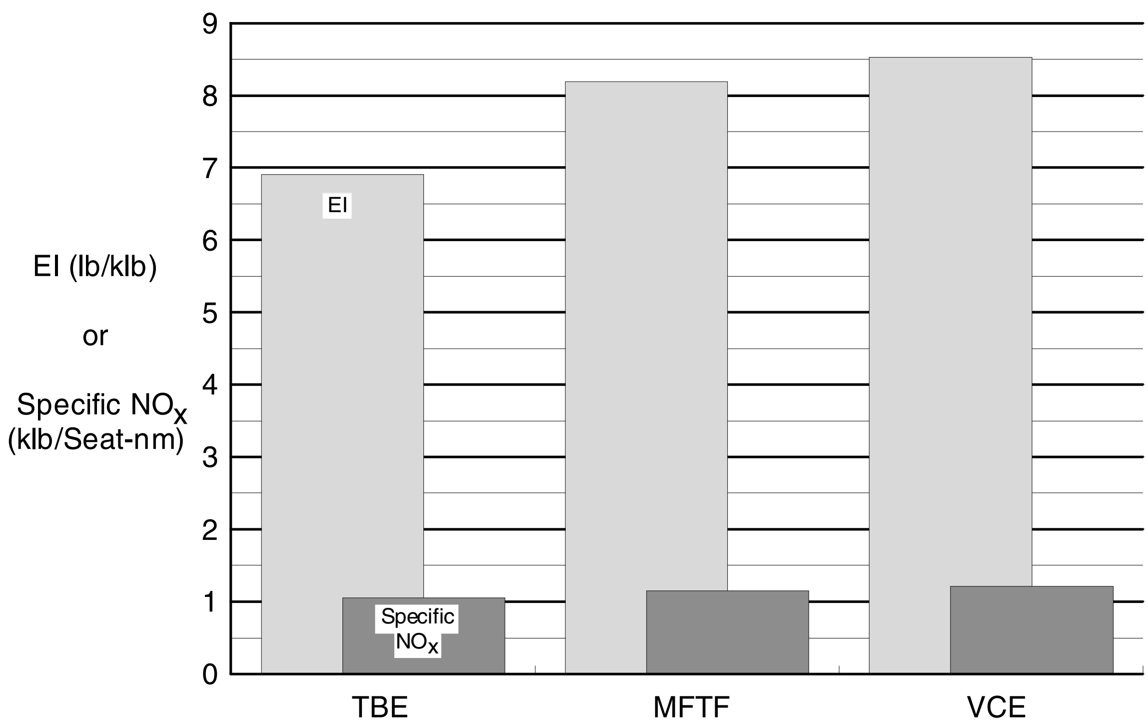

Figure 60.—Emissions index and specific NO_X comparison: 1993 cycle ground rules, standard takeoff, Boeing HSCT

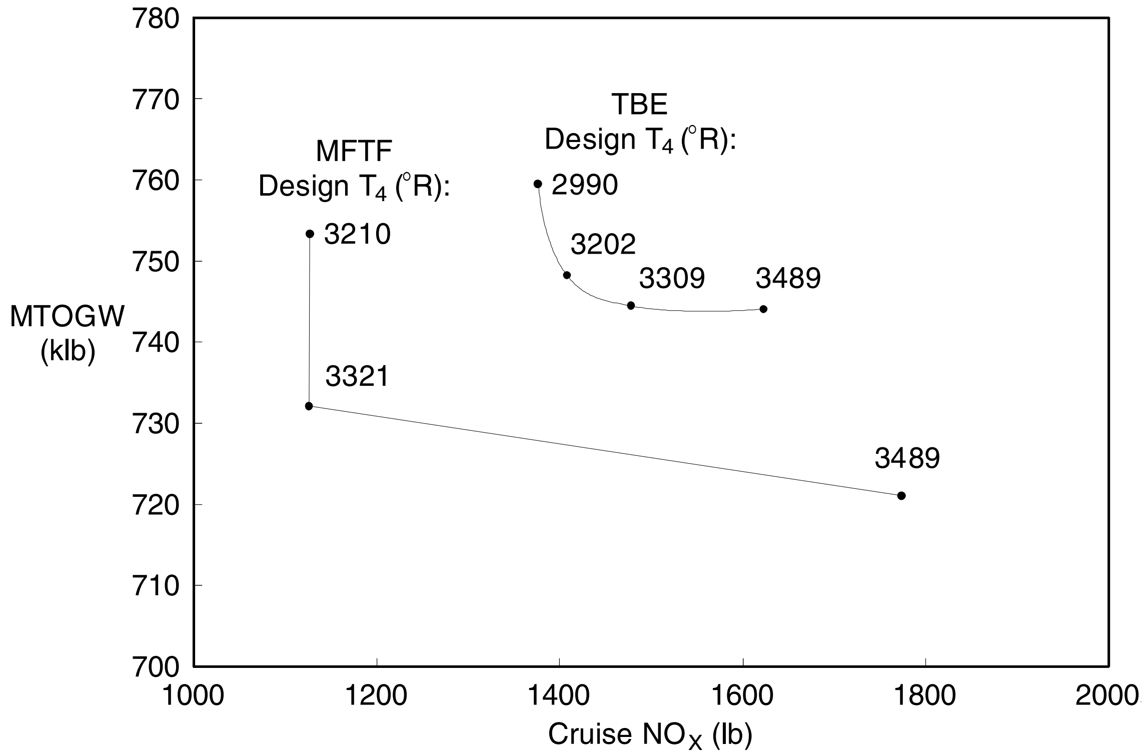

Figure 61.—Achieving lower emissions by lowering T_4 (1993 TBEs 3010, 3021, 3031, 3041, and 1993 MFTFs 5093, 5193, 4293, standard takeoff, Boeing HSCT)

REPORT DOCUMENTATION PAGE			Form Approved OMB No. 0704-0188

1. AGENCY USE ONLY (*Leave blank*)	2. REPORT DATE	3. REPORT TYPE AND DATES COVERED
	February 2005	Technical Memorandum

4. TITLE AND SUBTITLE

A Comparative Propulsion System Analysis for the High-Speed Civil Transport

5. FUNDING NUMBERS

WBS–22–714–09–46

6. AUTHOR(S)

Jeffrey J. Berton, William J. Haller, Paul F. Senick, Scott M. Jones, and Jonathan A. Seidel

7. PERFORMING ORGANIZATION NAME(S) AND ADDRESS(ES)

National Aeronautics and Space Administration
John H. Glenn Research Center at Lewis Field
Cleveland, Ohio 44135–3191

8. PERFORMING ORGANIZATION REPORT NUMBER

E–14934

9. SPONSORING/MONITORING AGENCY NAME(S) AND ADDRESS(ES)

National Aeronautics and Space Administration
Washington, DC 20546–0001

10. SPONSORING/MONITORING AGENCY REPORT NUMBER

NASA TM—2005-213414

11. SUPPLEMENTARY NOTES

This research was originally published internally as HSR007 in October 1995. Responsible person, Jeffrey J. Berton, organization code PBA, 216–977–7031.

12a. DISTRIBUTION/AVAILABILITY STATEMENT

Unclassified - Unlimited
Subject Category: 07 Distribution: Nonstandard

Available electronically at http://gltrs.grc.nasa.gov

This publication is available from the NASA Center for AeroSpace Information, 301–621–0390.

12b. DISTRIBUTION CODE

13. ABSTRACT ***(Maximum 200 words)***

Six of the candidate propulsion systems for the High-Speed Civil Transport are the turbojet, turbine bypass engine, mixed flow turbofan, variable cycle engine, Flade engine, and the inverting flow valve engine. A comparison of these propulsion systems by NASA's Glenn Research Center, paralleling studies within the aircraft industry, is presented. This report describes the Glenn Aeropropulsion Analysis Office's contribution to the High-Speed Research Program's 1993 and 1994 propulsion system selections. A parametric investigation of each propulsion cycle's primary design variables is analytically performed. Performance, weight, and geometric data are calculated for each engine. The resulting engines are then evaluated on two airframer-derived supersonic commercial aircraft for a 5000 nautical mile, Mach 2.4 cruise design mission. The effects of takeoff noise, cruise emissions, and cycle design rules are examined.

14. SUBJECT TERMS

Jet propulsion; Supersonic aircraft; Turbine engines; Aircraft engines; Aircraft noise; Noise prediction-aircraft

15. NUMBER OF PAGES

105

16. PRICE CODE

17. SECURITY CLASSIFICATION OF REPORT	18. SECURITY CLASSIFICATION OF THIS PAGE	19. SECURITY CLASSIFICATION OF ABSTRACT	20. LIMITATION OF ABSTRACT
Unclassified	Unclassified	Unclassified	